THE UNIVERSITY OF CHICAGO

THE MORPHOLOGICAL DIVERSITY OF COCCOLITHOPHORES ACROSS ENVIRONMENTS, GEOGRAPHIC SPACE, AND GEOLOGIC TIME

A DISSERTATION SUBMITTED TO

THE FACULTY OF THE DIVISION OF THE PHYSICAL SCIENCES

IN CANDIDACY FOR THE DEGREE OF

DOCTOR OF PHILOSOPHY

DEPARTMENT OF THE GEOPHYSICAL SCIENCES

BY

MARITES VILLAROSA GARCIA BARIŞ

CHICAGO, ILLINOIS

DECEMBER 2017

To my husband, Tristan, and in memory of my friend John K. Adams.

TABLE OF CONTENTS

List of Figures

List of Tables

ABSTRACT

In this dissertation, I explore how the morphological diversity of coccolithophores, a major group of eukaryotic phytoplankton, manifests at different scales—from the subspecies level as the functional consequences of form, to the biogeographic patterns of disparity of families. The first part of this dissertations evaluates whether the minute morphologies of coccoliths and coccospheres can affect how a cell interacts with its fluid environment. From these biomechanical sinking experiments, I find that the size and shape of coccoliths can slow sinking velocity, and that coccospheres exhibiting asymmetric arrangements of coccoliths will reorient while sinking, demonstrating the relevance of these features. Next, I explore the spatial and environmental structure of morphological diversity in the modern ocean, by quantifying and comparing disparity across biomes and latitudes. Similar to other groups, such as marine invertebrates and flying terrestrial vertebrates, there is no clear gradient to disparity across either latitudes or biomes in this group; in fact, different regions are indistinguishable with respect to morphological disparity. This homogeneity is likely a result of the cosmopolitan range of most extant families. Finally, I examine the potential distortion of morphological disparity in fossil samples which are predominantly made up of disarticulated coccoliths, by analytically degrading extant assemblages. Coccolith morphology is poorly correlated with coccosphere morphology, but makes a reasonable proxy for whole-organism morphology. The disparity of fossil and dead assemblages is indistinguishable from that of the living assemblages, for biome and latitudinal assemblages, and for the families that could be examined. This work serves to buttress and inform future paleontological work on coccolithophorid morphological diversity, as well as to provide insights into the role of different coccolith arrangement and coccosphere shape.

ACKNOWLEDGMENTS

This dissertation is a result of many years of mentoring, fruitful discussions, and persistent encouragement from both my advisor, Michael Foote, and committee, Kevin Boyce, David Jablonski, and Susan Kidwell. I am grateful that they believed in my ability to take on this ambitious project, and never gave up on me throughout the process. This dissertation also benefited greatly from the help of other faculty, post-docs, and students, at the University of Chicago. I am indebted to Maureen Coleman and Michael LaBarbera for helping me understand the world of plankton, and without whose feedback and guidance, chapters 2 and 3 would not have been possible. I also thank Graham Slater and Mark Webster for useful discussion of projects and ideas related to those covered in this dissertation. Thank you to Kathleen Ritterbush and Christina Belanger for useful discussion throughout the development and completion of this project, and for their wisdom on how to be an academic scientist. Thank you to my fellow students for the years of comradery and intellectual discourse. A special thanks to Kristen Jenkins Voorhies, Nadia Pierrehumbert, Peter Smits, Tristan Betzner, David Bapst, Stewart Edie, Andres Baresch, Joseph Walkowicz, Peter Tierney, Nicole Bitler Kuehnle, Amy Henry, and especially my fantastic office-mate Jon Mitchell. I am also thankful for the help I received from the department's administrative and research staff—especially Brian Lynch, Gerry Olack, David Taylor, Katie Casey, and Jess Valle— , Elizabeth Eakin and Carolyn Johnson from The Committee on Evolutionary Biology, and the Physical Sciences Division's Dean of Students, Miranda Swanson.

I extend my deepest gratitude to the International Nannoplankton Association and The Micropalaeontological Society, for their welcoming community, whose expertise, feedback, and

constructive challenge helped hone the work presented herein. A special thank you to Marie-Pierre Aubry, David Bord, and Rehab Salem who took me under their wing and brought me up to speed with nannofossil taxonomy and identification. Thank you to Jeremy Young and Michal Kucera for fielding and discussing a plethora of questions and ideas. A very special thanks to Jeremy Young, Jackie Lees, Paul Bown, and all the other Mikrotax/Nannotax contributors whose work with the database made my work possible. I thank my funding sources, The Gurlly Fund, The Hinds Fund, The Micropalaeontological Society Grant in Aid, ASLO Travel Fund, and The Graduate Student Affairs Travel Grant for their generous support of this project and its presentation.

Finally, I want to express my profound appreciation to my incredible and loving husband, Tristan Betzner, who not only discussed the intricacies and nuances of my research, but also helped me find the mental and emotional strength to do the work daily, and to my supportive family who may not totally understand why I set out on this journey, either because they are non-academic folks of many talents or because they are cats, but nonetheless accompanied me on this journey.

CHAPTER 1

INTRODUCTION

The importance of marine primary producers is widely recognized, and while copious studies have examined the effects of environmental change on primary production (D'Hondt et al. 1998, Eleson et al. 2005, Palumbo et al. 2013), more work remains to be done on the response of primary producers themselves. Phytoplankton show varied responses to major environmental perturbations and ecological turnover events on different time scales. Over large temporal scales, they exhibit periods of high and low taxonomic diversification and/or extinction, often coincident with major environmental changes (Katz et al. 2004, Erba 2006, Aubry 2007), and display morphological macroevolutionary trends in form, such as the Cenozoic decrease in size observed in coccolithophores and the reduction of test weight observed in radiolarians (Schmidt et al. 2006). On shorter time scales, the physiology of the individuals composing a population can change in a matter of days (i.e. a few generations) and ecological communities turn over seasonally, at times existing in large but ephemeral blooms visible from space.

Unicellular eukaryotic plankton benefit from their cellular physiology, such as organelles and a cytoskeletons, which allow for intricate morphologies (Butterfield 2015), both organic, as in the case of dinoflagellates and acritarchs, and mineralized, as in the case of diatoms, foraminifera, and coccolithophores. Both organic and mineralized forms are frequently preserved, yielding a high-resolution fossil record that can ultimately be linked to phylogenies based on the soft anatomy and molecular data. The fossil remains of mineralizing plankton have frequently been employed as biostratigraphic indices of particular time intervals and events, environmental indicators, or packets of geochemical data. These fossil structures also represent

whole organisms and so are good operational units for evolutionary studies, which is the focus of this dissertation.

1.1 Motivation for the Present Research

Before proceeding with paleontological studies of morphological diversity, certain aspects of a study system must be understood. First, an implicit assumption when conducting paleontological studies of morphological diversity is that the morphology of interest is biologically relevant to the evolution of the group in question. There are many examples of morphological forms that arise accidentally and are non-adaptive features (Gould & Lewontin 1979), and though these must have some biological consequences, as there is at least a metabolic cost to their production and development, these features may not do a good job of tracking the evolutionary dynamics of a group. Second, there is an underlying assumption that the difference in morphological diversity observed through time is greater than the amount of variation introduced by sampling different latitudes and longitudes or environments. Thus, the effect of geographic or spatial variation on values of morphological diversity must be also be evaluated. Third, the process of fossilization is often assumed to introduce minimal biases, such that the diversity patterns through time are robust and represent reality. The robustness of the fossil record to preservational bias has been demonstrated many times, especially when applied to questions of large-scale taxonomic richness and diversification, (e.g. Wagner 2000, Kidwell & Holland 2002, Alroy et al. 2008, Holland 2009) and the work that has addressed a similar question pertaining to morphological diversity seems to also support the idea of a robust record (e.g. Foote 1997, but see Mitchell 2015), although this aspect has been explored to a lesser extent.

In this dissertation, I address these three assumptions in turn. First I test the fluid dynamical consequences of coccolithophore morphology, which has been a challenge to study due to the miniature scale of these organisms, a problem I circumvent by constructing larger physical models used in sinking experiments. Next I investigate the biogeographic and environmental structure of morphological disparity in extant coccolithophores across the world's ocean. Last, I evaluate the potential biases introduced through the process of fossilization by degrading the morphological disparity of extant live-collected coccolithophores to dead and fossil conditions, i.e. reducing the species pool and excluding morphological features evident only in intact complete tests. In this way, I lay the foundation for building extensive paleontological studies utilizing these nannoplankton.

1.2 Biology and Paleontology of Coccolithophores

To provide further context for the chapters that follow, this section summarizes some of the principal features of coccolithophore biology and paleontology.

Coccolithophores are unicellular haptophyte algae in the class Prymnesiophyceae, which synthesize calcium carbonate scales known as coccoliths. These scales exhibit a wide range of complex scale morphologies—solid paired discs (e.g. placoliths), stems or spines (e.g. salpingiform, phenoliths), walled rings (e.g. muroliths), wigwam-like struts (as in *Wigwamma arctica.*), etc.— and the arrangement of these plates around the cell, known as the coccosphere, is also highly variable in overall shape and architecture. Coccoliths are synthesized intracellularly in a vacuole and subsequently exocytosed to the surface (Billard and Inouye 2004). The coccolithophorid life cycle consists of an independent haploid stage and an independent diploid stage; cells in either of these stages are capable of asexual reproduction, and

the haploid cells are also capable of sexual reproduction. Some species have unmineralized cells in the haploid stage, though many species bear mineralized scales of a different structure, known as holococcoliths or nannoliths; these holococcoliths are distinguished from the heterococcoliths typical of the diploid stage by their architecture, composed of many more, and smaller crystallites (Young & Henriksen 2003). Different species often exhibit the same holococcolith morphology, and so there is a many to one mapping between these two kinds of coccoliths (Billard and Inouye 2004). For many taxa (orders Isochrysidalles, and Coccolithales), heterococcolith formation begins with a proto-coccolith ring composed of what are termed V and R units, distinguished from each other based on the orientation of the long axis of each crystal (Young & Henriksen 2003). Coccolith morphology is fairly plastic and lacks homology at any structural level beyond that of crystallographic units, which only applies to taxa wherein the VR units are clearly recognizable (Young et al. 2004). The pattern and organization of these units are often conserved among families and can be used to characterize these groups (Young et al. 2004). Since it is possible to observe crystal structure via light microscopy, which is thus frequently used in systematic work, the previously established groupings between species and genera are likely fairly robust (Bown et al. 2004). High genetic variability exists in modern representatives, with species frequently harboring various distinct genotypes raising the possibility of cryptic speciation (Saez et al. 2004). Nonetheless, fossil systematists have historically still erred on the side of over splitting, mostly in the interest of better specifying biostratigraphic intervals (Bown et al. 2004).

Coccolithophores have undergone multiple periods of diversification and taxonomic turnover (Aubry 1998, Bown 1998a, 2004, Perch-Nielsen 1985a, 1985b). They have been major primary producers in Earth's oceans since the Jurassic (De Vargas, 2007); the oldest known

fossil coccolith dates back to the Triassic (some 235 Mya) (Bown 1998b), and molecular phylogenies predict non-armored, single-celled ancestors of one form or another to have arisen in the Neoproterozoic (Medlin et al. 1997). Their fossil record largely consists of disarticulated coccoliths but coccospheres can be preserved, even in sediments dating to the Triassic (Bown et al. 2014, Mai 1997, Mai 1999). Although their diversity, measured as the number of genera in a given stage, has declined since the Paleogene (Bown et al. 2005), extant coccolithophores exhibit a great deal of morphological diversity. At the same time, Aubry (2007) demonstrates evidence that coccolithophores have undergone convergence in overall (i.e. coccosphere) form (Aubry 2007), Young and colleagues (2004) have also proposed convergence in coccolith shape, and it is possible that biocalcification in this group may have originated independently multiple times (DeVargas et al. 2007).

Cenozoic coccolithophores never reach the species richness that the group had in the Cretaceous, and their diversification rates have fluctuated greatly since then (Bown et al. 2004). They also ceased to be as profuse a sediment builder in the Cenozoic compared to the Mesozoic, when they formed vast chalk deposits globally. Although diversity increases briefly in the Miocene, the remainder of the Neogene is characterized by declining diversity. Despite the overall declining diversity trend during the Cenozoic, several authors remark on the notably different morphologies that arise during some of these biodiversity events. Bown et al. (2004) note that the majority of taxonomic innovation evolved during the Paleocene radiation and, from a qualitative comparison of assemblages, the morphological differences observed between the epochs of the Cenozoic is greater than the difference observed between Cretaceous stages. Aubry (2007) argues that coccolithophores become more specialized during the Pliocene, based on the observed tendency towards smaller coccosphere and coccolith sizes across multiple lineages, in

contrast with the larger more heavily calcified forms of the early Cenozoic and late Mesozoic. The intricate jointed appendages of some members of the family Syracosphaeraceae stand out as an example of unusual and specialized coccolith forms that arose in the Cenozoic (Aubry 2009, Young et al. 2009), and modern taxa such as the members of genus *Solisphaera*, with their characteristic flat-bottom hemispherical form made up of at least three distinct coccolith forms, present examples of specialized coccosphere morphology. These remarkable structures beg further investigation into the evolutionary patterns and dynamics of coccolithophorid morphology, which may ultimately follow a different trajectory than their taxonomic richness.

Today, coccolithophores remain a cosmopolitan and ecologically important group of marine phytoplankton, though perhaps the term mixotrophic is more appropriate as there are several documented cases of plausible heterotrophy in this group (e.g. Aubry 2009, Thompson et al. 2012, Hagino 2012). They are found in all ocean basins with some species, like *Emiliania huxleyi,* having a cosmopolitan distribution. Their species richness is highest in warm, low-productivity, open ocean settings and in areas of restricted circulation (Winter et al. 1994). When conditions are favorable, some coccolithophores (r-strategist) can form large blooms in cooler, nutrient-rich waters. The highest mean biomass values are found between 40°S and 50°S in the Southern Hemisphere and 50°N and 60°N in the Northern Hemisphere, declining in both cases towards the poles and equator (O'Brien et al. 2013).

Winter et al. (1994) grouped coccolithophore species into five latitudinal zones encompassing distinct nannofloras associated with the movements of, as they referred to them, major water masses. For example, they note that *Gephyrocapsa muellerae* is common to abundant in the temperate zone and in upwelling waters, but not anywhere else, and *Reticulofenestra sessilis* is found only in the tropical zone (Winter et al. 1994). On the other

hand, some species, such as members of the family Noelaerhabdaceae are abundantly common in both the temperate and tropical zones, displaying a cosmopolitan distribution. The boundaries of these latitudinal zones are neither static nor hard, and while this scheme is useful as a first order pattern, but does not take into account coastal currents, upwelling regions, or other smaller scale oceanographic features, and does not capture water-depth partitioning (Winter et al. 1994).

Further dissimilarity between assemblages stems from the variations in conditions and the history of different oceans even at comparable latitudes. The Atlantic Ocean is recognized as having the highest diversity of coccolithophorid species (Winter et al. 1994), and also the highest mean biomass (~1.7 $\mu g_{Carbon}/L$) (O'Brien et al. 2013). In contrast, the Pacific Ocean, the second most studied ocean with respect to coccolithophores, has a lower nannofloral richness and a mean biomass of 0.3 $\mu g_{Carbon}/L$ (O'Brien et al. 2013), but is subject to distinct seasonal events such as monsoons (Winter et al. 1994). Species and assemblages are further differentiated within each of these basins. There is even some evidence that different morphologies dominate coccolithophorid assemblages at specific habitats (Young 1994), but different morphologies need not correspond to different environments (Quinn et al. 2005).

In summary, coccolithophores are unusual both as phytoplankton and as biomineralizing organisms. Their morphology makes them an ideal system to study, as it links their modern biology and ecology to a rich fossil record in deep time. Furthermore, their planktonic lifestyle offers a contrast and complement to studies of morphological diversity focused on benthic marine fauna and terrestrial fauna.

CHAPTER 2

THE EFFECT OF COCCOSPHERE MORPHOLOGY ON WHOLE-ORGANISM SINKING BEHAVIOR

2.1 Abstract

Many eukaryotic phytoplankton bear morphologically complex mineralized tests. The biological consequences of these structures and their configurations in a laminar fluid environment are poorly understood owing to the difficulties in making field observations, but the fluid-dynamic consequences associated with different morphologies can be tested biomechanically. Sinking experiments utilizing scaled-up physical models of coccolithophores exhibiting three of four basic coccosphere types (placolith, umbelliform, and floriform) reveal a non-linear and non-monotonic relationship of sinking velocity with coccolith size and shape. Stalked coccoliths and other morphologies that extend a plankter's effective surface away from the cell significantly reduce sinking rates and yield lower Stokes radii than forms without such structures. Asymmetric arrangements of coccoliths shift the position of the center of gravity and result in consistent reorientation, with the coccolith mass facing downwards. These experiments demonstrate that the morphology of these minuscule structures and their arrangement can influence the overall fluid dynamics of a cell.

2.2 Introduction

The morphology of plankton, especially mineralized plankton, is generally assumed to affect their sinking behavior (e.g., Smayda 1970). How a cell behaves in the water column and its interactions with the fluid environment have critical ramifications for its ability to remain in favorable environmental conditions. Mineralized structures should generally promote sinking, since such materials are denser than a cell and can constitute a significant fraction of a plankter's weight. The opal in diatoms can be as much as 50% of their dry weight (Strickland 1965), and the weight of a single coccolith can vary anywhere from <5pg to almost 150pg depending on the species (Beaufort 2005). Eppley et al. (1967) observed that unmineralized cells of *Emiliania huxleyi* sink 4.5 times more slowly than normally mineralized cells. However, the effect of this added weight might be reduced by the intricate and ornate nature of planktonic forms, which can impede sinking by increasing drag. For example, removing the protruding chitinous fibers in the diatom *Thalassiosira flurrantitis* increases the sinking rate from 3.8 μm/s to 6.6 μm/s, even though these fibers are denser than other parts of the organism (1495 kg/m^3 vs 1112 kg/m^3) (Walsby and Xypolyta 1977).

Smayda (1970) stressed three key points about the relationship between sinking rate, cell size, and cell surface area. First, for any given shape, larger cells sink faster than small cells, a pattern that holds true across different eukaryotic phytoplankton, and for both actively growing and senescent cells. Second, sinking is controlled by the overall size of a colony, rather than the size of individual colonial cells. Third, the sinking rate of a single cell is inversely related to the surface area to volume ratio. Note, however, that projections, such as setae in diatoms, were not taken into account in Smayda's experiments and that the surface area to volume ratio itself is not size-independent (it has dimensions of L^{-1}).

Although many groups of eukaryotic phytoplankton bear striking ornamentation, coccolithophores exhibit a particularly complex suite of morphologies, especially given their minute size (on average 5-20 μm). Not only do coccolithophores synthesize ornate calcitic scales (known as coccoliths) in many different shapes and sizes, but these coccoliths can be arranged in a variety of configurations on the cell to form tests known as coccospheres. Coccolithophores differ from diatoms, radiolarians, and planktonic foraminifera in that they produce no other extracellular extensions beyond the coccosphere, with the exception of the haptonema and flagella that are present in motile forms. Thus, the coccosphere defines the morphology of the coccolithophore which functionally interacts with the environment.

There have been many proposed functions for coccoliths, in addition to their effect on sinking velocity. The coccosphere creates a physical boundary between the cell and its environment, but whether or not this boundary is advantageous remains unclear. On the one hand, such a layer can buffer a cell against drastic environmental changes, such as salinity changes (Sikes and Wilbur 1982). On the other hand, it can hinder exchange between the cell and its environment, which might be the case for cells that shed most or all of their coccoliths when grown in restricted nutrient conditions (Paasche 2001). Coccoliths might also serve as a barrier to pathogens, but such interactions can be complex. For example, giant phycodnaviruses seem unable to recognize naked haploid cells of *Emiliania huxleyi*, resulting in higher viral loads in the calcified diploid cells (Frada et al. 2008). Indeed, exposure of diploid populations to phycodnaviruses induces a transition to the unmineralized haploid stage, contrary to what might be expected if the coccoliths protect against pathogens.

Another popular – but still unconfirmed – idea is that the elaborate protrusions of many coccospheres serve as deterrents to predation. However, both naked and calcified cultures of *E.*

huxleyi and *Hyemomonas* (now *Pleurochrysis*) *carterae* suffer equivalent copepod grazing pressures (Sikes and Wilbur 1982); moreover, coccospheres frequently occur in fecal pellets of copepods, salps, and other zooplankton (Norris 1997, Roth et al. 1975). It has been suggested that specialized coccoliths could play a role in bacterial harvesting (Aubry 2009), based on some cases of heterotrophy in coccolithophores (Brand 1994), and given that the accumulation of organic matter on coccoliths could result in biofouling (Manton et al. 1984). However, direct evidence for such harvesting is lacking. Thus, although their specific functions are still uncertain, the variety and complexity of coccoliths suggest that they play a notable role in the biology of these organisms (Young 2009).

The function of the overall morphology of the coccosphere has received less attention than that of individual coccoliths, though it is arguably just as important to coccolithophorid biology. Within a given population, the number of coccoliths in a coccosphere varies ontogenetically, with immature cells, characteristic of populations with high growth rates, bearing small coccospheres with few coccoliths of shorter lengths (Henderiks 2008, Gibbs et al. 2013). Young (1994) outlined three distinct coccosphere types – placolith-bearing, floriform, and umbelliform – each with its own characteristic biogeographic patterns and morphology; a fourth "miscellaneous" category is also recognized, encompassing forms that do not have a clear ecological characterization and cannot be grouped with the aforementioned types. These miscellaneous coccosphere types dominate specific environments but are exhibited by multiple phylogenetic groups, suggesting the presence of ecological convergence. Among the distinct types, placolith-bearing taxa are often bloom-forming species, dominant in eutrophic environments (Okada and Honjo 1973), and have been posited as early succession, *r*-selected taxa whose rapid growth would benefit from accelerated sinking (assuming that faster sinking, in

fact, aids in nutrient uptake; Young (1994), following Margalef (1967)). In contrast, taxa with umbelliform-type coccospheres are most abundant in low-latitude oligotrophic waters (Kleijne 1989) and exhibit low abundances in sea floor sediments. These taxa are thought to be late-succession, K-selected taxa, which could benefit from decelerated sinking in order to remain at favorable water depths. Finally, taxa with floriform-type coccoliths are abundant well below the surface mixing zone of the ocean, and should also benefit from reduced sinking in order to retain their position within the deep photic zone.

Disentangling how shape affects sinking behavior can be challenging, especially when working with living organisms. Therefore, we investigate whether these three distinct coccosphere morphologies, which are thought to reflect discrete ecological lifestyles, differ in sinking rates and behaviors using scaled-up physical models in an appropriately scaled, and thus more viscous fluid. These models allow variation in specific features, such as coccolith shape and size, while holding other traits constant, such as cell size and mass. Such experiments reveal the aspects of coccosphere morphology that are most relevant to sinking behavior and thus the specific ways in which that morphology modulates either the velocity or trajectory and orientation of sinking.

2.3 Methods

2.3.1 Reynolds Number Calculations

At their minuscule size, coccolithophores exist in environmental conditions where viscous forces are greater than inertial forces, i.e. low Reynolds number conditions. The Reynolds number is a ratio of the relative magnitude of viscous forces to inertial forces in a fluid, expressed as follows

$$Re = \frac{\rho UL}{\mu}$$

where rho (ρ) is the density of the fluid, *U* is the velocity of the object moving through the fluid, *L* is a characteristic length of the object (in this case the radius), and mu (μ) is the dynamic viscosity of the fluid.

One of the guiding principles of fluid dynamics is the observation that, for two objects of the same shape, equality of Reynolds number implies both identity of force coefficients (e.g. drag coefficient, pressure coefficient, etc.) and identity of flow patterns around the two objects. Knowing the Reynolds number of living coccolithophores allows us to create a physically valid scaled experiment by offsetting the change in the object's size with a corresponding change in the viscosity of the fluid. Based on the data reported in Smayda (1970) (Table 2.1), living coccolithophorid cells exist at Reynolds numbers of ~10^{-5}. In order to build larger physical models for ease of observation and construction, we offset this increase in size by substituting a more viscous fluid for sea water, namely Karo® Light Corn Syrup, a complex solution of sucrose and other sugars (Table 2.2). Fluid flow is completely laminar below a Reynolds number of ~10^{-1} (condition generally referred to as creeping flow or Stokes flow), and there generally are minimal differences in flow patterns between different Reynolds number values below this threshold. Our models operate at a Reynolds number of 10^{-2} (Table 2.1; also see Appendix A for detailed calculations and parameters). Although extrapolating from these experimental values to quantify daily sinking rates would not be meaningful or realistic, we are confident that both the patterns of sinking and relative sinking rates are realistic and informative, because the experiments are still at creeping flow conditions.

Table 2.1. Reynolds number calculated for the models herein, and for the taxa reported in Smayda (1970), which exhibit a placolith-type morphology. See Appendix A for the parameters used in these calculations. Selection of representative taxa based on the similarity of coccolith size relative to coccosphere size, as opposed to absolute coccolith diameter.

Model/ Observation	[Representative] taxon	Characteristic length (radius) in meters	Reynolds number	Empirical Mean sinking rate(m/day)
Floriform	*Florisphaera profunda*	13.5×10^{-3}	3×10^{-2}	NA
Umbelliform	*Discosphaera tubifera*	13.5×10^{-3}	2×10^{-2}	NA
Small placoliths	*Reticulofenestra parvula*	5.7×10^{-3}	2×10^{-2}	NA
Medium placoliths	*Gephyrocapsa ericsonii ericsonii*	5.7×10^{-3}	2×10^{-2}	NA
Large placoliths	*Emiliania huxleyi var. corona*	5.7×10^{-3}	1×10^{-2}	NA
Smayda (1970)	*Cricosphaera elongata*	16×10^{-6}	4×10^{-5}	0.25
Smayda (1970)	*Coccolithus huxleyi* (calcified)	5×10^{-6}	8×10^{-5}	1.4
Smayda (1970)	*Coccolithus huxleyi* (naked)	4×10^{-6}	1×10^{-5}	0.27
Smayda (1970)	*Cyclococcolithus fragilis* (smallest palmelloid)	20×10^{-6}	3×10^{-3}	13

2.3.2 Stokes radii calculations

Because our models differ strongly in shape and have different masses, especially in the case of the umbelliform model, a more appropriate measure for comparison would be to compare their Stokes radii, i.e. the radius of a theoretical sphere of the same mass and terminal velocity as the object of interest. We applied equation 15.12 in Vogel (1994), and equation 11.2 in Vogel (2006), specific to low Reynolds number conditions.

Eq. 15.12 $$mg - \frac{4}{3}\rho_f g\pi a^3 = 6\pi\mu a U$$

Eq. 11.12 $$\frac{mg}{6\pi\mu a} = \frac{2a^2 g(\rho_0 - \rho_f)}{9\mu}$$

where m is the mass of the model (and the theoretical sphere of interest), g is the acceleration due to gravity (9.8 m/s^2), U is the observed terminal velocity, μ is the dynamic viscosity of the fluid, a is the Stokes radius [of the theoretical sphere], ρ_0 is the density of the sphere, and ρ_f is the density of the fluid. To use equation 15.12, one needs to measure the mass and terminal velocity of the object of interest (Vogel 1994). However, when buoyancy is significant, mass can be substituted for the product of the volume of the theoretical sphere and the excess density between the sphere and the surrounding fluid (Vogel 2006), as in equation 11.2. Empirical model volumes used herein are based on the weight difference from the model suspended in water and when suspended in air. This methodology was susceptible to mass loss resulting from the incidental boiling of some of the water when under vacuum, and so this high variability (Appendix A) resulted in higher standard errors when applying equation 11.2 (Figure 2.4). Vacuuming was employed in order to be certain that no air bubbles were trapped in the bead, which would significantly throw off density estimates.

Computational calculations were carried out in R using the optimize() function (R Core Team 2015), and cross-verified in Mathematica using the Solve[] function (Wolfram Research Inc. 2016). The Stokes radii are presented both with units (Table 2.3) and as dimensionless values that are thus size-independent (Table 2.3; Figure 2.5). In the latter case, the resulting Stokes radii are divided by the actual radius of the model and can be read as a proportion of the actual radius, for example, with a dimensionless Stokes radius of 0.34, the model is comparable to a theoretical sphere that is 34% of the model's actual volume. Although dimensionless Stokes radii generally fall between 0 and 1, it is nonetheless possible to have values that are greater than 1. The length measurement presented as the actual radius of the floriform model yields a

dimensionless Stokes radius greater than 1 because it is the radius at the widest circumference of the hemisphere of coccoliths. Similarly, the length presented as the actual radius of the umbelliform model is based on the widest circumference of the model (stalked coccoliths included). These actual radii reflect the size of the area that would realistically interact with the fluid environment better than the length of the central portion of the models (see next section).

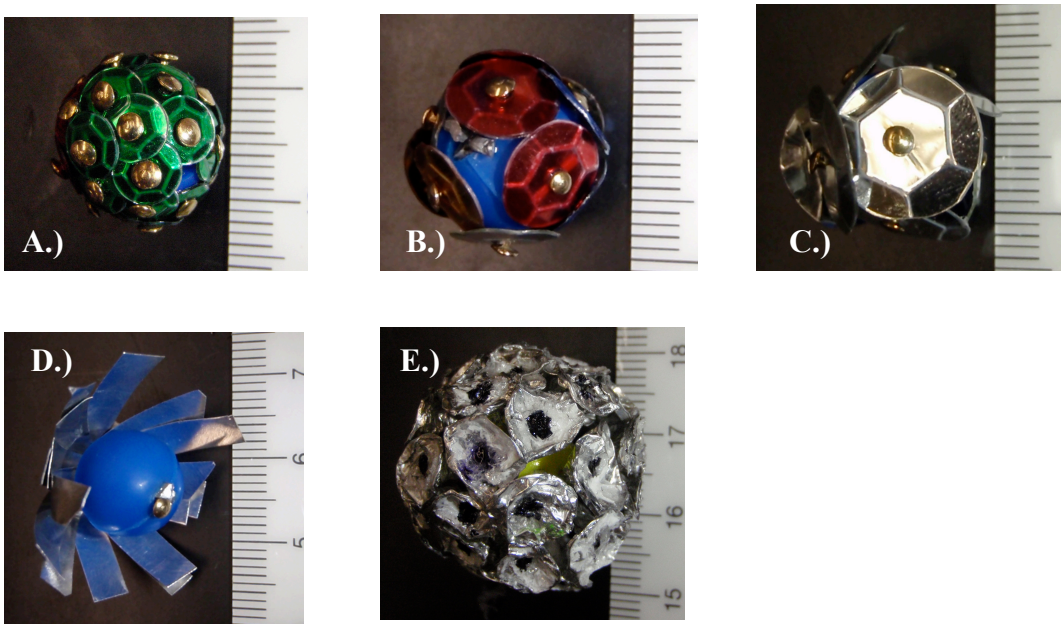

Figure 2.1. Coccosphere models Physical models used in sinking experiments. A.) Placolith model with small coccoliths. B.) Placolith model with medium coccoliths. C.) Placolith model with large coccoliths. D.) Floriform model. E.) Umbelliform model.

2.3.2 Coccolithophore Model Construction

We recreated Young's (1994) three distinct coccosphere types using spherical rubber beads (diameter of 11.5 mm) as the base 'cell' of our coccolithophore, to which were added shortened steel dress-making pins as anchors for model coccoliths (Figure 2.1) of a variety of materials (see below). The rubber beads were chosen because they resisted deformation during pin insertion and were of lower density than our model coccoliths, which were aluminum and/or

plastic. The mean mass of all model types was 2.17g (± 0.0054g (1SE)), excluding the umbelliform model and the extended placotlith model (described at the end of this section), which has a mass of 4.20g (discussed below). Because it was critically important to have the same mass across all models, we added a small amount of lead to the center of the bead of each model to bring the mass of each model to 2.17g. Adding mass to the center of the models minimally interferes with the position of the center of gravity, so we believe the models are reasonable approximations of the living cells, since the majority of the mass is distributed on the outer surface of the cell and models.

Placolith-type coccospheres, exhibited by such taxa as *Emiliania huxleyi, Calcidiscus leptoporus,* and *Umbilicosphaera sibogae,* consist of coccoliths bearing two shield-like structures connected by a central tube. These coccoliths slide into one another and interlock to form a tight sphere around the cell (Figure 2.1A–C). We used plastic sequins of three different sizes (5 mm, 8 mm, and 10 mm diameter) to model placolith coccoliths and determine the effect of coccolith diameter on sinking behavior. The final coccosphere radius for all versions of the placolith model was 5.75 mm, with mass ranging from 2.16g to 2.18g (Appendix A).

Umbelliform coccospheres, such as exhibited by *Umbellosphaera tenuis, U. irregularis,* and *Discosphaera tubifera*, are grossly spherical, but their coccosphere is formed by stalked and flaring coccoliths, resembling trumpet bells, that project some distance out from the cell's surface to form a second layer of calcite, separated from the underlying cell largely by seawater (Figure 2.1E). We used aluminum foil to create the flaring trumpet bells on the ends of steel dress-making pins (total of 43), and secured the flared bells to the pins using cyanoacrylate glue. These stalks were roughly 6 mm in height; the overall diameter of the model was 25 mm. Each

individual umbelliform coccolith weighed more than a given placolith coccolith, due to the large amount of metal used, so the final mass of the model was 4.20 g.

Floriform-type coccospheres, exhibited by such deep-photic zone taxa as *Florisphaera profunda* and *Gladiolithus flabellatus,* have an asymmetric arrangement of polygonal coccoliths concentrated at one end of the cell, leaving a naked opening at the other pole (Figure 2.1D). This model was constructed by overlapping relatively rigid aluminum strips, which were attached to the rubber bead at a single point using a clipped dressmaker pin. These strips were able to slide over one another; experimental drops in which the strips failed to maintain the desired full hemisphere were disregarded. The maximum diameter of the floriform model was 27 mm and its mass was 2.16 g. In corroborative experiments, a small counter weight of the same mass as the aluminum coccoliths was added in order to evaluate the effect of the position of the center of gravity on the model's sinking dynamics (see section 2.5.2 in the discussion).

Lastly, we created a model much like the large placolith model in mass and construction, but with the plastic sequins on longer pins, to evaluate whether simply extending the coccoliths at a distance from the coccosphere is sufficient to produce a similar sinking behavior as was observed in the umbelliform model. This model had a radius of 25mm and a mass of 2.15g.

2.3.5 Experimental Tank Set-Up

The drop-tank was a glass vessel 29.2 cm in diameter and 42 cm in height, filled with approximately 7 gallons (~27L) of Karo® Light Corn Syrup (Figure 2.2). The large diameter (>20 body lengths) of the drop-tank minimized wall effects and allowed the models to reach terminal velocity well before the middle 10 cm of the tank, where we recorded observations and settling velocities. Models were released through a single hole in the lid of the tank and fell down

the center of the tank, with the vertical plane of observation defined by a laser sheet (Lasiris Inc Magnum SP 750 mW laser sheet generator). Each model was dropped a minimum of ten times (Appendix A). Runs wherein models sank off-center from this vertical plane were disregarded and not counted as part of the ten run minimum. Minute, naturally occurring bubbles acted as flow tracers and allowed us to visualize flow patterns as the model moved through the fluid. Settling velocities were calculated based on the time to traverse a 10cm section in the middle of the tank; this allowed sufficient space for the model to reach terminal velocity and still be well above the bottom of the tank, so as to reduce wall effects. Video was taken for three of the runs of each model, using a high definition camera (stills from videos shown in Figure 2.5). Observations were conducted at two different points in the year (March and September 2013) and so the fluid properties for the Karo syrup at these two different times are presented below in Table 2.

Fluid	***Density (kg/m^3)***	***Dynamic viscosity (kg/m•s)***
Karo syrup @ 23°C (3/5/ 2013)	*1362*	*3.689*
Karo syrup syrup @ 23°C (10/7/2013)	*1339*	*4.141*
Seawater @ 20°C	*1024*	*0.001072*

Table 2.2. Properties of Karo syrup used in experiment. Ambient temperature was 23°C throughout the duration of the experiments. We use the seawater properties reported in Vogel (1994) Table 2.1 as a scaling baseline for these experiments.

2.3.6 Data Analysis

The aforementioned fluid mechanical calculations were conducted in Mathematica (Wolfram Research Inc. 2016), Microsoft Excel (2016) and R (R Core Team 2015). We used a

one-way ANOVA test to compare the mean sinking velocities among the placolith bearing models, followed by a Tukey's Honest Significant Difference test, and evaluated the effect of coccolith size. Both were conducted using the MASS package in R (R Core Team 2015). Additional statistics, e.g standard deviations, were obtained using built-in functions in Microsoft Excel and from the MASS and stats package in R (R Core Team 2015). The datasets utilized in this chapter are included as Appendix A.

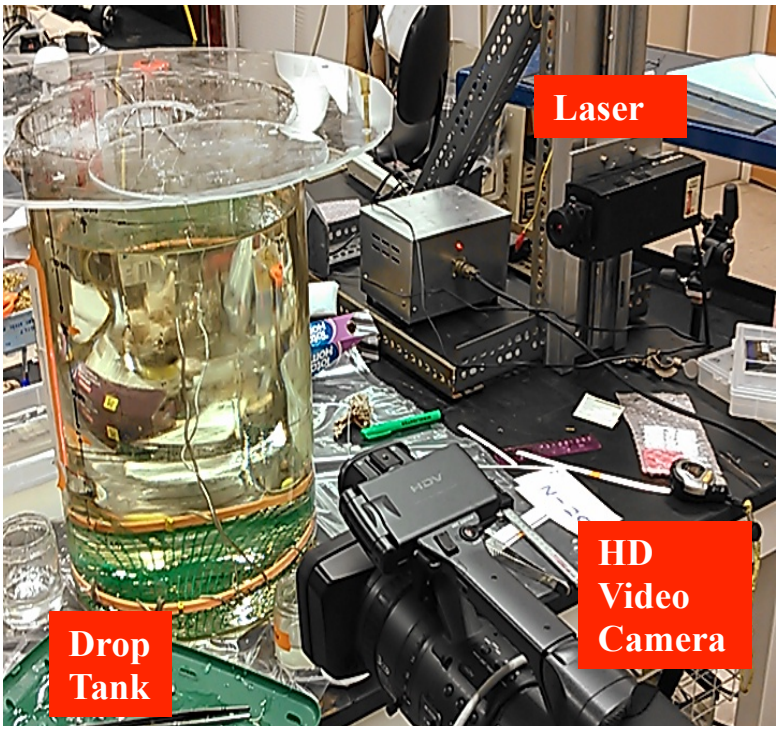

Figure 2.2. Experimental tank set-up, featuring tall cylindrical glass tank, laser field set-up, and high definition camera.

2.4 Results

2.4.1 Comparing sinking velocities

When comparing variants within the same coccosphere type, in this case the placolith-type morphology, the effect of coccolith diameter on sinking speed is non-monotonic

and non-linear (Figure 2.3A). The mean sinking velocities for the different models are significantly different from one another as determined by one-way ANOVA test (Figure 2.3B; $F(2,24.6)=207.31$, p-value << 0.001). The model with medium-sized coccoliths (coccolith diameter=8 mm; average $U = 0.010 \pm 0.0004$ m/s (1 SE)) sank faster than the model with large coccoliths (10 mm, $U = 0.0076 \pm 0.0003$ m/s (1 SE)) (Figure 2.3B; Tukey Honest Significant Difference= 0.0027, adjusted p-value ~0.00), but only marginally faster than the model with smaller coccoliths (coccolith diameter= 5 mm; average $U = 0.0095 \pm 0.0005$ m/s (1 SE)) (Figure 2.3B; Tukey Honest Significant Difference= -0.00086, adjusted p-value <<0.001). The model with the small-sized coccoliths (5 mm) sank faster than the model with large coccoliths (8mm) (Figure 2.3B; Tukey Honest Significant Difference= 0.0018, adjusted p-value ~0.00).

Comparing between different coccosphere types, the floriform coccosphere model has a mean observed sinking velocity ($U = 0.0077 \pm 0.0006$ m/s (1 SE); ~0.29 diameters/second) which is comparable to the placolith models. However, the umbelliform model has much slower mean observed sinking velocity ($U = 0.0053 \pm 0.0004$ m/s (1 SE); ~0.21 diameters/second).

When comparing all of the models using their calculated Stokes radii (Table 2.3), the floriform and umbelliform models have the smallest dimensionless Stokes radii (Figure 2.4), irrespective of which equation is used. The placolith bearing models have larger Stokes radii, which are closer in value to the model's actual radii (Table 2.1). When using equation 15.12, which explicitly includes the observed sinking velocities, the pattern is concordant with the results of the direct sinking velocity comparison (Figure 2.3A); the medium sized placolith model has the fastest sinking velocity and also the smallest Stokes radius, followed by the small placolith model, and lastly the large placolith model. When using equation 11.2, the small-sized

placolith model has the smallest Stokes radius, followed by the medium-sized placolith model, and finally the large-sized placolith model.

2.4.2 Comparing sinking behavior

The pattern of motion of a cell as it moves through a fluid may be just as important as its sinking velocity, and so we also compared the sinking trajectory and behavior of the different coccosphere models (see Figure 2.5). All placolith models moved through fluid swiftly and resembled a sphere moving through an ideal fluid (Vogel 1994, 2006): these models maintain a single orientation (no rotation or spinning) and minimally disturb the surrounding fluid, that is, the fluid separates in front of the model and reunites behind it without any recirculation, such as eddies or a wake. The umbelliform model also behaves much like a sphere moving through an ideal fluid, sinking in a straight trajectory without recirculation behind it, but it sinks more slowly than the placolith models. In contrast, the floriform model quickly reorients as it sinks so that the coccolith end of the model faces the direction of oncoming flow (i.e., orients in the direction of gravity).

Model	Mean Stokes Radius (dimensionless)	Standard Error	Mean Stokes Radius (meters)	Standard Error
Floriform (Vogel 1994)	**0.283**	0.114	**0.00383**	0.00154
Floriform (Vogel 2006)	**0.503**	0.0024	**0.00679**	3.24E-05
Small placolith (Vogel 1994)	**0.825**	0.254	**0.00474**	0.00146
Small placolith (Vogel 2006)	**1.164**	0.00530	**0.00679**	3.05E-05
Medium Placolith (Vogel 1994)	**0.8958**	0.380	**0.00515**	0.00219
Medium Placolith (Vogel 2006)	**1.150**	0.00498	**0.00661**	2.86E-05
Large Placolith (Vogel 1994)	**1.716**	1.515	**0.00986**	0.00871
Large Placolith (Vogel 2006)	**1.181**	0.00289	**0.00679**	1.66E-05
Umbelliform (Vogel 1994)	**0.725**	0.00147	**0.00907**	0.00186
Umbelliform (Vogel 2006)	**0.704**	0.00236	**0.00880**	2.948E-05

Table 2.3. Stokes Radii for all models, presented as dimensionless radii and radii in meters.

2.3.A)

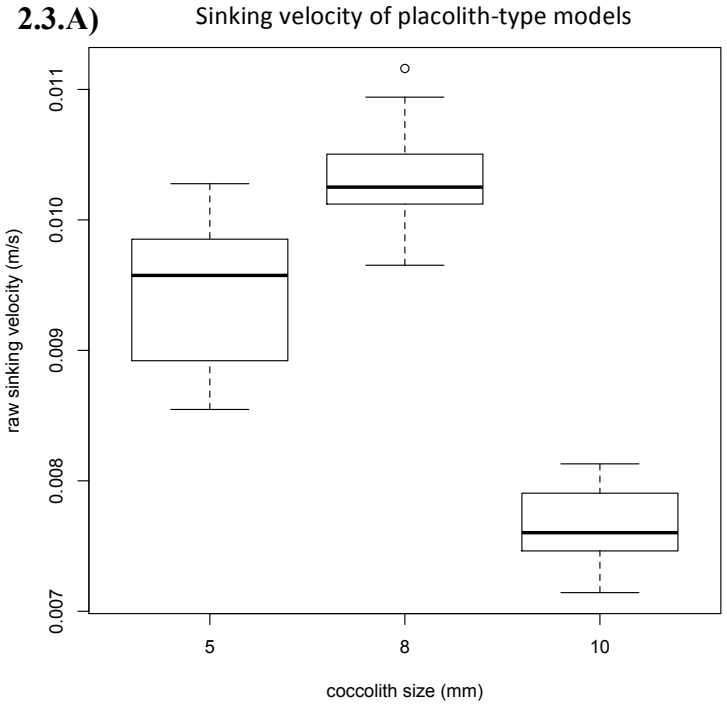

2.3.B)

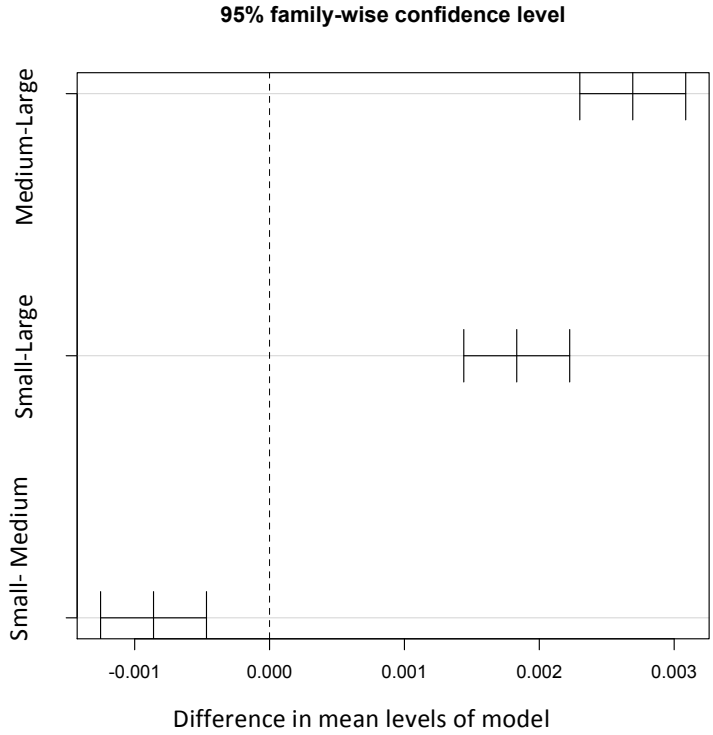

Figure 2.3. Comparison of terminal sinking velocity of placolith models. A.) Boxplots of raw sinking velocities by model. B.) 95% Confidence level for pairwise comparisons using Tukey's Honest Significance Tests, ANOVA $F(2,24.6)= 207.31$, p-value << 0.001.

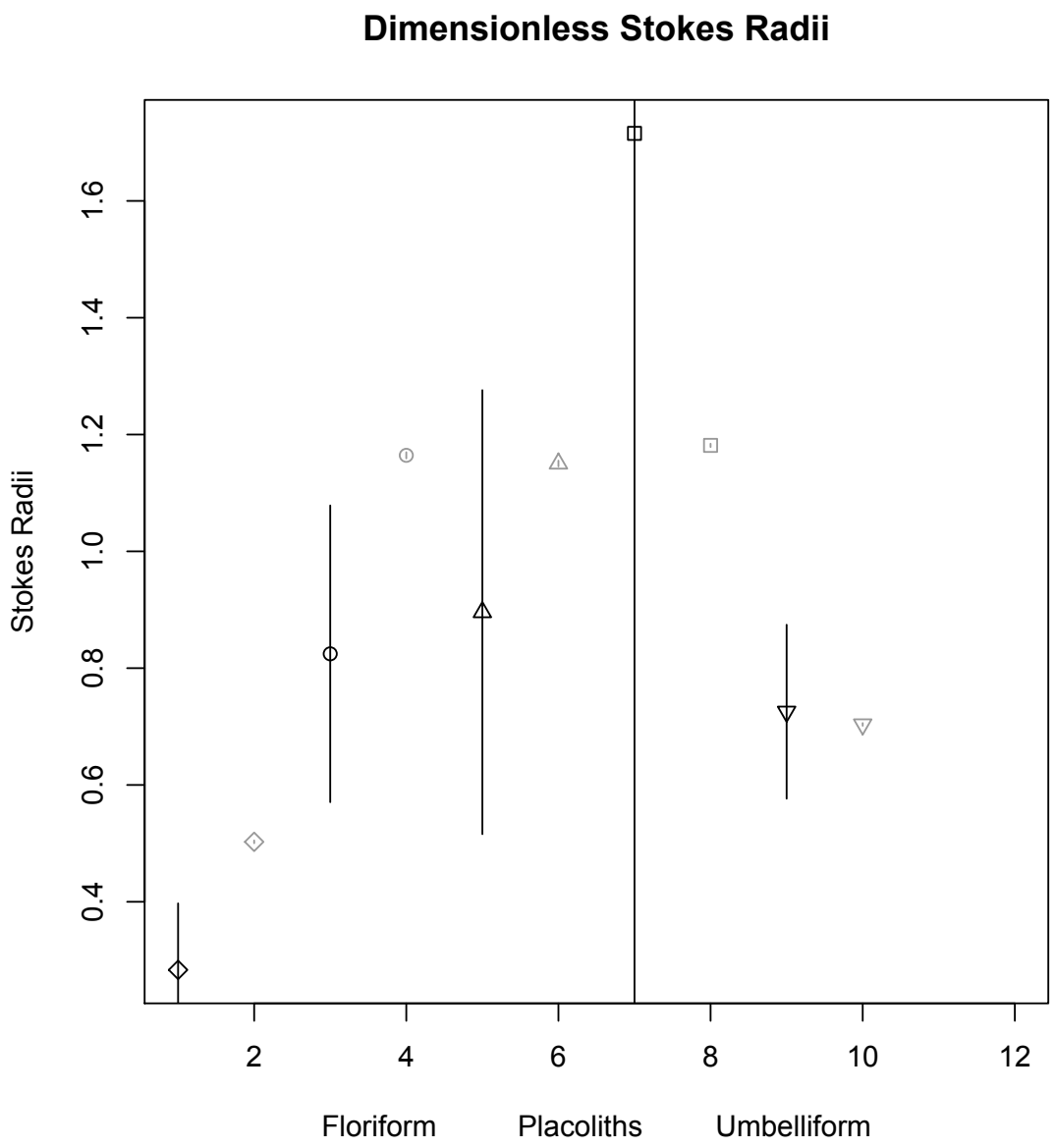

Figure 2.4. Dimensionless Stokes radii for all models. Error bars (small dash inside point) represent the standard error. Values calculated using equation 15.12 in Vogel (1994) are represented in black. Values calculated using equation 11.2 in Vogel (2006) are represented in gray. Floriform model radii = open diamonds, small placolith model radii = open circles, medium placolith model radii = right-side up triangles, large placolith model radii = open squares, and umbelliform model radii = up-side down triangles.

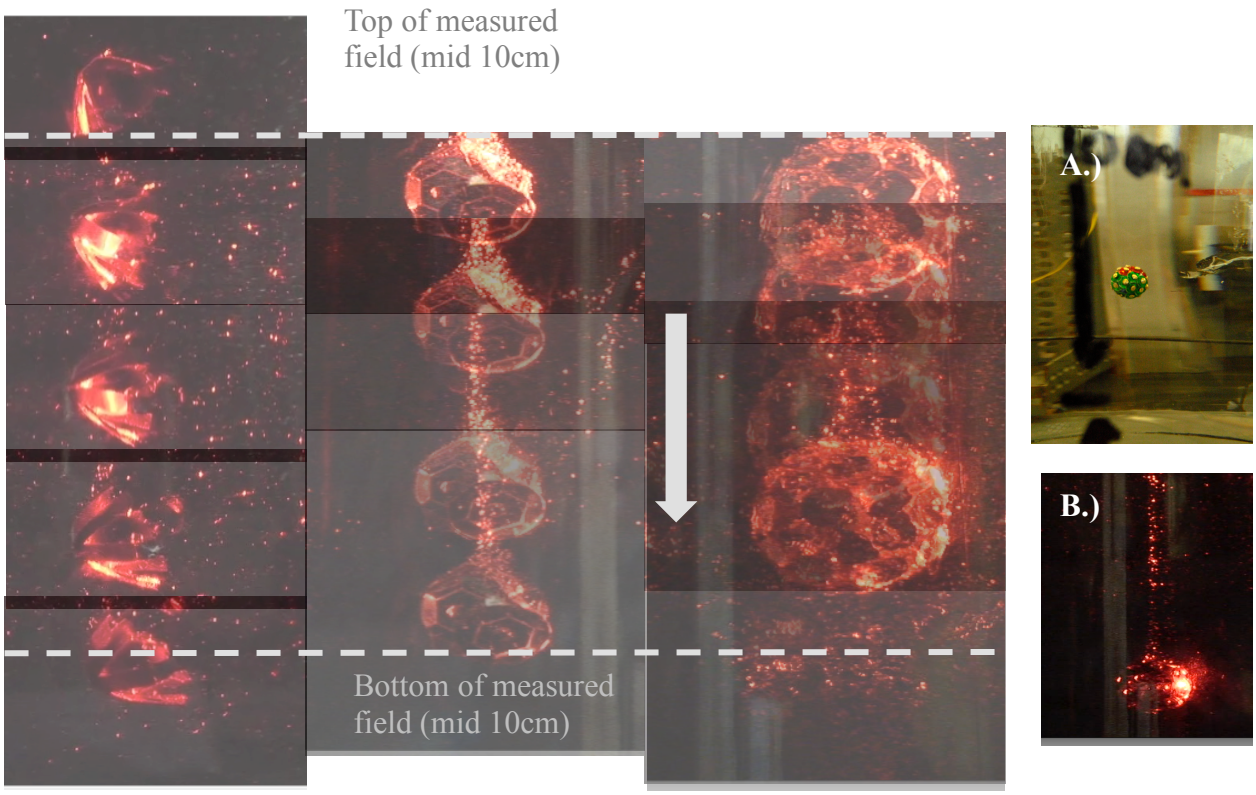

Figure 2.5. Photo overlay of sinking time steps for the floriform model, large placolith model, and umbelliform model. Images are taken 3 seconds apart. The dashed lines represent the top and bottom of the middle 10cm of the tank, used for sinking velocity observations. Grey arrow indicates the direction of motion for all models. All models shown are illuminated by laser sheet; inset A.) model illuminated by ambient light, B.) same model illuminated by laser sheet.

This behavior occurs quickly (within two model diameters) and consistently regardless of the initial orientation of the model, suggesting that an asymmetric arrangement of coccoliths can be used to maintain a specific orientation in the water column.

2.5 Discussion

2.5.1 The Realism of these Experiments

All of our models operated at a Reynolds number of approximately 10^{-2}, and so comparisons of sinking behavior and relative sinking velocities among models are valid. Given that the experimental Reynolds number is greater than that of living cells, the daily sinking

velocities that we would extrapolate are much higher (158.9 m/day to 518 m/day) than those reported from laboratory observations by Smayda (1970) for isolated coccolithophorid cells and the smaller palmelloid cells of *Cyclococcolithus* [now *Oolithotus*] *fragilis*. Nonetheless, the relative differences in sinking rate among our models reflect real disparities in behavior and the patterns are likely to hold at much lower Reynolds numbers.

A key factor in recreating realistic morphology, specifically with respect to the center of gravity and moment of inertia of coccospheres, is the relative difference in density between a cell and its coccoliths, which we prioritized over recreating an exact Reynolds number. Aluminum has approximately the same density (2700 kg/m^3) as calcite (2710 kg/m^3), and so this difference is reasonably recreated in our models. Thus, the observed reorientation of the floriform model resulting from the polarization of weight towards a single pole of the cell, is likely also realistic. However, the density of the rubber beads used was lower than that of water so the density difference of these components may be more pronounced than the difference seen in living cells.

2.5.2 Fluid Mechanically Important Features of Morphology

Among the array of coccosphere types tested here, coccolith size and shape are important in determining sinking velocity, but disentangling the specific effects of each is not straight-forward. Consider the floriform model, with its distinct polygonal coccolith morphology. Its Stokes radius is similar in raw value to the raw values of the Stokes radii of the placolith models (Table 2.3), suggesting that its sinking rate is comparable to that of the other morphologies. However, the dimensionless Stokes radius of the floriform model is significantly different, which suggests that for its size, the model is actually sinking slower than the placolith models. The umbelliform model has a larger raw Stokes radius than all of the other models suggesting a faster

sinking rate. However, when we consider the size-independent value (i.e. dimensionless), its Stokes radius is smaller than those of the placolith models, but not as small as the floriform model (Figure 2.5). This reasoning suggests that, despite the floriform model's increased mass, the increased surface area away from the cell resulting from the stalked nature of the umbelliform coccoliths may be increasing drag and slowing its settling velocity.

To further explore this, we built an alternative version of the large placolith model, with its coccoliths stilted on longer pins so that they are elevated ~1cm from the rubber bead base (same sequins of 10 mm-diameter, same coccolith count (8), and similar mass of 2.15 g). This caused its sinking rate to slow to 63% of that for the model with the coccoliths flushed (0.002 m/s versus 0.006 m/s). Because this study is only preliminary and confirmatory we did not have as many replicates as with the other models, and because it was done years later, the properties of the test Karo syrup have changed enough to require reevaluation. It is plausible that the non-monotonic relationship between sinking rate and coccolith size exhibited by the placolith models (Figure 2.3A) is attributable to an increase in surficial irregularity of the models but that quality is difficult to quantify and so we cannot draw definitive conclusions on this matter.

Coccolith size and shape do not appear to affect the sinking trajectory of a cell: the placolith models and the umbelliform model, which have different coccoliths, are all fundamentally spherical in coccosphere morphology and maintain a constant orientation while sinking in a straight path. In contrast, the asymmetric, non-spherical floriform coccosphere does play a role in determining the trajectory of sinking; this asymmetrical model reorients so that the mass of coccoliths lies below the center of gravity. Coccosphere asymmetry, a trait that is present in multiple, phylogenetically distant taxa, is thus evidently an effective way to establish and maintain a particular orientation in the water column. Taxa such as *Syracosphaera pulchra*

derive their asymmetry from the overall arrangement of otherwise identical coccoliths, whereas other taxa such as *Pappomonas weddellensis* derive their asymmetry from specialized coccoliths of differing shapes.

From these experiments alone, it is unclear whether the reorientation of the floriform model results from the poleward shift in the center of gravity or from the anisotropy of the shape. An anisotropic shape will tend to rotate as it moves through a fluid and finds a hydrodynamically stable orientation, whereas isotropic shapes will maintain their starting orientation (Vogel 1994). To disentangle these effects, we conducted two follow up experiments; as with the alternate placolith model, these experiments are preliminary in that they do not have as many replicates as the rest of the experiments presented here and were conducted years later. In the first, we changed the model's center of gravity by adding a counter weight of the same mass as the coccoliths at the opposite pole; if the reorientation is due to the position of the center of gravity, this modification, which shifts the center of gravity away from the coccolith pole, would hinder the reorientation. In the second experiment, we removed most of the asymmetry in shape (center of mass unchanged in position) by binding the coccoliths flush against the surface of the central bead; if the reorientation is due to the position of the center of gravity and not the hydrodynamics of the shape, then the bound model would still reorient

We found that, when the model with a counter weight is dropped in Karo syrup it reorients so that the axis connecting the coccolith pole and the counter-weight pole is nearly perpendicular to the direction of gravity (i.e. weighted poles point left and right), regardless of coccoliths being splayed or bound. When the model is dropped without the counter weight and bound, the model reorients with the coccolith pole pointing downwards. These results suggest that at low Reynolds numbers, reorientation is more strongly affect by the position of the center

of gravity than simply the asymmetry in shape, although the latter could offset the center of mass and result in reorientation.

2.5.3 Linking morphology and ecology

These experiments demonstrate that these coccosphere types, differentiated by the shape of constituent coccoliths and their arrangement around the central cell, interact in significantly different ways with the fluid environment and could thus potentially constitute different ecological groups, as suggested by Young (1994). As might be predicted from their tighter coccospheres, placolith-type coccospheres sink at faster rates than umbelliform-type coccospheres. Floriform-type coccospheres have a much slower sinking rate than the other shapes, and their tendency to reorient might promote photosynthetic activity (Gartner & Bukry 1969), allowing light direct access to the cell through the naked pole while the mass of coccoliths may refract ambient light back to the cell because the index of refraction of calcite is higher than that of water. Our experiments addressed only the sinking rates and sinking behaviors of cells; other experiments are required to evaluate the photosynthetic utility of particular shapes and sinking orientations.

Some of the morphological characters we examined show intriguing biogeographic patterns, hinting at large-scale ecological importance. For example, large coccoliths are more prevalent at high latitudes (Saez et al. 2003, Geisen et al. 2004, Herrmann et al. 2012a), a pattern that seems to hold true for the entire Cenozoic (Herrmann et al. 2012b). Bear in mind that coccolith size is closely tied to cell size, which changes ontogenetically and in response to growth (Henderiks 2008, Gibbs et al. 2013). Although coccolith size clearly influences sinking, these other physiological traits may be stronger drivers of environmental sorting. Our results

address the consequences of morphology and can help constrain potential ecology but are of course not the whole story.

It is important to keep in mind that how morphotypes differ hydrodynamically is critical in assessing the potential for the ecological groupings in Young (1994), and that not all morphological variation will sort spatially. Although *Florisphaera profunda var. profunda, F. profunda var. elongata,* and *F. profunda var. rhinocera* differ in the shape of the anterior edge of the body coccoliths, and although natural populations in the Indian Ocean exhibit different modal coccolith sizes, the three morphotypes co-occur at the same depths and both *Florisphaera profunda var. profunda* and *F. profunda var. elongata* occur in high abundances (Quinn et al. 2007). The overlap in mean coccolith sizes and the fact that the overall coccosphere size does not vary greatly may preclude spatial sorting of morphologies in this species, at least as far as we can tell based on the likely effects of that morphology on sinking.

2.6 Conclusions

We demonstrate that different coccosphere morphologies can play an important role in the sinking behavior of a coccolithophore, either by changing surface area and thus changing drag and the sinking velocity, or by altering the center of mass and thus hydrodynamic properties to alter the orientation of the cell. These different forms could differentiate ecologically on the basis of these effects, although many other aspects of their biology were not considered in this study (e.g. metabolism and life history strategies). In order to understand coccolithophorid ecology and biogeographic patterns, we need to understand the consequences and trade-offs related to different traits. Starting from first principles, as we have done here, can help constrain the potential biological importance of different forms and identify fruitful avenues of research.

CHAPTER 3

THE LACK OF BIOGEOGRAPHIC STRUCTURE OF COCCOLITHOPHORID MORPHOLOGICAL DIVERSITY IN MODERN OCEANS

3.1 Abstract

Although taxonomic diversity, often reported as species richness, is spatially partitioned on the globe, there is limited evidence that morphological diversity has an analogous global structure among major groups of marine invertebrates and flying terrestrial vertebrates. Although surface temperatures are important to the biology of heterotrophs, they are on or more trophic levels further removed from the effect of insolation than their ultimate food source, primary producers, which might exhibit a stronger spatial structure. I investigate whether morphological diversity in coccolithophores, a major group of eukaryotic phytoplankton, is spatially structured in the world's oceans. Analysis of 76 characters shows invariant morphological diversity across latitudes and biomes, yielding similar values of mean pair-wise distances and similar suites of morphologies. Polar latitudes can be differentiated from other latitudes when analyzed using canonical variates analysis (CVA), but both latitudes and biomes remain indistinct from one another in principal coordinate space (PCO). Regions are also indistinguishable when conducting pair-wise comparisons using linear discriminant analysis (LDA) with shared species excluded, suggesting that the high degree of homogeneity may instead result from the near-cosmopolitan extent of families. This finding suggests that the geographic distribution of morphologically distinct clades, i.e. families, is more influential than species' distributions in establishing large-

scale spatial structures of morphological diversity in coccolithophores. Similar considerations regarding the dispersal potential of those taxonomic units that encompass distinct morphological suites should be applied when studying such patterns in other organisms.

3.2 Introduction

3.2.1 The ubiquity of global diversity gradients

The latitudinal diversity gradient characterizes so many biological groups that it has been dubbed Earth's first-order biodiversity pattern (Willig *et al*. 2003; Hillebrand 2004; Krug *et al*. 2009). In general, the number of species and higher taxa decreases from the tropics to polar latitudes, reflecting a gradient of insolation and temperature, although in some cases, the trend is inverted or the peak is otherwise shifted away from the tropics (Willig *et al*. 2003). Taxonomic richness has also been shown to follow other spatio-environmental gradients such as altitude (Stevens 1992), water depth (McClain & Etter 2005), and nutrients (Bedford *et al*. 1999). In contrast to species richness, it is not yet clear whether morphological diversity, also termed morphological disparity, shows a similar biogeographic structure (Table 3.1).

Several studies have focused on the spatial patterns of selected characters thought to be functionally and thus ecologically important, such as cell size and body size or mass (Hillebrand 2004, San Martin *et al.* 2006, Barton *et al*. 2013, but see Roy & Martien 2001). However, functional diversity is not the same as morphological diversity, as the latter includes aspects of morphology that are non-adaptive or for which a function is unknown and so encompasses multiple biological signals and tradeoffs. While functional traits may exhibit latitudinal trends, morphological diversity need not follow suit; more congruency between functional diversity and

morphological diversity can be observed when traits are optimized for a single function, but this is rarely done since a given body part often serves multiple purposes (see Wainwright 2007).

3.2.2 On Regional Morphological Diversity

Studies focused on the geographic patterns of disparity for a single clade mostly find that different regions can harbor different amounts of disparity, but there is mixed support for a salient latitudinal or environmental gradient (Table 3.1). For example, gastropods in the family Strombidae demonstrate no clear spatial structure in mean disparity, a pattern that is indistinguishable from that obtained through random sampling (Roy *et al*. 2001). Their heterogeneous pattern of morphological diversity is also largely incongruent with the distribution of species richness, which peaks in the tropical shelf environments in the Philippines and New Guinea and radiates outward to the rest of the Indo-Pacific (Roy *et al*. 2001); species-poor areas, such as the 20°x20° cell just south of Madagascar, can express the same mean disparity as species-rich areas, such as the 20°x20° cell that includes the Java Sea (Roy *et al*. 2001). Similarly, corals in the genus *Porites,* whose taxonomic richness radiates out from Southeast Asia into both the Indian and Pacific Oceans, also lack a clear spatio-environmental pattern, which may be a result of phyletic or ecological limits on morphological diversity (Mohedano-Navarrete *et al.* 2008). When the Pacific Ocean is treated as a separate entity from the Indian Ocean, values of disparity become more similar, further reducing the effect of latitude (tropical vs subtropical) and hemisphere (Northern versus Southern) (Mohedano-Navarrete *et al.* 2008).

Authors	System	Taxonomic level	Geographic scale	richness correlates to disparity?	Evidence for latitudinal gradient in disparity?	Evidence for environmental gradient in disparity?
Roy et al. 2001	Marine snails (Strombidae)	82 species from one family	Indo-Pacific ocean (20°x20° long/lat cells)	Most, no	No, in all regions mean disparity is similar	NA
Mohedano-Navarrete et al. 2008	Corals (*Porites*)	52 species from one genus	Indo-Pacific ocean (20°x20° long/lat cells)	No	No, all regions mean disparity is similar	NA
Neige 2003	Cuttlefish (Sepidae)	160 species from one family	Continental shelf area in Eastern hemisphere	No	No relationship with latitude or longitude	NA
Ricklefs 2012	Continental birds (Passeriformes)	>6,000 species in one order	11 biogeographic regions	No	No	No
Jønsson et al. 2015	Continental birds (Passeriformes)	1329 species from one order (divided into 4 subclades)	4 biogeographic regions (Neotropics, Australasia, Afrotropics, Orient)	No	NA	No, average size and shape variation is invariant.
McClain 2005	Deep sea snails	76 species in 8 families	Bermuda, 196m-5042m	No	NA	No, comparable disparity when rarefied
McClain et al. 2004	Deep sea snails	37 species in multiple families	5 lower bathyal and 5 abyssal samples in North Atlantic ocean	Mixed	NA	Non-linear correlation (summed range) over depth, but similar average dissimilarity
Villalobos & Arita 2014	Neotropical bats (Chiroptera)	101 species in 8 families	Nested cells (4°x4° to 0.5°x0.5°) in Tehuantepec, Mexico	No	NA	No, morphospace volumes invariant and similar to null model
Villarosa Garcia (this study)	Nannoplankton (Coccolithophores)	104 species in 14 families	34 Pelagic provinces in all oceans	No	No, similar disparity values and morphospace volumes	No, invariant disparity values and morphospace volumes

Table 3.1. Summary of previous studies focusing on spatio-environmental patterns of morphological diversity.

When the Pacific Ocean is treated as a separate entity from the Indian Ocean, values of disparity become more similar, further reducing the effect of latitude (tropical vs subtropical) and hemisphere (Northern versus Southern) (Mohedano-Navarrete *et al.* 2008). Studies focused on ecological assemblages similarly find minimal support for a spatio-environmental structure to regional morphological diversity (Table 3.1). For example, mean disparities in deep-sea gastropod assemblages from the abyssal plain (water depths 3310m to3834m) are indistinguishable from a random sample and reflect an attenuation of the diversity of forms exhibited in lower bathyal assemblages (water depths 4680m to 4853m) (McClain *et al*. 2004). Deep-sea snails in the Western North Atlantic (transect from Gay Head, Massachusetts to Bermuda) also exhibit constant disparity values across depth, but the range of morphologies is correlated with the number of species in a community (McClain 2005). Continental assemblages of passerine birds are indistinguishable across the Neotropics, Afrotropics, Orient, and Australasia, with an average misclassification rate of ~64% (>90% is generally considered good) and mixed support for priority effects between first and second-wave colonizers (Jønsson *et al*. (2015). Nested regional assemblages of Neotropical bats are also indistinguishable from one another, irrespective of the size of the area sampled (Villalobos & Arita (2014)).

3.2.3 The Utility of Studying Marine Primary Producers

The aforementioned studies focused on metazoan groups, which although commonly conforming to latitudinal and environmental clines, are also tracking their ultimate food source – primary producers. Aquatic primary producers demonstrate spatial patterns of taxonomic richness (Stomp *et al*. 2011, Barton et al. 2010) and might be more sensitive to such gradients

given not only their requirement to inhabit favorable temperatures, light, and nutrient conditions, but also their spatial entrainment, which in marine phytoplankton results in distribution patterns paralleling physical oceanographic features (see Margalef 1979 and Follows et al. 2007 for discussion on establishment of spatial patterns).

Here, I examine the biogeographic structure of morphological diversity in a group of extant, unicellular haptophytes, the coccolithophores. Coccolithophores synthesize intricate calcitic scales known as coccoliths, which can form a plethora of arrangements on a cell's surface, collectively known as the coccosphere, and morphological features of both coccoliths and coccospheres have been used to study their biodiversity and evolution in the present day and in the paleontological record (Kahn & Aubry 2006, Triantaphyllou *et al.* 2008, Poulton *et al.* 2011, Aubry *et al.* 2005, Aubry 2007, Blaj *et al.* 2010, Bord 2013, Gibbs *et al.* 2013, Henderiks 2008, Henderiks & Pagani 2008, Herrmann *et al.* 2012, Reitan *et al.* 2012). The latitudinal and environmental distribution of coccolithophorid species richness, which show taxonomic richness peaking in the subtropics (Winter *et al* .1994), has also been well studied at various scales in all ocean basins, making them an ideal group for study (Okada & Honjo 1973, Okada & Honjo 1975, Okada & McIntyre 1979, Winter *et al.* 1994). This analysis addresses the first-order question of whether coccolithophorid morphological diversity, measured as regional disparity, traces biome and/or latitudinal clines, and whether that diversity is partitioned by region. I then consider how the geographic distribution of families, as compared to the geographic distribution of species, may influence the establishment of spatio-environmental structure to morphological diversity.

3.3 Methods

3.3.1 Biogeographic Units of Organization

Coccolithophorid biogeography is evaluated using the presence/absence of taxa in pelagic biogeographic provinces that follow Spalding *et al*. (2012) and Longhurst (2007) – i.e. regions delimited by stable (or seasonally recurring) oceanographic conditions, harboring distinct biological assemblages. Analytically, I treat species as if they occur throughout each province in which they have been sampled, irrespective of sampling season and species abundance, as the aim of this study is to examine the total morphological diversity that exists in these regions and individual seasonal censuses are not available for all regions of the world ocean. Local (within-province) changes in coccolithophorid community composition can manifest as variation in the relative abundances of species and morphogenotypes, as seen in the Norwegian-Icelandic Sea (Dylmer *et al.* 2013) and the Gulf of Manfredonia (Balestra *et al.* 2008), or as changes in species composition (Dimizia *et al*. 2008, Hagino *et al.* 2005). In many of these regional cases the most dramatic ecological changes occur during the winter months, when bloom-forming species like *Emiliania huxleyi* dominate samples. More pronounced seasonal changes in community composition can be seen along interregional transects, especially when crossing different latitudinal and biome zones, for example, within the North Sea and into Svalbard (Charalampopoulou *et al*. 2011), and the Northwest Atlantic (Okada & McIntyre 1979). The spatial scale for such observations is most similar to the geographic scale of focus in this study, but again, because not all regions of the world are sampled across different seasons, seasonal changes are not explored herein. Although seasonal changes between morphotypes of the same taxon have been observed (Kahn & Aubry 2006, Triantaphyllou *et al.* 2008, Henderiks *et al.*

2012), I have selected morphological characters that are generally constant among morphotypes of the same species (see following subsection on coding morphological characters).

Geographic occurrence data are restricted to water-column samples to the exclusion of samples from core tops or sediment traps. This information is drawn from literature sources, e.g. the Atlas of living coccolithophores (Winter & Siesser 1994) and the Nannotax3 database (http://www.mikrotax.org/Nannotax3/index.html; accessed May 1, 2017) (file of species locality information provided by Jeremy R. Young, personal correspondence). I have included only occurrences that are recorded at a spatial scale that is at least as fine as that of the biogeographic province and that are accompanied by at least one coccosphere image (a requisite for corroborating taxonomic assignment and assuring minimal post-mortem lateral transport). For example, an observation with locality information reported as "Western Mediterranean Sea" is included because it is finer than province-scale (i.e the Mediterranean Sea pelagic province), whereas an observation with locality reported as "Western Atlantic Ocean" would be excluded because it is too broad and thus difficult to assign to a specific province. The data set of geographic occurrences and the associated metadata of literature sources for that data are included as Appendix D "Geographic Occurrence Data" and will be made available on Dryad (Table 3.3A and 3.3.B).

Because organisms interact with their integrated environment, rather than with any single environmental factor on its own, I examine the question of environmental gradients of disparity using the prevailing conditions of biomes, e.g. the oligotrophic nature of all gyres. Pelagic biogeographic provinces can be organized by biome type (*sensu* Spalding *et al*. 2012), herein defined as groups of provinces with common oceanographic features (e.g. boundary current systems, mid-oceanic gyres, semi-enclosed seas, etc.) and similar ecosystems. Several planktonic

groups of organisms were considered when delimiting these biomes (Longhurst 2007, Spalding *et al*. 2012). Although many of these defining organisms are much larger than coccolithophores, these environmental boundaries are likely also applicable to the latter, which, by virtue of their minuscule size are more susceptible to passive entrainment in physical oceanographic features. Any given province may represent multiple biome types (e.g. shallow semi-enclosed sea), although most provinces represent only one biome type.

The second part of this study addresses the regional differences in morphological diversity partitioned by latitude. My latitudinal scheme follows Winter *et al*. (1994) and is specifically constructed using the distribution of coccolithophorid taxa and assemblages (See Appendix E "Map of Biogeographic provinces" for map with hand-drawn province boundaries tracing and adding to Winter *et al*., 1994; Google Earth file will be made available on Dryad). Some pelagic provinces, such as those characterized by western boundary currents, can span several traditional latitudinal belts, but because the latitudinal boundaries in Winter *et al*. (1994) conform to the fluid bounds of ocean currents (see Figure 3 in text), most are easily assigned to a single latitudinal belt using their framework. There are a few exceptions for which latitudinal assignment is based on the nature of prevailing oceanographic conditions, e.g. sea surface temperature. For example, the Agulhas Current biogeographic province is assigned to the subtropical belt, since it is a western boundary current sourced from the warm waters off the eastern coast of Madagascar.

3.3.2 Taxonomic classification

I examined 104 living coccolithophorid taxa, which I will refer to as species, following the systematic classification of Young et al. (2003). There is open discussion regarding cryptic

speciation and the status of a number of these species as species complexes (Saez *et al.* 2003), but this discussion lies beyond the scope of this work. These species are distributed across 14 clades operationally treated as families, whose grouping is based on clades recovered from a phylogeny of 18S RNA sequences constructed following the methodology in Hagino *et al*. (2009). Not all erected coccolithophorid families are represented in this phylogeny, e.g. Pappospheraceae, and in such cases families are delimited following Young *et al*. (2003). Families that are unsupported as monophyletic clades are denoted with an asterisk following their taxonomic name.

3.3.3 Coding Morphological Characters

I use discrete morphological characters in order to generate a set of characters comparable across all coccolithophores that are not necessarily explicitly used in developing taxonomic schemes (Figure 3.1 shows examples of characters and their coding for five species). I coded 76 discrete binary characters – 44 related to coccoliths, 32 related to coccospheres – for 104 living taxa (Figure 3.1). Binary characters work well to characterize the dramatic differences between coccolithophorid taxa, as there are few homologous features across different families, beyond the tracing of individual crystal units in a few groups (Young *et al.* 2004). Coccoliths vary not only in their morphology (e.g. number of cycles, degree of ornamentation, etc.) but also in how they are arranged into coccospheres (e.g. overlapping, abutting, one layer, multiple layers, etc.). Coccospheres also can vary in overall shape from elongate to spherical, and can even display asymmetric profiles. A character is coded as "1" if it is expressed by a given taxon, "0" if it is not expressed, and "NA" if the character cannot physically be realized (Figure 3.1). For example, taxa having coccospheres that consist of a single layer of coccoliths would have

"NA" for the character "outer layer covers most (>50%) of inner layer", as it refers to morphologies with more than one mineralized layer. Both coccolith and coccosphere traits likely capture diverse aspects of coccolithophorid biology. For example, both kinds of characters affect the sinking velocity and fluid behavior of a cell (as discussed in Chapter 2), although it is important to consider that not all characters are necessarily ecologically, functionally, or taxonomically important.

I limit this study to heterococcoliths, the coccolith morphology expressed exclusively by diploid cells of mineralizing coccolithophorid taxa (Cros et al. 2000). While this omits information about the haploid life stage of these organisms, the many-to-one matching between diploid and haploid life stages (Geisen 2002) and the fact that many haploid-diploid pairings remain unknown would make it difficult to interpret any biogeographic patterns inclusive of both life stages. These characters are not meant to reproduce systematic relationships between taxa, but instead to consider the total morphological diversity of coccolithophores. However, they nonetheless recover the 12 familial groupings when ordinated using principal coordinate analysis (PCO) (Figure 3.2). The dataset of all 76 characters for the 104 species utilized in this study is listed as Appendix B "Binary Character Data" and will be made available through Dryad (See Appendix C "" for explanation of each character).

3.3.4 Quantifying regional morphological diversity

Regional morphological diversity is measured as the mean squared distance between all member species in a biome or latitudinal assemblage. Distances were calculated using the Gower dissimilarity coefficient (for examples of use, see Bellwood *et al.* 2014, and Hopkins & Smith 2015), which accounts for both the number of different character states as well as the number of

characters that can be compared for a given taxonomic pair, allowing for 'NA' values in character sets (Gower 1971). Since the distances in the similarity matrix associated with this coefficient are metric if there are no missing values (following the triangle inequality), they are analogous to Euclidean distances (Gower 1966, Gower 1986). The corresponding pairwise distances are Euclidean if they are positive and semi-definite (Theorem 6 in Gower 1986), and can therefore easily translate into a Euclidean space (Gower 1971, Gower1986). For this reason, I present the morphospace based on these distances using principal coordinate axes (PCO), which reduce the dimensionality of multivariate data (Gower 1966). PCO analyses were conducted using the `cmdscale()` function in the MASS package in R (R Core Team 2015).

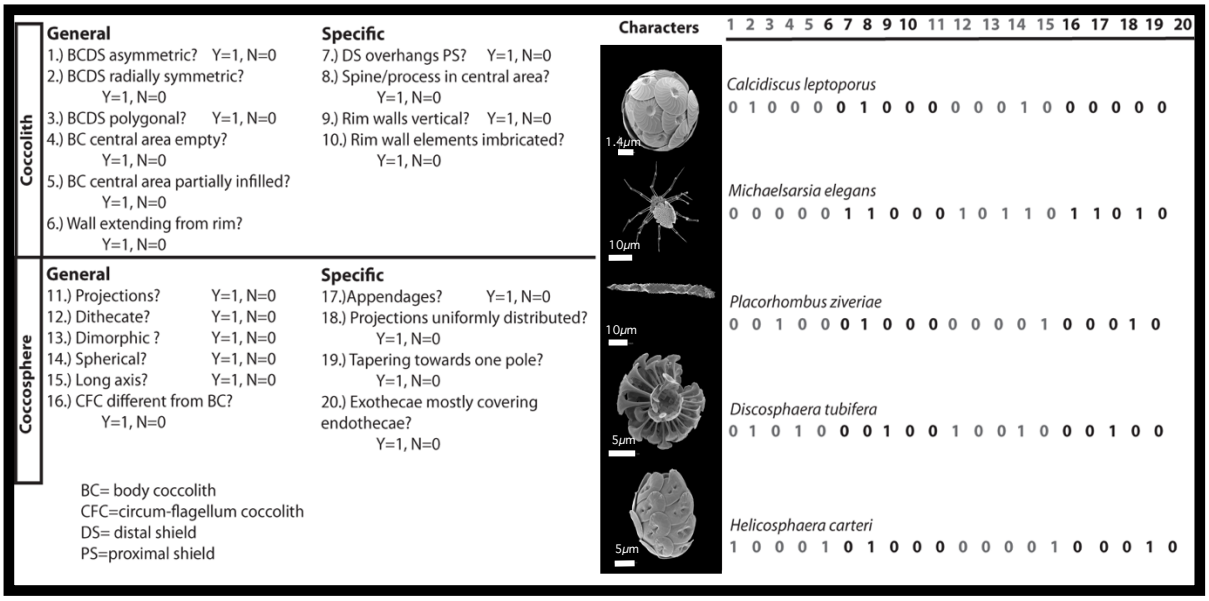

Figure 3.1. Examples of morphologic characters and coding examples for five species. General characters pertain to overall form, while specific characters pertain to specific features of the coccosphere or coccolith. Images from the Nannotax website (www.mikrotax/org/Nannotax3) reproduced by permission of Dr. Jeremy R. Young.

3.3.5 Analyzing Dissimilarity in Regional Morphological Suites

Regional assemblages were further differentiated using canonical variate analysis (CVA), which maximizes the overall differences between the means (centroids) of regional groups (assigned *a priori*) rather than using the differences between species. This method establishes a new coordinate system by scaling multiple descriptor variables, in this case the first 15 of the aforementioned principal coordinate axes, relative to the within-group variance and covariance, then representing the data in a reduced number of canonical variate axes or scores (Albrecht 1980, Campbell & Atchley 1981, Campbell 1984). Canonical variate analysis was conducted using the lda function in the MASS package in R (R Core Team 2015) (N.B. Linear discriminant analysis identifies axes that maximize group separation and projects all data points onto those axes). I carry out a separate set of pair-wise comparisons to assess the effect of shared taxa, explained below.

3.3.6 Testing for the Effect of Shared Taxa

Taxonomic composition exhibits considerable regional redundancy, which could play a role in homogenizing disparity. In order to assess the potential masking effect of shared taxa, I exclude them from regional pairwise comparisons of distances along linear discriminant axes (Sneath & Sokal 1973), which were calculated using the lda function in the MASS R package (R Core Team 2015). Focusing on pairwise comparisons minimizes data loss, as only those species shared between the paired regions are excluded (as opposed to all non-endemic species).

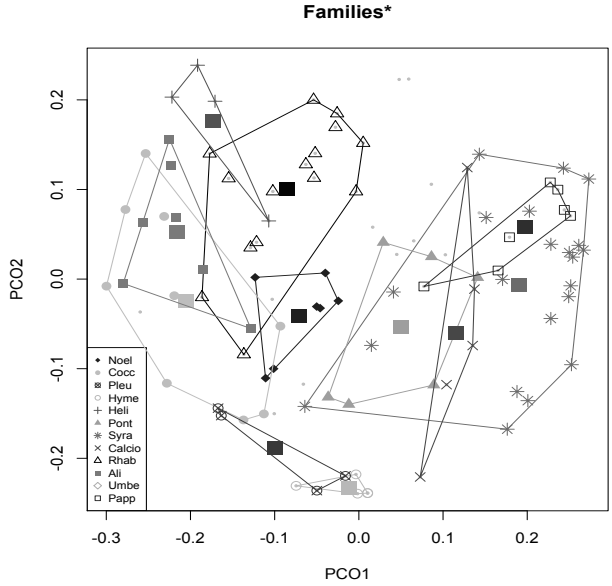

Figure 3.2. Distribution of coccolithophorid species in morphospace coded by family assignment, calculated from the pairwise Gower distances between all species; only first two principal coordinate axes of variation depicted. Large squares denote family centroid position of *Noelrhabdaceae* (Noel, dark grey open circles), *Calcidiscaceae*+ *Coccolithaceae* (Cocc, dark greysolid circles), *Pleurochrysidaeae* (Pleu, light gray circle w/ X), *Hymenomodaceae* (Hyme, solid diamonds), *Helicosphaeraceae* (Heli, crosses), *Pontosphaeraceae* (Pont, solid triangle), *Rhabdosphaeraceae* (Rhab, open triangles), *Syracosphaeraceae* (Syra,*), *Calciosolenaceaea* (Calcio, X), *Pappposphaearceae* (Papp,open diamond), and *Alisphaeraea* (Ali, solid square). Small light-gray points in the background denote species *incertae sedis* and *Umbilosphaeraceae.*

I test for low rates of misclassification, which is simply the proportion of taxa in assemblage A that are incorrectly classified as being from assemblage B; less than 10% misclassified specimens can be considered good, 11% to 20% I considered fair, 21% or greater I considered poor. However, an imbalance between the samples size of the two assemblages compared can artificially inflate the percent of correctly classified taxa. Receiver Operating Characteristic (ROC) graphs factor in the number of incorrect positive classifications, since they depict the trade-off between the rate of correctly assigned positives (Positives correctly assigned/ (True Positives + False Positives)), and the rate of incorrectly assigned positives (Negatives incorrectly classified/ (True Negatives + False Negatives)). Therefore, in these bivariate plots, each point represents a single attempt of classification, with values closest to (0,1) representing perfect classification and the diagonal (1:1) representing random guessing (Fawcett 2006). A concise way to summarize that information is by reporting the area under the ROC curve (AUC),

which is calculated herein using the `auc()` function from the pROC package in R (Robin *et al.* 2011) on the prior probabilities of assignment of a given taxon in assemblage A to A, rather than being assigned to assemblage B. Area values between 1.0 and 0.90 are considered excellent fits, 0.90 and 0.80 fair, while areas of 0.5 or lower are no better than random guessing (Fawcett 2006). This method allows for the evaluation of the goodness of misclassification-based discrimination.

3.4 Results

3.4.1 Biome and Latitudinal Disparity is Homogeneous

I assessed regional disparity for both latitudinal and biome assemblages by averaging the squared distances among all constituent species in each assemblage. Polar, temperate, subtropical, and tropical latitudes have indistinguishable disparity values (~0.31), irrespective of the number of species in each assemblage (Figure 3.3A). Similarly, gyres, eastern boundary currents, western boundary currents, semi-enclosed seas, and transitional biomes all have indistinguishable disparity values (~0.31), regardless of the number of species in each assemblage (Figure 3.3B).

3.4.2 Regional Morphological Suites are Mostly Indistinguishable

Geographic regions exhibiting similar disparity may nonetheless have distinct suites of morphologies; disparity measures the variance among forms, not their positions in morphospace. I recover 66 positive eigenvalues, each explaining ≤13% of the variation. Ordination using principal coordinate analysis (PCO) reveals clustered centroids and comparable convex-hull

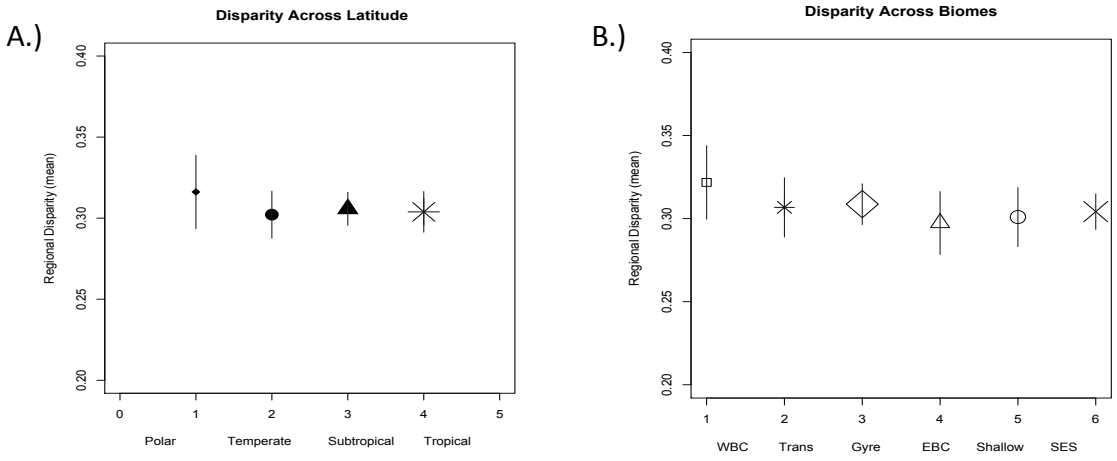

Fig 3.3. Morphological disparity by region, taken as the mean squared distances between all species in a region with its standard error **A.)** Data binned by latitude (size of icon reflects the relative number of species) and **B.)** Data binned by biomes (WBC= western boundary currents, Trans= transition, Gyres=gyres, EBC= eastern boundary currents, Shallow= shallow marine environments, SES= semi-enclosed seas).

volumes, calculated using the `chull()` function in the *grDevices* package in R (R Core Team 2015), which occupy most of the morphospace for all biomes and all latitudes on the first two PCO axes, with the exception of the polar latitude assemblage, which has a smaller convex hull (Figure 3.4).

Canonical variates analysis (CVA) significantly discriminates between polar latitudes and all other latitudes along CVA score 2 (Figure 3.5A; Table 3.3B) and minimally discriminates temperate latitudes from subtropical and tropical latitudes along CVA score 2 (Figure 3.5A; Table 3.3B). Western boundary biomes are slightly separated along CVA score 1, but not to the same degree as in the latitudinal comparison since biome centroids are tightly clustered (Figure 3.5 B), and their convex hulls greatly overlap (Figure 3.5B).

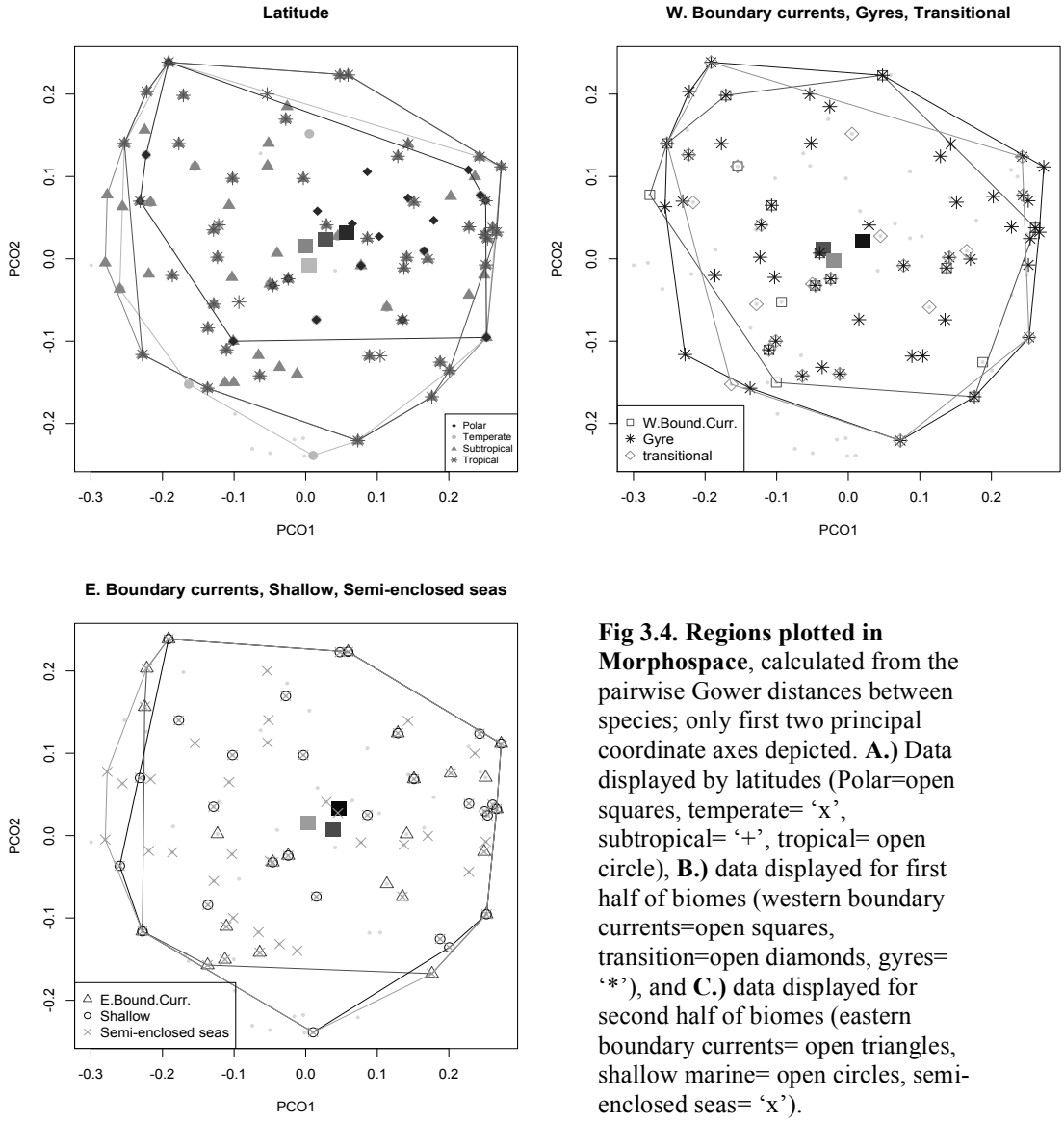

Fig 3.4. Regions plotted in Morphospace, calculated from the pairwise Gower distances between species; only first two principal coordinate axes depicted. **A.)** Data displayed by latitudes (Polar=open squares, temperate= 'x', subtropical= '+', tropical= open circle), **B.)** data displayed for first half of biomes (western boundary currents=open squares, transition=open diamonds, gyres= '*'), and **C.)** data displayed for second half of biomes (eastern boundary currents= open triangles, shallow marine= open circles, semi-enclosed seas= 'x').

3.4.3 Shared Species have Some Effect on Disparity

The inclusion of redundant species can result in groups appearing less distinct under CVA and may play a role in quantifying similar disparity values, so it is important to examine the similarity between the suites of morphologies in each assemblage without shared species. On average, ~95% of species are correctly classified in pair-wise comparisons involving polar latitudes (all have AUC >0.95), while an average of ~65% of species are correctly classified when comparing non-polar latitudes to one another (Table 3.3A). On average ~72% of species are correctly classified between biomes, with only two examples of only fair classification; one comparison having a low AUC value— Western boundary currents compared to semi-enclosed seas (81.70%; AUC =0.80)— and the other with fair AUC value— western boundary currents to shallow (80%; AUC=0.83) (Table 3.3A). Some biome pairs, such as gyre versus semi-enclosed seas, are probably imbalanced with respect to the number of species in each regional class (n=16 and n=66, respectively) (Table 3.3A). Such imbalance has potential to inflate the accuracy of classification, but most of these imbalanced comparisons nonetheless have high rates of misclassification, and so the inference that many species are misclassified is conservative. In contrast, roughly 95% of species are correctly classified in pair-wise comparisons involving polar latitudes (all have AUC >0.95), while an average of ~65% of species are correctly classified when comparing non-polar latitudes to one another (Table 3.3B).

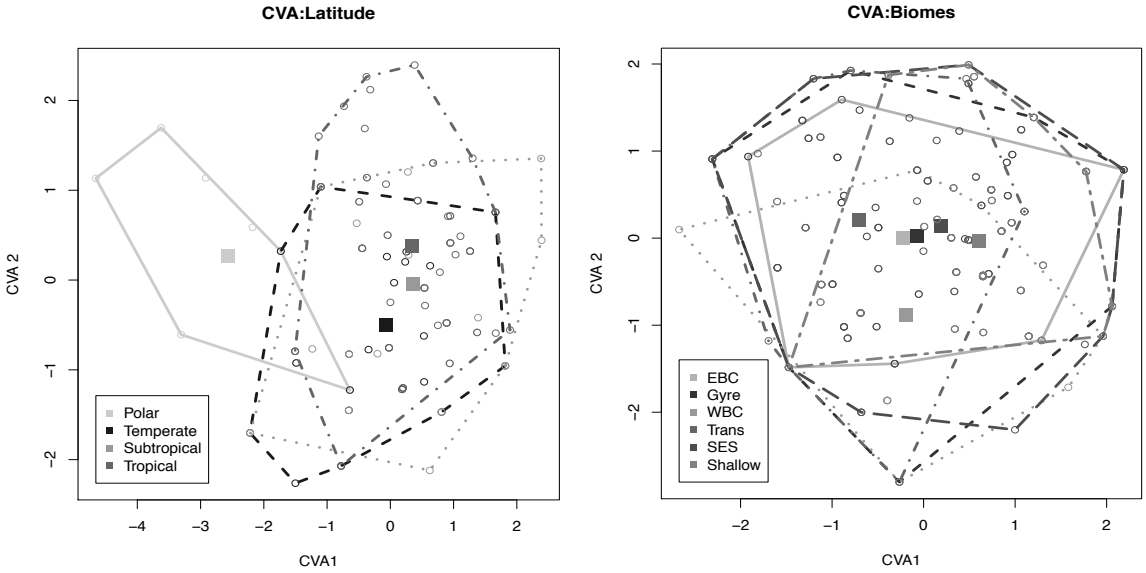

Fig 3.5. Canonical variate analysis (CVA) of the first 15 principal coordinate axes binned by region. A.) Data binned by latitude. Solid squares denote group centroids. Convex hulls: polar assemblage = light-gray solid line polygon; temperate assemblage = medium gray dashed polygon; subtropical assemblage= dotted medium gray polygon; tropical assemblage= dark gray dashed and dotted polygon. **B.)** Data binned by biomes. Solid squares denote group centroids. Convex hulls: Eastern boundary current assemblage= dark gray solid line polygon; Gyre assemblage = small-dash medium gray dashed line; Western Boundary Current assemblage= dotted medium gray polygon; Transitional assemblage= medium grey, dashed and dotted polygon (left-most centroid); Semi-enclosed Seas= dark grey large-dash polygon; Shallow= medium gray alternating large-and-small-dashed polygon.

	Biomes							
Family	Eastern Boundary	Gyre	Western Boundary	Transitional	Semi-enclosed.Sea	Enclosed Sea	Shallow	**Total species in family**
Noel	4	6	4	5	5	0	2	7
Calc+Cocc	3	4	3	1	6	0	2	9
Pleur	0	0	0	1	0	0	0	5
Hymn	0	0	0	0	1	0	1	5
Heli	2	4	2	1	3	0	1	4
Pont	1	5	0	2	4	0	1	6
Syra	8	15	3	3	20	0	12	21
Calcio	3	5	1	2	3	0	1	6
Rhab	0	6	1	3	11	1	6	15
Ali	1	2	0	3	5	0	0	7
Umb	1	1	1	0	2	0	2	2
Papp	1	3	0	3	2	0	0	7
IS	0	1	1	1	4	0	1	10

Table 3.2. A.) Number of unique coccolithophorid species by family across Biomes. Noel= *Noelrhabdaceae*; Calc+Cocc= *Calcidiscaceae* and *Coccolithaceae;* Pleur= *Pleurochrysidaeae*; Hyme= *Hymenomodaceae;* Heli= *Helicosphaeraceae* (crosses); Pont= *Pontosphaeraceae*; Rhab= *Rhabdosphaeraceae*; Syra= *Syracosphaeraceae;* Calcio= *Calciosolenaceaea*; Papp= *Papposphaearceae* ; Alis=*Alisphaeraea* ; Umb=*Umbilosphaeraceae*; IS= *incertae sedis*.

	Polar				Temperate					Subtropical				Tropical			
Family	ATL	PAC	ARC	ANT	ATL	MED+	PAC	ARC	ANT	ATL	PAC	MED+	IND	AMS	ATL	IND	PAC
Noel	1	0	1	2	6	0	0	0	0	4	5	5	2	3	1	0	3
Calc+Cocc	1	0	1	0	1	0	1	0	1	5	2	6	4	3	1	0	3
Pleur	0	0	0	0	1	0	0	1	0	0	0	0	0	0	0	0	0
Hymn	0	0	0	0	0	0	0	1	0	0	0	0	0	0	0	0	0
Heli	1	0	1	0	1	0	0	0	0	3	1	3	2	2	1	0	1
Pont	0	0	0	0	1	0	0	0	0	4	3	4	0	3	1	0	0
Syra	2	0	2	0	1	0	1	3	5	11	3	17	5	11	5	0	1
Calcio	1	0	1	0	2	0	1	1	0	5	1	3	4	4	0	0	2
Rhab	0	0	0	0	2	1	1	0	2	1	2	10	2	9	0	1	0
Ali	1	0	1	0	1	0	0	1	2	2	0	5	0	0	1	0	0
Umb	0	0	0	0	0	0	0	0	0	2	1	2	1	2	1	0	2
Papp	3	0	4	2	3	0	1	0	0	1	0	2	0	0	0	0	1
IS	0	0	2	5	0	0	1	0	1	1	1	4	0	0	0	0	0

Table 3.2. B.) Number of unique coccolithophorid species by family across Latitudes. All ocean basin counts include both northern and southern hemisphere, where relevant.

3.5 Discussion

Coccolithophores apparently do not express a latitudinal cline of morphological diversity. Although some metazoan clades lack a latitudinal trend of morphological diversity (Table 3.1), many express more interregional variation in mean values of disparity than do coccolithophores. The homogeneity in disparity values documented herein parallels that observed for multi-family ecological assemblages, such as Neotropical bats (Villalobos & Arita 2014), continental birds (Jønsson *et al*., 2015, Ricklefs 2012), and deep-sea snails (McClain 2005, McClain *et al*., 2004). It is possible that the high homogeneity observed in certain metazoan groups results from the high dispersal potential of these groups, as is also true of planktonic organisms. However, studies focused on a single clade tend to exhibit more regional heterogeneity in disparity values, regardless of whether they have high dispersal potential (e.g., strombid gastropods (Roy *et al*., 2001) and *Porites* corals (Mohedano-Navarrete, et al. 2008)) or are only somewhat limited by dispersal, e.g., cuttlefish (Neige 2003); the aforementioned groups nonetheless lack a distinct

spatial structure to morphological diversity. It is thus conceivable that the hierarchical level of study, and whether the focus is on a single monophyletic clade or several clades, factors into our ability to detect patterns of morphological diversity. Biogeographic studies of planktonic diatoms (Cermeño and Falkowski 2009) and foraminifera (De Vargas et al. 1999) suggest that planktonic groups are not dispersal-limited, an idea that has been proposed for multiple unicellular eukaryotic groups (Finlay 2002). The broad geographic extent, and thus the taxonomic overlap between regional assemblages of coccolithophorid species resulting from their high dispersal ability, is seemingly not a key factor in homogenizing morphological diversity across regions. This conclusion is based on the fact that regions bear similar suites of forms even when shared species are disregarded. It appears more likely that the homogeneity observed in coccolithophores is due to the near-cosmopolitan geographic distribution of all but two of the families examined herein (Table 3.2), given that each family is morphologically distinct (Figure 3.2). Coccolithophorid families are indeed widespread (see Table 3.2): of the 12 families included, only 2 are restricted in their biome occurrences, i.e. Pleurochrysidaceae and Hymenomonadaceae, both of which are predominantly found in coastal and freshwater environments (Heimdal, 1993). The Pleurochrysidacea occur only in the transitional biome (i.e. the North Atlantic current) and the Hymenomonadaceae occur in the shallow marine biome and semi-enclosed seas (i.e. the Northern European continental shelf) (see Table 3.2A and data on geographic occurrences). The story changes slightly when considering latitudes within different ocean basins, because 6 of the 12 families have less than 50% occupation of all possible latitudinal-ocean bins (Table 3.2B). In both the canonical variate analyses and pairwise linear discriminant analyses, polar latitudes stand out as different. This distinction may simply result

Biome i	No. spp i	Biome J	No. spp j	Proportion correct	Proportion of pooled spp in i	Proportion of pooled spp in j	AUC
E. Boundary	24	Gyre	52	0.684	0.316	0.684	0.642
E. Boundary	24	W. Boundary	16	0.725	0.6	0.4	0.820
E. Boundary	24	Transitional Semi-enclosed	25	0.694	0.490	0.510	0.752
E. Boundary	24	Sea	66	0.756	0.267	0.733	0.704
E. Boundary	24	Shallow	29	0.698	0.453	0.547	0.815
Gyre	52	W. Boundary	16	0.794	0.765	0.235	0.788
Gyre	52	Transitional Semi-enclosed	25	0.688	0.675	0.325	0.729
Gyre	52	Sea	66	0.602	0.441	0.559	0.643
Gyre	52	Shallow	29	0.679	0.642	0.358	0.728
W. Boundary	16	Transitional Semi-enclosed	25	0.707	0.390	0.610	0.831
W. Boundary	16	Sea	66	0.817	0.195	0.805	0.799
W. Boundary	16	Shallow	29	**0.8**	0.356	0.644	**0.833**
Transitional Semi-enclosed	25	Sea	66	0.758	0.275	0.725	0.762
Transitional Semi-enclosed	25	Shallow	29	0.778	0.463	0.537	0.879
Sea	66	Shallow	29	0.695	0.695	0.305	0.661

Table 3.3.A.) Table showing the percent of taxa misclassified between biome pairs (e.g. proportion of gyre taxa misclassified as eastern boundary current taxa) when species shared between the two regions being compared are excluded. Taxa are assigned as either occurring in biome i, as compared to biome j based on linear discriminant analysis of morphological data. Fewer than 10% misclassified specimens is considered good, 11% to 20% is considered fair, 21% or greater is considered poor. Cases with 80% correct assignment (20% misclassification) are highlighted in bold. Imbalances in samples are tested using receiver operon curves, with the area under that curve (AUC) (Area values between 1.0 and 0.90 are considered excellent fits, 0.90 and 0.80 fair, while areas of 0.5 or lower are no better than random guessing (Fawcett 006)).

Biome i	No. spp i	Biome J	No. spp j	Proportion correct	Proportion of pooled spp in i	Proportion of pooled spp in j	AUC
Polar.realms	8	Temp.realms	30	**0.921**	0.211	0.790	**0.969**
Polar.realms	8	Subtrop.realms	28	**0.972**	0.222	0.778	**0.991**
Polar.realms	8	Trop.realms	37	**0.956**	0.178	0.822	**0.997**
Temp.realms	30	Subtrop.realms	28	0.638	0.517	0.483	0.731
Temp.realms	30	Trop.realms	37	0.702	0.448	0.552	0.774
Subtrop.realms	28	Trop.realms	37	0.615	0.431	0.569	0.663

Table 3.3.B) Table showing the percent of taxa misclassified between latitude pairs (e.g. proportion polar taxa misclassified as tropical taxa) when species shared between the two regions being compared are excluded. Taxa are assigned as either occurring in biome i, as compared to biome j based on linear discriminant analysis of morphological data. Convention as in Table 3.3.A.

from only two families being present in the Antarctic (with 5 other taxa present whose taxonomic affiliation beyond genus is uncertain (*incertae sedis*)), whereas 7 of the 12 families occur in the polar Arctic (Table 3.2B). Bear in mind that a diverse range of morphologies can be captured with only a handful of families, as each one extends widely in morphospace (Figure 3.2).

Examining each family on its own reveals a variety of latitudinal distributions. Once again, the Hymenomonidaceae (6% occupation of latitudinal-ocean bins) and Pleurochrysidaceae (12% occupation of latitudinal-ocean bins) are restricted in their latitudinal extent, occupying only temperate latitudes. The Papposphaeraceae are predominantly found at polar and temperate latitudes. The Pontosphaeraceae are predominantly subtropical, with some temperate and tropical occurrences in the Atlantic Ocean. The Alisphaeracea is predominantly found in the Atlantic Ocean and Arctic Ocean but also has two occurrences in temperate Antarctic provinces and several occurrences in the Mediterranean and adjacent seas. The Umbellosphaeraceae is predominantly subtropical, extending into the temperate and tropical latitudes in the Atlantic Ocean and Pacific Ocean.

3.6 Conclusion

Coccolithophores do not exhibit a latitudinal or biome-based structure to their morphological diversity. Different regions of the world harbor very similar suites of morphologies, with the exception of polar latitudes, which are distinct. This overarching homogeneity in morphological diversity is not a result of the broad geographic range of species, but rather the near-cosmopolitan geographic dispersion of families, which are morphologically

distinct. With families forming morphologically distinct units and having little spatial partitioning, there is minimal spatial structure of morphological diversity in this group.

When studying spatial patterns of morphological diversity we need to consider the dispersal capacity of the appropriate hierarchical group. Plankton families are apparently not dispersal limited, and it is possible that their families along with flying birds and some marine invertebrates with pelagic larvae have sufficiently broad dispersal to yield homogenous patterns of disparity. It is thus not surprising to see less distinct patterns in their morphological diversity. As such, any potential regional distinctions can be minimized, especially in the case of plankton, which are found throughout most of the world's oceans.

Although an intriguing aspect of biodiversity, there are many yet-unknown interactions between morphological diversity of a community or clade and its biogeographic extent. These present-day patterns, or lack thereof, are intriguing, but ultimately the mechanistic processes behind them, including the role that hierarchy might play in establishing those patterns, require deeper comparative investigation. It is also important to examine the evolution of a group's morphological diversity in the geologic past, before its constituent taxa attained their present broad distribution, and before they had saturated all known morphologies.

CHAPTER 4

ASSESSING PALEONTOLOGICAL PATTERNS OF DISPARITY WHEN COCCOSPHERES ARE EXCLUDED FROM THE FOSSIL RECORD

4.1 Abstract

The fossil record of coccolithophores consists predominantly of individual scales known as coccoliths, since the complete test, i.e. the coccosphere, usually disarticulates in the early stages of fossilization. As a result, the nature of the coccolithophorid fossil record may bias our understanding and interpretations of their morphological diversity through time. Although some coccospheres can be reconstructed based on the geometry of their constituent coccoliths, this approach cannot be applied to the majority of families. Here, I ask whether coccolith-based distances are correlated with coccosphere-based distances, and whether these two character sets capture the same taxonomic and spatial patterns of disparity. In general, coccosphere-based distances tend to exhibit a greater range of values, which are larger on average than coccolith-based distances. I find that the overall correlation between the two distances is weak and highly variable across families. Additionally, I assess the biases resulting from preservation on the fidelity of a coccolith-only record by degrading the taxonomic list of regional assemblages (biomes and latitudes) to encompass just those genera known from 0-0.2mya (subfossil assemblage) and 0.2mya-1 mya (fossil assemblage), using occurrence data recorded in the Neptune database. Under these simulations, disparity values of both latitudes and biomes of the

subfossil and fossil assemblages are indistinguishable from the disparity values of the living assemblages. Measuring family disparity in subfossil and fossil assemblages is complicated by the fact that most living species are not present in core tops, and so to develop a complete understanding of disparity in the past, fossil taxa must be included. Paleontological studies of coccolithophorid morphological disparity can be fairly robust, depending on scope and questions, but caution needs to be exercised when interpreting the resulting patterns.

4.2 Introduction

The fossil record of coccolithophores, like those of many organisms with complex skeletons and tests, is predominantly represented by a single (or a few) parts of the organism, in this case coccoliths, since coccospheres, which are held together by an overlapping layer of organic scales, often fall apart even before settling to the sea floor (Bown et al.2014). In studying their biodiversity, we accept the record for what it is, but our interpretations from this data can be made more robust with an understanding of the potential biases and distortions arising from preservation of a record that is dominated by a single element of a complex test. Fossil coccospheres are rare but have nonetheless been recovered from exceptionally well preserved faunas, from the Paleogene of Tanzania (Bown et al. 2014), Cretaceous of Gulhemmergberg, The Netherlands (Mai 1997) and Southeast Limburg, The Netherlands (Mai 1999), and even the Jurassic of England (Young & Bown 1991). Even in cases where coccospheres are missing, it is possible to infer their characteristics from their constituent coccoliths. Henderiks (2008) and Gibbs et al. (2013), for example, have geometrically reconstructed fossil coccospheres using coccolith length (constrained for ontogeny using living cells) and implemented this methodology to understand the evolution of cell size, which is key in controlling the cell's exchange of waste

and nutrients with its environment. However, these methods hinge upon a strong geometric relationship between spherical coccospheres and their constituent monomorphic coccoliths, and so cannot be directly applied to clades having non-spherical and/or polymorphic coccospheres, especially types without a modern analog. A frequently employed strategy for studying the evolutionary history of nannoplankton is to focus on those taxa that preserve well and are well represented in the record, such as *Emiliania huxleyi* and *Coccolithus pelagicus*, but this approach presents a limited view of the total biodiversity of the group.

To fully evaluate morphological diversity of all coccolithophorids through time and space, we need a way to evaluate all taxa within the context of a coccolith-based record. Is it possible to recover concordant patterns of morphological diversity using just coccoliths, also considering the other biases introduced by typical preservation scenarios? If the preserved parts of the organism also faithfully record the same biological patterns as the traits missing from the record, then we circumvent the need to find that which is missing. In this study, I investigate the correlation between these two different character sets using extant coccolithophores whose coccosphere morphology is known and thus determine whether coccoliths can act as reasonable proxies for coccospheres when evaluating the morphological diversity of families.

A related inquiry that first needs to be addressed is whether the preserved parts are a faithful record of the whole organism. Considering character set comparisons based strictly on hard parts, Hopkins (2017) has reassuringly demonstrated that morphological disparities and evolutionary rates based on cranidium morphometrics in trilobites faithfully match those calculated using discrete traits reflecting more of the whole organism's morphology. Furthermore, patterns of morphological disparity in middle Triassic pterosaurs based on cranium morphometrics are concordant with those of limb lengths (Foth et al. 2012), despite different

data treatment (see Hopkins 2017 for discussion of the biases introduced by different data treatment). Analogously, I test whether coccoliths act as good proxies for whole-organism morphology of coccospheres.

Lastly, measures of disparity are sensitive to fossilization bias, but could prove more robust if the fossil assemblages are a reasonably random and representative sample of the living community. Even weak preservational bias can distort both the mean and variance of an ecological assemblage in predictable ways, in clades that are taphonomically fragile (Mitchell 2015). While most coccoliths are taphonomically robust, there are some with particularly long and delicate elements that are seldom found in the sedimentary record, and coccospheres harboring delicate coccoliths are commonly left out of the record entirely. I test whether regional assemblage disparity under the typical preservation conditions of fossil and younger assemblages is representative of the disparity of the living assemblage by degrading modern regional assemblages to just those taxa present under different scenarios of preservation.

4.3 Methods

4.3.1 Character Coding

As in Chapter 3, I coded 76 discrete binary characters —44 coccolith characters and 32 coccosphere characters— in 104 extant coccolithophorid species, covering 12 families. These characters were chosen in order to capture as much of the morphology as broadly as possible, and so are not necessarily traits employed for systematics. Taxonomy is based on phylogenetic relationships following Hagino et al. (2009), when applicable, and otherwise following the systematics of Young et al. (2003).

4.3.2 Fossil and Dead Assemblages

The marine microfossil record is not exempt from taphonomic bias or incompleteness but it is an exceptional study system due to its high resolution and global coverage (Lazarus 2011). More specifically, the record of nannofossils, while sensitive to calcium-carbonate dissolution (Lloyd *et al.* 2011), is frequently employed for biostratigraphic correlation and chronology (Perch-Nelsen 1985). Modern-day sediment traps indicate some amount of lateral transport (Honjo 1976), but our understanding of past taxonomic richness in this groups likely stems from reasonably reliable representation of formerly living communities.

My taxonomic lists of fossil and subfossil (a.k.a. dead) assemblages are based on microfossil occurrences in the Neptune Database (Lazarus et al. 1994). The Neptune Database is sourced from International Ocean Drilling Project (IODP) and Deep Sea Drilling Project (DSDP) cores, which have global coverage across all ocean basins. The data records used in this study were downloaded through the Paleobiology Database and are current as of 2007, since the on-going migration from CHRONOS to The Neptune Sandbox Berlin host made new digital downloads difficult. I refer to the subfossil assemblage as a dead assemblages, consisting of samples ranging in age from 0myr to 0.2myr, here distinguished from classical "death assemblages" which refer to the recently accumulated subfossil material local to a specific site. These absolute ages are based predominantly on the magnetostratigraphic data in Bergen et al. (1985), as in the original presentation of the Neptune Database, with more recent website updates allowing the user to apply age calibrations from the Gradstein et al. 2004 and 2012 geologic time scales, and the updated magnetostratigraphy of Berggren et al. (1995), based on Cande & Kent (1995). Choosing such a wide interval is conservative, since it likely includes more material than specifying core tops alone, but is still shorter than the average evolutionary turnover time for

microfossils (Lazarus 2011). I arbitrarily defined the fossil assemblage as samples ranging in age from 0.2myr to 1.5myr, in order to control the amount of time averaging exhibited by the data. I excluded fossil species that lack living representatives, without which coccosphere morphology is likely unknown (see Table 4.1 for full list of extant species and genera represented).

Because few families have more than three extant member species observed in the fossil record, I switch from using species to instead using genera for between-family disparity comparisons (see section 4.3.5 for more details).

4.3.3 Coccoliths as Proxies for Coccospheres

In order to evaluate the performance of coccolith morphology as a general proxy for coccosphere and complete morphology, I first examined whether morphological distances based on each of these datasets are strongly correlated. I evaluate this correlation based on logically independent distances, using a random spanning tree algorithm (Wilson 1996; Benjamini *et al.* 2001). With n species, there are $n(n\text{-}1)/2$ between-species distances, but only $(n\text{-}1)$ of them are logically independent. For example, knowing the distance between species A and B, and the distance between species B and C, provides information about the distance between A and C. In practice, these redundancies have little effect on the estimate of mean among-species distance, but they do artificially reduce the standard error of disparity measures if all distances are treated as if they were independent. In such algorithms, the morphospace, in this case all between-species pairwise distances calculated using the Gower dissimilarity (Gower 1968, Gower 1971), is explored by starting at a randomly chosen point (i.e., a species), and visiting another point (i.e. another species' position in that same space) that has not yet been visited, until all points have

been incorporated into a tree. The mean squared length of the path segments is then a logically independent measure of disparity. Since each run yields a different path length, I report the mean of 1,000 correlations, evaluated using Pearson's correlation coefficient, along with an associated standard error.

Fossil Assemblage Species	Dead Assemblage Species
Gephyrocapsa oceanica	Gephyrocapsa oceanica
Oolithotus fragilis	Oolithotus fragilis
Hayaster perplexus	Umbilicosphaera sibogae
Umbilicosphaera sibogae	Helicosphaera carteri
Helicosphaera carteri	Helicosphaera hyalina
Helicosphaera hyalina	Helicosphaera wallichii
Helicosphaera wallichii	Pontosphaera discopora
Pontosphaera discopora	Pontosphaera japonica
Pontosphaera japonica	Syracosphaera pulchra
Pontosphaera multipora	Syracosphaera histrica
Pontosphaera syracusana	Calciosolenia murrayi
Scyphosphaera apsteinii	Discosphaera tubifera
Scyphosphaera porosa	Umbellosphaera irregularis
Syracosphaera pulchra	
Syracosphaera histrica	
Calciosolenia murrayi	
Discosphaera tubifera	
Umbellosphaera irregularis	

Table 4.1. Extant taxa that are recovered from Neptune Database as "dead assemblage species" (ages 0.0myr to 0.2myr) and as "fossil assemblage species" (ages 0.2myr to 1.5myr).

4.3.4 Regional Disparity Under Different Preservation Scenarios

Even if coccoliths prove to be poor proxies for coccospheres, it is nonetheless possible that they could capture the same overall patterns, should both character sets respond similarly to the same biological and environmental factors. In the present-day oceans, there is a weak gradient of disparity across environments (biomes and latitudes), but notably variable values of disparity by family. Since families do exhibit different values of disparity, while different biomes

and latitudes exhibit nearly identical values (Chapter 3), these two divisions provide alternate case studies to test for bias resulting from the fossilization process, which could reduce or inflate disparity and thus alter the relational patterns between regions and families.

Thus, I ask whether the mean regional disparity is robust to preservation by degrading the complete modern assemblage (all extant species), derived using both coccolith and coccosphere traits, to a "subfossil (a.k.a. dead)" assemblage (age =0-0.2myrs) derived using only coccolith traits, and to a "fossil" assemblage (age=0.2myrs-1.5myrs) derived using only coccolith traits. The disparity of the living assemblage is provided in Table 4.3 for full comparison. Disparity for each scenario is calculated using the same random spanning tree algorithm describe above on the between-species Gower distances, with a bootstrapped standard error.

4.3.5 Family Disparity Under Different Preservation Scenarios

Because very few families have more than three extant species represented in core material, I instead use genera to calculate family disparity, which yields more fossil occurrences because extinct species in extant genera count towards that genus's fossil occurrence. It is not unusual to use genera in fossil studies (e.g. Foote 1997; Aubry 1998; Foote & Miller 2013), but in order to substitute one for the other, congeneric species must be more similar to one another than to species outside that genus, and the distance between genera needs to yield a disparity value comparable to that produced by taking all species into account. Although comparable, the genus-based distances would never be exactly the same as the species-based distances because the genus-based distances exclude the within-genus variation by construction.

I test for concordance among distance measures by comparing the disparity of each family using the Gower distance between species; the between-species distances in principal

coordinate space (PCO) (derived from the aforementioned distances); and the between-genus distances in PCO space, measured as the Euclidean distance between genus centroids across 40 PCO axes. Although both Euclidean and Gower distances are squared distances, I make no assumptions about the linearity of the relationship between both sets of distances and so use Spearman rank correlation, which assigns a rank to the values and compares the ranking rather than the values themselves. I then apply the same random spanning tree algorithm method as employed to compare regional disparity, only this time on the between-genera distances in PCO space, under different preservation scenarios. Disparity is reported as the mean of 1000 replicates, along with a bootstrapped standard error.

4.4 Results

4.4.1 Comparing morphological distances

Coccolith-based distances are weakly correlated with coccosphere-based distances across the whole group (Figure 4.1A. Pearson correlation =0.19, SE=0.097), but are strongly correlated with distances derived from both characters sets (Figure 4.1B. Pearson correlation=0.77, SE=0.038). That this second correlation is stronger is to be expected, as it reflects a whole-versus-part comparison, in contrast to the previous part-versus-part comparison. For most families, the mean coccosphere distance is greater than the mean coccolith distances, and the two are often weakly correlated, i.e. not significant (Table 4.2). Only the Hymenomodaceae (cor=0.85, p =0.089) and the Calciosoleniaceae (cor=0.92, p=0.0093) show a strong correlation between coccolith and coccosphere characters, although both groups have few (<5) species.

4.4.2 Genera as Proxies for Species

As explained above, to use genera as proxies for species in assessing disparity, we need to test whether the two taxonomic levels yield comparable patterns. Across the whole coccolithophore group, the average between-species distance (0.30) is greater than the average distance between genera (0.25) (Table 4.3). The difference in values is to be expected because the mean among-species distance reflects both among- and within-genus distances. However, the rank order of family disparities calculated using the Euclidean distances between genus centroids

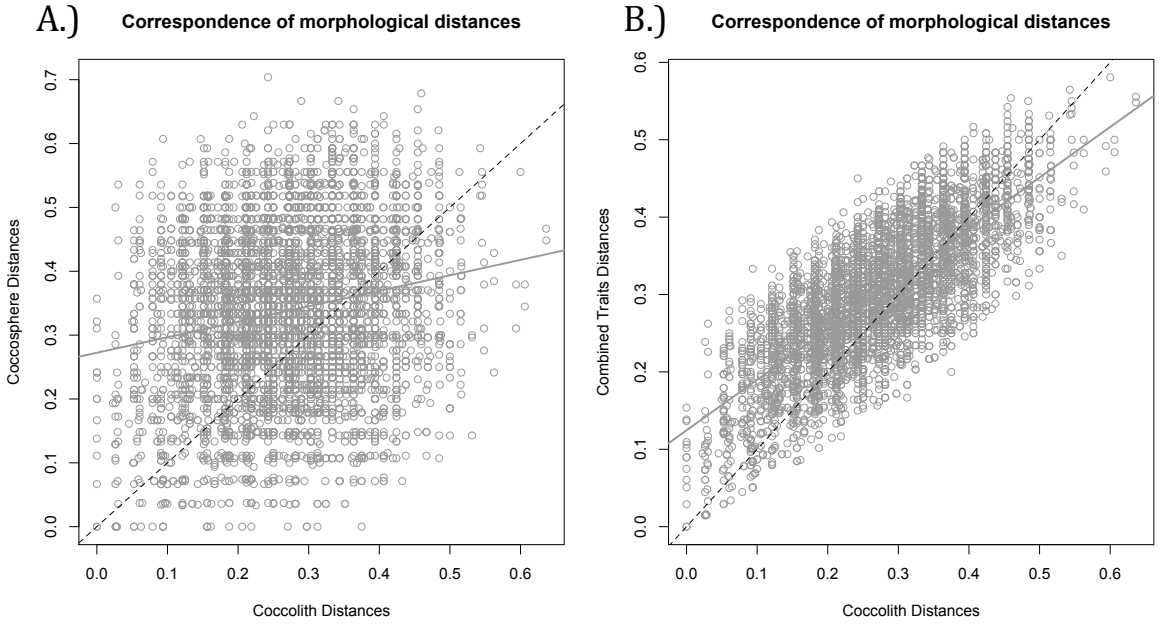

Figure 4.1. A.) Correspondence between coccosphere-based distances and coccolith-based distances, calculated as the Gower Distance. **B.) Correspondence between coccolith-based distances and Gower Distances** derived using both character sets. Linear regression for the data set shown in grey, 1:1 line shown as dashed black line.

in principal coordinate (PCO) space has a low correspondence to the rank order of family disparities calculated using the between-species Gower distances taken from the original binary characters (Table 4.3, Spearman's rho=0.59, p=0.13.). This shuffling is most likely a result of three families— the Papposphaeraceae, the Pontosphaeraceae, and the Hymenomonadaceae— that decrease in disparity when using genera-based Euclidean distances (Table 4.3).

Correlation between CL & CS (species-based Gower Distances)		
Family	**Pearson's Correlation**	**p-value**
Noelaerhabdaceae	0.387	0.345
Cocco+Calcidiscaceae	0.149	0.336
Pleurochrysidaceae	-0.0537	0.521
Hymenomonadaceae	0.847	0.0889
Helicosphaeraceae	-0.293	0.356
Pontosphaeraceae	-0.113	0.484
Syracosphaeraceae	0.186	0.195
Calciosoleniacea	0.9200	0.0093
Rhabdosphaeraceae	0.205	0.238
Alisphaeraceae	0.342	0.370
Umbellosphaeraceae	-0.0306	0.664
Papposphaeraceae	0.0920	0.294

Table 4.2. Correlation between coccolith-based distances and coccosphere based distances by family, calculated using Pearson's correlation coefficient on 1000 replicates of logically independent distances from all calculated between-species Gower distances. Values in grey are based on two or fewer pairwise distances.

Family disparity using species-based Gower distances: Coccolith(CL) & Coccosphere(CS) traits			*Family disparity using genus-based Euclidean distances: CL & CS traits*	
Family	**Living Disparity**	**Living SE**	**Living Disparity**	**Living SE**
Noelaerhabdaceae	0.142	0.114	0.0748	0.00470
Cocco+Calcidiscaceae	0.217	0.110	0.194	0.0376
Pleurochrysidaceae	0.200	0.0816	NA	NA
Hymenomonadaceae	0.227	0.0580	0.0823	0.00751
Helicosphaeraceae	0.250	0.138	NA	NA
Pontosphaeraceae	0.165	0.166	0.112	0.0125
Syracosphaeraceae	0.213	0.0426	0.139	0.0293
Calciosoleniacea	0.225	0.332	0.249	0.0620
Rhabdosphaeraceae	0.177	0.0670	0.162	0.0208
Alisphaeraceae	0.167	0.141	NA	NA
Umbellosphaeraceae	0.0145	0.500	NA	NA
Papposphaeraceae	0.235	0.0761	0.185	0.0329

Table 4.3. Disparity by family, taken as the mean of species-base Gower distances. Reported standard errors are calculated based on 1000 bootstrap values.

4.4.3 The Effect of Preservation on Family Disparity

Measuring family disparity in dead and fossil assemblages is complicated by the fact that half of the living genera are not present in the top of sediment cores (dead assemblage) and only a handful of families are represented by two or more genera. For this reason, I was only able to examine the effect of preservation bias on three families, namely the Noelaerhabdaceae, the Pontosphaeraceae and the Coccosphaeraceae+Calcidiscaceae clade. In these three clades,

	Family disparity using genera-based Euclidean distances							
	CL & CS traits		*CL only*					
Family	**Living Disparity**	**Living SE**	**Living Disparity**	**Livin g SE**	**Dead Disparity**	**Dead SE**	**Fossil Disparity**	**Fossil SE**
Noel	0.0748	0.0047	0.0929	0.333	0.0749	0.0047	0.0747	0.0047
Cocc+Calci	0.194	0.0376	0.265	0.200	0.221	0.0512	0.221	0.0512
Pleur	NA	NA	NA	NA	NA	NA	NA	NA
Hyme	0.0822	0.0075	0.134	0.334	NA	NA	NA	*NA*
Helic	NA	NA	NA	NA	NA	NA	NA	NA
Pont	0.112	0.0125	0.0360	0.500	0.101	0.0103	0.101	0.0103
Syra	0.139	0.0293	0.0993	0.200	NA	NA	NA	NA
Calcio	0.249	0.0620	0.143	0.500	NA	NA	NA	NA
Rhab	0.162	0.0208	0.148	0.125	NA	NA	NA	NA
Alis	NA	NA	NA	NA	NA	NA	NA	NA
Umbe	NA	NA	NA	NA	NA	NA	NA	NA
Papp	0.185	0.0329	0.171	0.200	NA	NA	NA	NA

Table 4.4. Disparity by family taken as the mean of genus-based Euclidean distances in principal coordinate space, under living, dead (a.k.a. subfossil), and fossil preservation scenarios. Reported standard errors are calculated based on 1000 bootstrap values. Noel= *Noelrhabdaceae*; Calc+Cocc= *Calcidiscaceae* and *Coccolithaceae;* Pleur= *Pleurochrysidaeae*; Hyme= *Hymenomodaceae;* Heli= *Helicosphaeraceae* (crosses); Pont= *Pontosphaeraceae*; Rhab= *Rhabdosphaeraceae*; Syra= *Syracosphaeraceae;* Calcio= *Calciosolenaceaea*; Papp= *Papposphaearceae* ; Alis=*Alisphaeraea* ; Umb=*Umbilosphaeraceae*;

disparity values are nearly identical under different preservation scenarios (Table. 4.4) and the rank order of the three families is well preserved (Spearman's rho living to dead= 1, p=0.33; living to fossil=1, p=0.33).

4.4.4 The Effect of Preservation on Regional Disparity

When simulating subfossil (a.k.a. dead) and fossil assemblages, their latitudinal disparity values are comparable to disparity values in extant assemblages (rho= 0.8, p=0.33; rho= 0.8, p=0.33. Figure. 4.3). Biome disparity values of both fossil and dead assemblages are not significantly different from those of the living assemblage (rho=0.18, p=0.71); note however that these exhibit high standard errors (mean fossil SE=0.12; mean dead SE=0.13; mean living SE=0.031). The near-identical regional disparity values of polar latitudes and Eastern boundary currents for both the dead and fossil assemblages is likely a result of the high reduction of an already small species pool for fossil and dead assemblages (Table 4.1). This reduction could also explain the high standard error for these regional assemblages (Figure. 4.3)**.** Disparity values for larger assemblages, like tropical latitudes and gyres, exhibit more divergent values, but these differences are not significant, despite having smaller standard errors (Figure 4.3).

4.5 Discussion

4.5.1 Coccoliths are Poor Proxies for Coccospheres

Across all extant coccolithophores examined herein, coccolith-based distances are poorly correlated with coccosphere-based distances, although within a given family the two can have greater correlation. The correlation between coccolith-based distances and distances derived from both character sets is much stronger, which is not surprising given the nested nature of these character sets. Thus, coccolith morphology is a poor proxy for coccosphere morphology

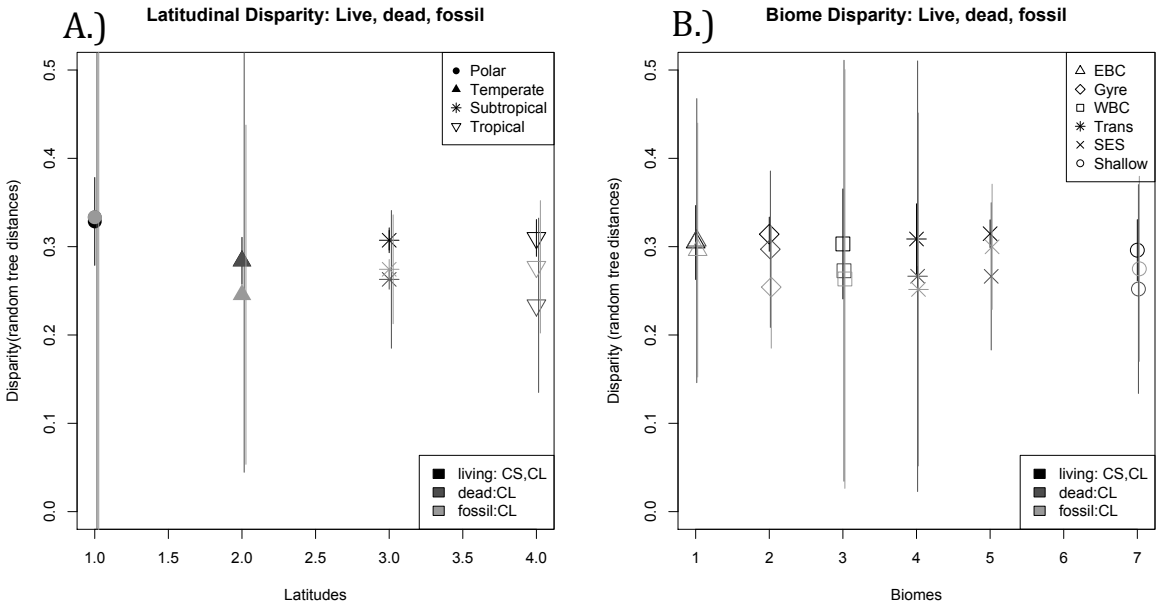

Figure 4.2. Regional assemblage disparity under different scenarios of preservation, presented as the mean of 1000 repetitions of the same mean squared length distance calculated using a random spanning tree algorithm for each regional assemblage. Living assemblages shown in black, dead assemblage shown in dark grey, and fossil assemblages shown in light grey. Standard error bars calculated using 1000 bootstrapped values. **A.)** Polar latitudes plotted as a solid circle, temperate latitudes plotted as solid upright triangle, subtropical latitudes plotted as an asterisk, and tropical latitudes plotted as an open upside down triangle**. B.)** Eastern boundary current biomes plotted as open upright triangles, gyre biomes plotted as open diamonds, Western boundary currents plotted as open squares, transitional biomes (*sensu* Spalding *et al.* 2012) plotted as asterisks, semi-enclosed seas (e.g. the Mediterranean Sea) plotted as 'X', and shallow biomes (e.g. The Malaysian shelf) plotted as open circles.

but a reasonable proxy for the whole-organism morphology, as is also the case for trilobite cranidia (Hopkins 2017).

The handful of families that exhibit a higher correlation between both sets of character-based distances are most promising for clade-focused fossil studies based on coccoliths, as it is likely that the coccolith and coccosphere traits are responding to similar factors and would thus likely yield patterns concordant with the missing coccosphere data. Even so, every attempt should be made to study the fossil diversity of the other clades with poor correspondence between coccolith and coccosphere data, which would greatly benefit from the inclusion of

coccosphere characters. As in Hopkins' (2017) trilobite study, coccospheres contribute additional information not captured by coccoliths, as reflected by the slight mismatch between the two character sets, and should be included in disparity studies whenever possible.

4.5.2 Disparity is Robust to Preservation

Again, very few extant species are found in the shallow fossil record (0 to 1.5 myr), and so attempting to gauge disparity in fossil samples cannot be done using solely extant taxa. Although genera can be good proxies for species when determining family or regional assemblage disparity, they are also often represented by one or two species in the sedimentary record, which unfortunately invalidates many of them for disparity calculations as only one pair-wise distance can be obtained from a single pair. This fact limited my examination of the effect of preservation bias to three families. In these three clades, disparity values are comparable under different preservation scenarios and their rank order is preserved, which is perhaps odd given the low rank-order correlation in living species (Gower distance) and living genera (Euclidean distance).

The conservation of rank of the Noelaerhabdaceae's disparity makes sense; both sets of distances (coccoliths and coccospheres) are relatively low in absolute magnitude, thus safeguarding its position at the bottom of the rank under the different preservation scenarios. The close correspondence between the disparity values of the Coccolithaceae+Calcidiscaceae clade under differing preservation scenarios makes sense because its coccolith distances reflect just as much diversity as coccosphere distances, so degrading this family, which is not limited to a handful of fossil or dead representatives, does not notably distort its aggregate disparity. The third family, the Pontosphaeraceae, thus hold their position in the middle of the rank by default.

Disparity values for different latitudes and different biomes are comparable under different simulated preservation scenarios. As shown in Chapter 3, the fact that only a handful of families are needed to represent the breadth of morphological forms results in minimal distortion; even depauperate regional assemblages, such as those of polar latitudes and Eastern boundary currents, under different preservation scenarios have enough families represented so as to have comparable disparity values. These results are in opposition but not contradiction to the findings of Mitchell (2015), because coccolithophorids are taphonomically more robust than birds and have a high-resolution fossil record. Fossil studies of the morphological diversity of different regional assemblages based solely on coccoliths are thus likely faithful representations of the diversity patterns in the once living community and are apparently minimally distorted by preservation.

4.6 Conclusions

Coccoliths serve as poor proxies for coccospheres in most coccolithophorid families, but are reasonable proxies for the whole-organism morphology in studies of disparity. Since coccosphere traits represent a fairly independent set of characters, nannofossil studies should make every attempt at including them whenever possible.

Genus-based distances are generally reasonable substitutes for species-based distances in evolutionary studies of morphological diversity, in that they usually preserve the rank-order of families. For the families that could be compared across different preservation scenarios, the relative rank-order of disparity among fossil and dead families using coccolith-only characters corresponds well to the rank-order of living families based on both character sets. Thus, it

appears that a coccolith-only record would preserve similar diversity patterns to those exhibited by the formerly living community.

The disparity among latitudinal and biome assemblages is highly robust to the biases introduced by preservation. Thus, the use of the coccolith-only record is fine when considering questions regarding the morphological diversity of regional assemblages, but bear in mind that values of biome disparity have large standard errors, which ultimately render all assemblage disparities comparable across preservation scenarios.

5 CONCLUSIONS

5.1 The Importance of Morphology at Different Scales

Morphology is one of the most accessible phenotypic aspects of an organism to study— it is visible in physical specimens and can be directly measured. The variety of studies on morphological diversity is unsurprising, but the concept of morphological diversity varies depending on the scope and scale of inquiry. On the one hand, there is the physiologically mediated morphological diversity of an individual, such as norms of reactions (see Bord 2013, for examples of intraspecific variation), and the diversity of forms expressed by an ecological community (see Okada & Honjo 1973, Okada & Honjo 1975, Okada & McIntyre 1979, Kahn & Aubry 2006, Triantaphyllou *et al.* 2008), both of which can be observed on ecological and experimental time scales. In these cases, the organisms are not necessarily evolving in response to their environment, although the diversity of that community is in part the result of the history of evolutionary responses both to the environment and other factors. Then, there is the morphological diversity of a single clade, such as the diversity of morpho-genotypes within a "species complex" (see Poulton *et al.* 2011, Henderiks *et al.* 2012), or the diversity of multiple or higher clades, which necessitate much longer time scales to observe their evolution, as distinct forms in genera, families, orders, classes, and phyla.

Chapter 2 dealt with morphology at the scale of an individual as it experiences its world on a day-to-day basis— does it sink or maintain its position in the water column? Despite the minuscule sizes of coccoliths and coccospheres, their diversity of forms can influence how a cell interacts with its environment and the consequent impacts on its ecology and physiology. This

sensitivity implies that the mineralized morphology of these organisms likely plays a critical role in the organism's daily life, perhaps to maintain a favorable position in the water column or to adjust position in the water column via sinking. From these observations, spatial and ecological patterns of morphological diversity might be postulated. However, observations in nature relate a more complex picture of how an individual's morphology translates into its habitat preferences, with mixed evidence for (e.g. Poulton *et al.* 2011) and against (e.g. Quinn *et al.* 2007) the vertical spatial partitioning of forms.

Chapter 3 shifts focus up to the scale of macroecology, investigating the distribution of morphological diversity of ecological entities, i.e. communities, and of evolutionary entities, here families across biogeographic space. In this case, bridging ecological and evolutionary ideas is facilitated by having the same operational units, those being species; cohabiting species can form ecological communities, but need not be closely related, whereas phylogenetically related species, which need not live in the same areas, form families. At the macroecological scale, there is striking homogeneity in biome and latitudinal suites of morphologies and regional disparity. This biogeographic pattern is likely a result of an underlying evolutionary pattern, namely the high dispersion and ultimately the wide geographic distribution of families. It makes sense that these large-scale patterns necessitate a longer temporal scope for adequate study, as attaining globally cosmopolitan distribution might take hundreds to thousands of years, and so the morphological patterns of interest must be considered over evolutionary and geologic time.

There is of course a challenge to bridging different scales, in terms of mechanisms, which has led to the distinct philosophical split between microevolutionists and macroevolutionists. Indeed, the work presented here largely deals with patterns of morphological diversity and is only the first step towards recognizing how a single facet of an individual's form translates to a

facet of a clade, among species or even families. Such avenues of study require a more temporally dynamic framework in order to illuminate the mechanisms that bridge these different hierarchical levels of organization. The findings presented in chapter 4 serve as scaffolding upon which to build these types of questions by offering guidance as to the completeness of the morphology needed to pursue different inquiries into coccolithophore ecology and evolution.

5.2 The Robustness of Environmental Assemblages

The work presented in this thesis sparks questions regarding the common practice of studying and using microfossil assemblages. Traditionally, it is the taxonomic composition of an assemblage that is utilized for biostratigraphy, paleoenvironmental reconstructions, plaeoceanography, etc., but suites of morphologies (Aubry 2007, Linnert *et al.* 2013) or alternatively the prevalence of indicator morphologies (e.g. Streng *et al.* 2004) are sometimes also examined. Relevant to the latter case, my work suggests that the morphological diversity of biome and latitudinal assemblages of nannoplankton are robust to preservation and, at least in modern seas, seem to minimally vary geographically. Because this is a result of their planktonic lifestyle, it is likely that older Paleogene and Mesozoic assemblages will also be fairly robust with respect to spatial distributions, with perhaps the exception of the early Triassic, when mineralized coccolithophorid forms first evolved and were less widespread than at present. Bear in mind that my study did not explore the taphonomic effect of facies type, which we know can change our picture of morphological diversity for benthic animals (Hopkins 2017), or other taphonomic factors, which could impact the observed diversity of forms (Mitchell 2015).

Also evident from this research is that environmental and geographic patterns of coccolithophorid morphological diversity likely have an important driver acting at evolutionary

time scales. Therefore, it is also important to understand the evolutionary dynamics of nannoplankton through time, since biotic events such as mass extinctions or dampened diversification (e.g. Oligocene Diversity minimum (Bown *et al.* 2004)) would affect both the standing diversity of forms and the robustness and homogeneity of regional morphological diversity, given that survivor and disaster taxa have smaller geographic ranges during the recovery interval (but also consider that taxa can exist in multiple small— but widespread— populations (Schueth *et al.* 2014)).

5.3 Future Neontological and Paleontological Studies

The work presented in this dissertation represents the first steps towards understanding the evolutionary history of coccolithophorid morphological diversity and the mechanisms that shape its environmental and biogeographic structure. In order to move forward, the group's morphological diversity needs to be assessed for both Cenozoic and Mesozoic stages, and such an assessment would greatly benefit from an extensive phylogeny of the haptophyte algae at large, ideally one that brings together molecular and fossil information (Lahr *et al.* 2014, Santoferrara *et al.* 2016). An inclusive phylogenetic framework allows us to place taxa within temporally long-lived lineages continuing from one geologic time period to another. This framework can thus circumvent analytic problems that may arise from working with short-lived species, a problem I encountered in Chapter 4 when calculating disparity using the few extant taxa that were known from the deep-sea sedimentary core record. Aside from quantifying the changes in morphological diversity through time, this framework would allow for the investigation and quantification of the rate of morphological evolution in targeted clades or all mineralizing prymnesiophytes. In addition to a complete and more importantly robust

phylogeny, a comprehensive study of morphological diversity in coccolithophores must include information from coccosphere-based traits. As suggested by my analyses in chapter 4, coccoliths alone may not be sufficient to recover the same taxonomic patterns of disparity as derived from including coccosphere characters. Thus, it is also important to continue to support innovative techniques aimed at recovering such delicate but informative structures from the fossil record.

To that end, I would first track coccolithophorid morphological disparity across the Cretaceous- Paleocene boundary, a pattern I would subsequently contrast with the dynamics of morphological diversity across the Paleogene-Neogene boundary. From the work of chapter 4, it seems adequate to code morphology according to genera in order to explore the dynamics of families, which makes the evaluation of each time slice less sensitive to the vagaries of species-level sampling. It is of course prudent to first check that Cretaceous and Paleogene genera are reasonable proxies for constituent species. The course-level analysis of the patterns of disparity through time does not rely on having a robust phylogeny, but as stated above, a phylogeny would greatly help comparing and following the continuation of lineages across these boundaries, particularly around the Cretaceous-Paleogene boundary. The most prominent phylogenies for Mesozoic taxa (Perch-Nielsen 1985a, Bown 1998) and for Cenozoic taxa (Perch-Nielsen 1985b, Aubry 1998) are largely based on stratophenetics, and the characters presented in this dissertation are separate and distinct from those utilized for these phylogenies.

The end of the Cretaceous is marked by the latest of the big five mass extinction, a catastrophe that deeply impacted the world's ocean (see Hallam & Perch-Nielsen 1990, Kump 1991, Thomas *et al.* 2006, Hull & Norris 2011); although only 9 of 131 known species make it through the event, they represent 5 of 14 families (Bown *et al.* 2004). It is however also possible that the group's Cenozoic morphological disparity would be comparable to its Cretaceous

disparity, if a handful of families can capture most of the group's morphological diversity. Aubry (1998) points out that over 70% of Cenozoic families originate during the Paleocene, and so it is possible that coccolithophorid morphological diversity actually increases from what it had been in the Mesozoic. What might change is the geographic extent of the families since their population numbers would be greatly reduced immediately following the extinction (except in the case of proliferating disaster taxa that form monocultures), and so the regional structure of disparity may be more heterogeneous than in the modern or in the Cretaceous, if families have reached all parts of the world ocean by the Maastrichtian. Coccolith size has not been constant throughout the Cretaceous— in general size increases from the Jurassic into the Campanian, stabilizes, but then declines during the Maastrichtian (Aubry *et al.* 2005, Aubry *et al.* 2012, Linnert *et al.* 2013)— so it is also possible that other aspects of morphology were also in flux at this time.

In contrast, there is severe but gradual biotic turnover during the Oligocene (Corliss *et al.* 1984); origination rates declined, and background extinction rates persisted at the same level as before (Bown *et al.* 2004). At this time taxa such as the genus *Disocoaster* that were prominent in the Paleogene decline (Aubry 1998, Schueth & Bralower 2015). This trimming of the phylogeny could result in reducing coccolithophorid morphological diversity. Aubry (2007, 2009) also notes a tendency for coccolithophores to converge on similar coccosphere and coccolith morphologies during the Pliocene, a trend that starts in the Miocene, so it is possible that morphological disparity would not subsequently increase during the mid-Miocene radiation. Unlike the environmental impacts of the end Cretaceous mass extinction, the Paleogene-Neogene transition is characterized by profound climatic and oceanographic changes that are sustained for the most part into the modern era, which have been shown to influence the distribution of

nannofossils (Beaufort & Aubry 1992). Therefore, the geographic structure of disparity in the Neogene need not be the same as that of the Paleogene or the Cretaceous, unless, again, there is enough time to allow for the broad dispersal of the majority of families across the world's ocean.

These two case studies would allow for the exploration of the patterns of coccolithophorid disparity in a situation of potentially increasing disparity and potentially decreasing disparity and would allow for more insight into the underlying mechanisms determining the environmental and geographic structure of morphological diversity.

REFERENCES

Albrecht, H. (1980). Multivariate analysis and the study of form, with special reference to canonical variate analysis. *American Zoologist*, 20(4), 679–693.

Aubry, M. P. (1998). Early Paleogene calcareous nannoplankton evolution: a tale of climatic amelioration. In M.P. Aubry, S. Lucas, & W. A. Berggren (Eds.) *Late Paleocene-Early Eocene climatic and biotic events in the marine and terrestrial records*, (pp.158-203). New York, NY: Columbia University Press.

Aubry, M. P. (2007). A major Pliocene coccolithophore turnover: change in morphological strategy in the photic zone. *Geological Society of America Special Papers*, 424, 25-51.

Aubry, M. P. (2009). A sea of Lilliputians. *Palaeogeography, Palaeoclimatology, Palaeoecology*, 284(1-2), 88–113.

Aubry, M., Bord, D., Beaufort, L., Kahn, A., & Boyd, S. (2005). Trends in size changes in the coccolithophorids, calcareous nannoplankton, during the Mesozoic: a pilot study. *Micropaleontology*, 51(4), 309–318.

Aubry, M., Rodriguez, O., Bord, D., Godfrey, L., Schmitz, B., & Knox, R. W. O. B. (2012). The first radiation of the Fasciculiths: morphologic adaptations of the coccolithophores to oligotrophy. *Austrian Journal of Earth Sciences*, 105(1), 29–38.

Balestra, B., Marino, M., Monechi, S., Marano, C., & Locaiono, F. (2008). Coccolithophore communities in the Gulf of Manfredonia (Southern Adriatic Sea): data from water and surface sediments. *Micropaleontology*, 54(5), 377–396.

Barton, A. D., Dutkiewicz, S., Flierl, G., Bragg, J., Follows, M. J. (2010). Patterns of diversity in marine phytoplankton. *Science*, 327, 1509-1511

Barton, A. D., Pershing, A. J., Litchman, E., Record, N. R., Edwards, K. F., Finkel, Z. V., … Ward, B. A. (2013). The biogeography of marine plankton traits. *Ecology Letters*, 16(4), 522–534.

Bedford, B. L., Walbridge, M. R., & Aldous, A. (1999). Patterns in nutrient availability and plant diversity of temperate North American wetlands. *Ecology*, 80(7), 2151–2169.

Bejamini, I., Lyons, R., Peres, Y., & Schramm, O. (2001), Special invited paper: uniform spanning forests. *The Annals of Probability*, 29(1), 1–65.

Bellwood, D. R., Goatley, C. H. R., Brandl, S. J., & Bellwood, O. (2014). Fifty million years of herbivory on coral reefs: fossils, fish and functional innovations. *Proceedings. Biological Sciences / The Royal Society*, 281(1781), 20133-20146.

Beaufort, L., & Aubry, M.-P. (1992). Paleoceanographic implications of a 17-M.Y.-long record of high-latitude Miocene calcareous nannoplankton fluctuations. *Proceedings of the Ocean Drilling Program, Scientific Results*, 120, 539–549.

Blaj, T., Henderiks, J., Young, J. R., & Rehnberg, E. (2010). The Oligocene nannolith *Sphenolithus* evolutionary lineage: morphometrical insights from the palaeo-equatorial Pacific Ocean. *Journal of Micropalaeontology*, 29(1), 17–35.

Bord, D. *Microevolution in coccolithophores: examples from the Paleocene-Eocene*, (Doctoral Dissertation). Rutgers University, 2013.

Bown, P.R. (Ed.). (1998a). *Calcareous nannofossil biostratigraphy*. London, UK: British Micropalaeontological Society Series, Chapman & Hall.

Bown, P. R. (1998b). Triassic. In P.R Bown. (Ed.). *Calcareous Nannofossil Biostratigraphy, British Micropalaeontological Society Series,* (pp. 29-33). London, UK: Chapman & Hall.

Bown, P. R. (2005). Calcareous nannoplankton evolution: a tale of two oceans. *Micropaleontology*, 51(4), 299–308.

Bown, P. R., Lees, J. A., Young, J. R. (2004). Calcareous nannoplankton evolution and diversity through time. In H. R. Thierstein & J.R. Young (Eds.) *Coccolithophores From Molecular Processes to Global Impact*, (pp. 481-508). Berlin Heidelberg. Germany: Springer-Verlag.

Bown, P. R., Gibbs, S. J., Sheward, R., & Sarah, O. (2014). Searching for cells: the potential of fossil coccospheres in coccolithophore research. *Journal of Nannoplankton Research, Coccolithophore 2014 Workshop Volume*, 5-21.

Campbell, N. A., & Atchley,. W. R. (1981). The geometry of canonical variate analysis. *Systematic Zoology,* 30,268-280.

Campbell, N. A. (1984). Canonical variate analysis - a general model formulation. *Australian Journal of Statistics*, 26(l), 86–96.

Cermeño, P., & Falkowski, P. G. (2009). Controls on diatom biogeography in the ocean. *Science*, 325(5947), 1539–41.

Charalampopoulou, A., Poulton, A. J., Tyrrell, T., & Lucas, M. I. (2011). Irradiance and pH affect coccolithophore community composition on a transect between the North Sea and the Arctic Ocean. *Marine Ecology Progress Series*, 431, 25–43.

Corliss, B. H., Aubry, Marie-Pierre, Berggren, W. A., Fenner, J. M., Lloyd, D., & Keigwin Jr., G. K. (1984). The Eocene/Oligocene boundary event in the deep sea. *Science*, 226(4676), 806–810.

Cros, L., Kleijne, A., Zeltner, A., Billard, C., & Young, J. R. (2000). New examples of holococcolith-heterococcolith combination coccospheres and their implications for coccolithophorid biology. *Marine Micropaleontology*, 39,1-34.

de Vargas, C., Norris, R., Zaninetti, L., Gibb, S. W., & Pawlowski, J. (1999). Molecular evidence of cryptic speciation in planktonic foraminifers and their relation to oceanic provinces. *Proceedings of the National Academy of Sciences of the United States of America*, 96(6), 2864–2868.

De Vargas, C., Aubry, M., Probert, I., & Young, J. (2007). Origin and evolution of coccolithophores: from coastal hunters to oceanic farmers. In P. G. Falkowski & A. H. Knoll (Eds.), *Evolution of Primary Producers in the Sea,* (pp. 251–286). Amsterdam, The Netherlands: Academic Press.

D'Hondt, S., Donaghay, P., Zachos, J., Luttenberg, D., & Lindinger, M. (1998). Organic carbon fluxes and ecological recovery from the Cretaceous-Tertiary mass extinction. *Science*, 282(5387), 276–9.

Dimiza, M. D., Triantaphyllou, M. V., & Dermitzakis, M. D. (2008). Seasonality and ecology of living coccolithophores in Eastern Mediterranean coastal environments (Andros Island, Middle Aegean Sea). *Micropalentology*, 54(2), 159–175.

Dylmer, C. V., Giraudeau, J., Hanquiez, V., & Husum, K. (2015). The coccolithophores *Emiliania huxleyi* and *Coccolithus pelagicus*: extant populations from the Norwegian-Iceland Seas and Fram Strait. *Deep-Sea Research Part I: Oceanographic Research Papers*, 98, 1–9.

Eleson, J. W., & Bralower, T. J. (2005). Evidence of changes in surface water temperature and productivity at the Cenomanian/Turonian boundary. *Micropaleontology*, 51(4), 319–332.

Eppley, R.W., Holmes, R. W., Strickland, J. D. H. (1967). Sinking rates of marine phytoplankton measured with a fluorometer. *Journal of Experimental Marine Biology and Ecology*, 1,191-208.

Erba, E. (2006). The first 150 million year history of calcareous nannoplankton: biosphere–geosphere interactions. *Palaeogeography, Palaeoclimatology, Palaeoecology*, 232(2-4), 237-250.

Fawcett, T. (2006). An introduction to ROC analysis. *Pattern Recognition Letters,* 27(8), 861–874.

Finlay, B. J. (2002). Global dispersal of free-living microbial eukaryote species. *Science*, 296(5570), 1061–1063.

Follows, M. J., Dutkiewicz, S., Grant, S., Chisholm, S. W. (2007). Emergent biogeography of mircobial communities in a model ocean. *Science*, 315,1834-1846.

Frada, M., Probert, I., Allen, M. J., Wilson, W. H., & de Vargas, C. (2008). The "Cheshire Cat" escape strategy of the coccolithophore *Emiliania huxleyi* in response to viral infection. *Proceedings of the National Academy of Sciences of the United States of America*, 105(41), 15944–9.

Geisen, M., Young, J. R., Probert, I., Saez, A. G., Baumann, K.-H., Sprengel, C., Bollman, J., Cros, L., De Vargas, C., Medlin, L. K. (2004). Species level variation in coccolithophores. In H. R. Thierstein & J.R. Young (Eds.) *Coccolithophores From Molecular Processes to Global Impact*, (pp. 327-366). Berlin, Heidelberg, Germany: Springer-Verlag.

Geisen, M., Billard, C., Broerse, A., Cros, L., Probert, I., & Young, J. (2002). Life-cycle associations involving pairs of holococcolithophorid species: intraspecific variation or cryptic speciation? *European Journal of Phycology*, 37(4), 531–550.

Gibbs, S. J., Poulton, A. J., Bown, P. R., Daniels, C. J., Hopkins, J., Young, J. R., … Newsam, C. (2013). Species-specific growth response of coccolithophores to Palaeocene–Eocene environmental change. *Nature Geoscience,* 6(3), 218–222.

Gower, J. C. (1967). Multivariate analysis and multidimensional geometry. *Journal of the Royal Statistical Society. Series D (The Statistician)*,17(1),13-28.

Gower, J. C. (1971). A general coefficient of similarity and some of its properties. *Biometrics*, 27(4), 857–871.

Hagino, K., Okada, H., & Matsuoka, H. (2005). Coccolithophore assemblages and morphotypes of *Emiliania huxleyi* in the boundary zone between the cold Oyashio and warm Kuroshio currents off the coast of Japan. *Marine Micropaleontology*, 55(1–2), 19–47.

Hagino, K., Takano, Y., & Horiguchi, T. (2009). Pseudo-cryptic speciation in *Braarudosphaera bigelowii* (Gran and Braarud) Deflandre. *Marine Micropaleontology*, 72(3-4), 210–221.

Hallam, A., & Perch-Nielsen, K. (1990). The biotic record of events in the marine realm at the end of the Cretaceous: calcareous, siliceous and organic-walled microfossils and macroinvertebrates. *Tectonophysics*, 171(1–4), 347–357.

Heimdal, B. R. (1993). Modern Coccolithophorids. In C. R. Tomas (Ed.), *Marine Phytoplankton: A Guide to Naked Flagellates and Coccolithphorids*, (pp. 147-249). San Diego, CA: Academic Press.

Henderiks, J. (2008). Coccolithophore size rules — reconstructing ancient cell geometry and cellular calcite quota from fossil coccoliths. *Marine Micropaleontology*, 67(1–2), 143–154.

Henderiks, J., & Pagani, M. (2008). Coccolithophore cell size and the Paleogene decline in atmospheric CO_2. *Earth and Planetary Science Letters*, 269(3–4), 576–584.

Henderiks, J., Winter, A., Elbrächter, M., Feistel, R., der Plas, A., Nausch, G., & Barlow, R. (2012). Environmental controls on *Emiliania huxleyi* morphotypes in the Benguela coastal upwelling system (SE Atlantic). *Marine Ecology Progress Series*, 448, 51–66.

Herrmann, S., Weller, A. F., Henderiks, J., & Thierstein, H. R. (2012a). Global coccolith size variability in Holocene deep-sea sediments. *Marine Micropaleontology*, 82-83, 1–12.

Herrmann, S., & Thierstein, H. R. (2012b). Cenozoic coccolith size changes—evolutionary and/or ecological controls? *Palaeogeography, Palaeoclimatology, Palaeoecology*, 333-334, 92–106.

Hillebrand, H. (2004). On the generality of the latitudinal diversity gradient. The *American Naturalist,* 163(2), 192–211.

Honjo, S. (1976). Coccoliths: production, transportation and sedimentation. *Marine Micropaleontology*, 1, 65–79.

Hopkins, M. J. (2017). How well does a part represent the whole? A comparison of cranidial shape evolution with exoskeletal character evolution in the trilobite family Pterocephaliidae. *Palaeontology,* 60(3), 309–318.

Hopkins, M. J., & Smith, A. B. (2015). Dynamic evolutionary change in post-Paleozoic echinoids and the importance of scale when interpreting changes in rates of evolution. *Proceedings of the National Academy of Sciences of the United States of America*, 112(12), 3758–3763.

Hull, P. M., & Norris, R. D. (2011). Diverse patterns of ocean export productivity change across the Cretaceous-Paleogene boundary: new insights from biogenic barium. *Paleoceanography*, 26(3), 1–10.

Jønsson, K. A., Lessard, J. P., & Ricklefs, R. E. (2015). The evolution of morphological diversity in continental assemblages of passerine birds. *Evolution*, 69(4), 879–889.

Kahn, A., & Aubry, M.-P. (2006). Intraspecific morphotypic variability in the Family Rhabdosphaeraceae. *Micropaleontology*, 52(4), 317–342.

Katz, M. E., Finkel, Z. V., Grzebyk, D., Knoll, A. H., & Falkowski, P. G. (2004). Evolutionary trajectories and biogeochemical impacts of marine eukaryotic phytoplankton. *Annual Review of Ecology, Evolution, and Systematics*, 35(1), 523-556.

Kleijne, A., Kroon, D., and Zeveboom, W. (1989). Phytoplankton and foramininferal frequencies in northern Indian Ocean and Red Sea surface waters. *Netherlands Journal of Sea Research*. 24, 531-539.

Krug, A. Z., Jablonski, D., Valentine, J. W., & Roy, K. (2009). Generation of Earth's first-order biodiversity pattern. *Astrobiology,* 9(1), 113–24.

Kump, L. R. (1991). Interpreting carbon-isotope excursions: Strangelove oceans. *Geology*, 19(4), 299-302.

Lahr, D. J. G., Laughinghouse, H. D., Oliverio, A. M., Gao, F., & Katz, L. A. (2014). How discordant morphological and molecular evolution among microorganisms can revise our notions of biodiversity on Earth. *BioEssays*, 36(10), 950–959.

Lazarus, D. B., (1994) Neptune: a marine micropaleontology database. *Mathematical Geology*, 26(7), 817-832.

Lazarus, D. B. (2011). The deep-sea microfossil record of macroevolutionary change in plankton and its study. In A. J. McGowan & A. B. Smith (Eds.), *Comparing the Geological and Fossil Records: Implications for Biodiversity Studies London, Special Publications, 358*, (pp. 141–166). London, UK: Geological Society, London.

Linnert, C., & Mutterlose, J. (2013). Biometry of Cenomanian-Turonian placoliths: a proxy for changes of fertility and surface-water temperature? *Lethaia,* 46(1), 82–97.

Lloyd, G. T., Smith, A. B., & Young, J. R. (2011). Quantifying the deep-sea rock and fossil record bias using coccolithophores. *Geological Society, London, Special Publications*, 358(1), 167–177.

Lohmann, H. (1913). Beiträge zur Charakterisierung des Tier- und Pflanzenlebens in den von der 'Deutschland' während ihrer Fahrt nach Buenos Ayres durchfahrenen Gebieten des Atlantischen Ozeans. II. Teil. *Internationale Revue der gesamten Hydrobiologie und Hydrographie,* 5(4), 343-504.

Longhurst, A. R. (2007). *Ecological Geography of the Sea.* San Diego, Academic Press.

Mai, H., von Salis Perch-Nielsen, K., Willems, H., and Romein, T. (1997). Fossil coccospheres from the K/T boundary section from Geulhemmerberg, The Netherlands. *Micropaleontology*. 43, 281–302.

Mai, H., (1999), Paleocene coccoliths and coccospheres in deposits of the Maastrichtian stage at the "type locality" and type area in SE Limburg, The Netherlands. *Marine Micropaleontology*, 36, 1–12.

Medlin L.K., Kooistra W.H.C.F., Potter D., Saunders G.W., Andersen R.A. (1997) Phylogenetic relationships of the 'golden algae' (haptophytes, heterokont chromophytes) and their plastids. In: D. Bhattacharya (Eds), *Origins of Algae and their Plastids. Plant Systematics and Evolution, Vol 11*. Vienna, Austria: Springer.

Margalef, R., (1967). The food web in the pelagic environment. *Helgoländer wissenschaftliche Meeresuntersuntersuchungen*. 15, 548-549.

Margalef, R. (1979). The organization of space. *Oikos,* 33, 152-159.

McClain, C. R. (2005). Bathymetric patterns of morphological disparity in deep-sea gastropods from the western North Atlantic basin. *Evolution,* 59(7), 1492–1499.

McClain, C. R., Johnson, N. A, & Rex, M. A. (2004). Morphological disparity as a biodiversity metric in lower bathyal and abyssal gastropod assemblages. *Evolution*, 58(2), 338–48.

McClain, C. R., & Etter, R. J. (2005). Mid-domain models as predictors of species diversity patterns. *Oikos*, 109, 555–566.

Microsoft. Microsoft Excel for Mac, Version 15.20.

Mohedano-Navarrete, a., Reyes-Bonilla, H., & Lopez-Perez, R. a. (2008). Species richness and morphological diversity of the genus *Porites* in the Pacific Ocean. *Proceedings of the 11th International Coral Reef Symposium,* (26), 7–11.

Neige, P. (2003). Spatial patterns of disparity and diversity of the Recent cuttlefishes (Cephalopoda) across the Old World. *Journal of Biogeography*, 30, 1125–1137.

O'Brien, C. J., Peloquin, A. J., Vogt, M., Heinle, M., Gruber, N., Ajani, P., Andruleit, H., et al. (2013). Global marine plankton functional type biomass distributions: coccolithophores. *Earth System Science Data*, 5, 259–276.

Okada, H., & Honjo, S. (1973). The distribution of oceanic coccolithophores in the Pacific. *Deep Sea Research*, 20 (2748), 355–374.

Okada, H., & Honjo, S. (1975). Distribution of coccolithophores in marginal seas along the western Pacific Ocean and in the Red Sea. *Marine Biology*, 31(3), 271–285.

Okada, H., & McIntyre, A. (1979). Seasonal distribution of modern coccolithophores in the Western North Atlantic Ocean. *Marine Biology*, 54, 319–328.

Paasche, E., (1962) Coccolith formation. *Nature (London),* 193, 1094-1095.

Paasche, E. (2001). A review of the coccolithophorid *Emiliania huxleyi* (Prymnesiophyceae) with particular reference to growth, coccolith formation and calcification-photosynthesis interactions. *Phycologia,* 40, 503-529.

Palumbo, E., Flores, J. a., Perugia, C., Petrillo, Z., Voelker, a. H. L., & Amore, F. O. (2013). Millennial scale coccolithophore paleoproductivity and surface water changes between 445 and 360ka (Marine Isotope Stages 12/11) in the Northeast Atlantic. *Palaeogeography, Palaeoclimatology, Palaeoecology,* 383-384, 27–41.

Perch-Nielsen, K. (1985a) Mesozoic calcareous nannofossils. In: H. M. Bolli, J. B. Saunders, & K. Perch-Nielsen (Eds.)*, Plankton Stratigraphy*, (pp. 329-426), Cambridge, UK: Cambridge University Press.

Perch-Nielsen, K. (1985b) Cenozoic calcareous nannofossils. In: H. M. Bolli, J. B. Saunders, & K. Perch-Nielsen (Eds.), *Plankton Stratigraphy*, (pp. 427-554). Cambridge, UK: Cambridge University Press.

Poulton, A. J., Young, J. R., Bates, N., Balch, W. M. (2011). Biometry of detached *Emiliania huxleyi* coccoliths along the Patagonia Shelf. *Marine Ecology Progress Series*. 443,1-17.

Quinn, P. S., Cortés, M. Y., & Bollmann, J. (2005). Morphological variation in the deep ocean-dwelling coccolithophore *Florisphaera profunda* (Haptophyta). *European Journal of Phycology*, 40(1), 123-133.

R Core Team (2015). R: A language and environment for statistical computing. R Foundation for Statistical Computing. Vienna, Austria. https://www.R-project.org/

Reitan, T., Schweder, T., & Henderiks, J. (2012). Phenotypic evolution studied by layered stochastic differential equations. *The Annals of Applied Statistics*, 6(4), 1531–1551.

Ricklefs, R. E. (2012). Species richness and morphological diversity of passerine birds. *Proceedings of the National Academy of Sciences of the United States of America*, 109(36), 14482–14487.

Robin, X., Turck, N., Hainard, A., Tiberti, N., Lisacek, F., Sanchez, J. C., & Müller, M. (2011). pROC: an open-source package for R and S+ to analyze and compare ROC curves. *BMC Bioinformatics*, 12, 77.

Roy, K., Balch, D. P., & Hellberg, M. E. (2001). Spatial patterns of morphological diversity across the Indo-Pacific: analyses using strombid gastropods. *Proceedings. Biological Sciences / The Royal Society*, 268(1485), 2503–2508.

Roy, K., & Martien, K. K. (2001). Latitudinal distribution of body size in north-eastern Pacific marine bivalves. *Journal of Biogeography*, 28(4), 485–493.

Saez, A. G., Probert, I., Geisen, M., Quinn, P., Young, J. R., & Medlin, L. K. (2003). Pseudo-cryptic speciation in coccolithophores. *Proceedings of the National Academy of Sciences of the United States of America*, 100(12), 7163-8.

San Martin, E., Harris, R. P., & Irigoien, X. (2006). Latitudinal variation in plankton size spectra in the Atlantic Ocean. *Deep-Sea Research Part II: Topical Studies in Oceanography,* 53(14–16), 1560–1572.

Santoferrara, L. F., Grattepanche, J.-D., Katz, L. A., & McManus, G. B. (2016). Patterns and processes in microbial biogeography: do molecules and morphologies give the same answers? *The ISME Journal*, 10(7), 1779–1790.

Schmidt, D. N., Lazarus, D., Young, J. R., & Kucera, M. (2006). Biogeography and evolution of body size in marine plankton. *Earth-Science Reviews*, 78(3-4), 239-266.

Schueth, J. D., Keller, K., Bralower, T. J., & Patzkowsky, M. E. (2014). The Probable Datum Method (PDM): a technique for estimating the age of origination or extinction of nannoplankton. *Paleobiology*, 40(4), 541–559.

Schueth, J. D., Bralower, T. J., Jiang, S., & Patzkowsky, M. E. (2015). The role of regional survivor incumbency in the evolutionary recovery of calcareous nannoplankton from the Cretaceous/Paleogene (K/Pg) mass extinction. *Paleobiology,* 41(4), 661–679.

Sikes, C.S., and Wilbur, K.M., (1982). Functions of coccolith formation. *Limnology and Oceanography*, 27, 18–26.

Šlapeta, J., Moreira, D., López-García, P., (2005). The extent of protist diversity: insights from molecular ecology of freshwater eukaryotes. *Proceedings of the Royal Society B*, 272(1576), 2073–2081.

Smayda, T. J. (1970). The suspension and sinking of phytoplankton in the sea. *Oceanography and Marine Biology Annual Reviews*. 8, 353-414.

Sneath, P. H. A., and Sokal, R. R. (1973). *Numerical Taxonomy*. San Francisco, CA: W. H. Freeman.

Spalding, M. D., Agostini, V. N., Rice, J., & Grant, S. M. (2012). Pelagic provinces of the world: A biogeographic classification of the world's surface pelagic waters. *Ocean & Coastal Management*, 60, 19–30.

Spencer-Cervato, C., (1999). The Cenozoic deep sea microfossil record: explorations of the DSDP/ODP sample set using the Neptune database. *Palaeontologia Electronica*, 2(2), 270 pp.

Stevens, G. C. (1992). The elevational gradient in altitudinal range: an extension of Rapoport's latitudinal rule to altitude. *The American Naturalist*, 140(6), 893–911.

Stomp, M., Huisman, J., Mittelbach, G., Litchman, E., & Klausmeier, C. (2011). Large-scale biodiversity patterns in freshwater phytoplankton. *Ecology*, 92(11), 2096–2107.

Streng, M., Hildebrand-habel, T., & Willems, H. (2004). Long-term evolution of calcareous dinoflagellate associations since the Late Cretaceous: comparison of a high- and a low-latitude core from the Indian Ocean. *Journal of Nannoplankton Research*, 26(1), 13–45.

Triantaphyllou, M., Dimiza, M., Krasakopoulou, E., Malinverno, E., Lianou, V., & Souvermezoglou, E. (2008). Seasonal variation in *Emiliania huxleyi* coccolith morphology and calcification in the Aegean Sea (Eastern Mediterranean). *Geobios*, 43, 99–110.

Thomas, E. (2007). Cenozoic mass extinctions in the deep sea: what perturbs the largest habitat on Earth? *Geological Society of America Special Papers*. 424, 25-51.

Thomas, E., Brinkhuis, H., Huber, M., & Röhl, U. (2006). An ocean view of the Early Cenozoic greenhouse world. *Oceanography*, 19(4), 94–103.

Villalobos, F., & Arita, H. T. (2014). Morphological diversity at different spatial scales in a Neotropical bat assemblage. *Oecologia*, 176(2), 557–568.

Vogel, S. (1994). *Life in Moving Fluids: The Physical Biology of Flow*. Princeton, N J: Princeton University Press.

Vogel, S. (2006). *Comparative Biomechanics.* Princeton, N J: Princeton University Press.

Wainwright, P. C. (2007). Functional versus morphological diversity in macroevolution. *Annual Review of Ecology, Evolution, and Systematics*, 38(1), 381–401.

Walsby, A. E., and Xypolyta, A. (1977). The form resistance of chitin fibers attached to the cells of *Thalassiosira fluviatilis* (Hustedt). *British Phycological Journal*, 12, 215-23.

Willig, M. R., Kaufman, D. M., & Stevens, R. D. (2003). Latitudinal gradients of biodiversity: patterns, scale, and synthesis. *Annual Review of Ecology, Evolution, and Systematics*, 34(1), 273–309.

Wilson, D.B., (1996), Generating random spanning trees more quickly than the cover time. *Proceedings of the twenty-eighth annual ACM symposium on Theory of computing (AC),* 296-303.

Winter, A., Jordan, R. W., & Roth, P. H. (1994). Biogeogrpahy of living coccolithophores in ocean waters. In A. Winter & W. G. Siesser, (Eds.), *Coccolithophores* (pp.160-177). Cambridge, UK: Cambridge University Press.

Winter, A., & Siesser, W. G. (1994). Atlas of living coccolithophores. P107-159Winter, A. & Siesser, W. G. (Eds.), In A. Winter & W. G. Siesser, (Eds.), *Coccolithophores* (pp. 107-159). Cambridge, UK: Cambridge University Press.

Wolfram Research, Inc., Mathematica, Version 10.4.

Young, J. R. (1994). Function of coccoliths. In A. Winter & W. G. Siesser, (Eds.), *Coccolithophores* (pp13-38). Cambridge, UK: Cambridge University Press.

Young, J. R., & Bown, P. R., (1991) An ontogenetic sequence of coccoliths from the Late Jurassic Kimmeridge Clay of England. *Palaeontology*, 34(4), 843-850.

Young, J.R., Bergen, J.A., Bown, P.R., Burnett, J.A., Fiorentino, A., Jordan, R.W., Kleijne, A., Niel, B.E. van, Romein, A.J.T. & von Salis, K. (1997). Guidelines for coccolith and calcareous nannofossil terminology. *Palaeontology*, 40/4, 875-912.

Young, J.R., Bown P.R., Lees J.A. (18 Jan 2016). Nannotax3 website. International Nannoplankton Association. http://ina.tmsoc.org/Nannotax3

Young, J. R., Geisen, M., Cros, Lluïsa, Kleijne, A., Sprengel, C., Probert, I., & Østergaard, J. B. (2003). A guide to extant coccolithophore taxonomy. *Journal of Nannoplankton Research Special Issue*, 1, 1–125.

Young, J. R., & Henriksen, K. (2003). Biomineralization within vesicles: the calcite of coccoliths. *Reviews in Mineralogy and Geochemistry*, 54(1), 189-215.

Young, J. R., Henriksen, K., Probert, I. (2004). Structure and morphogenesis of the coccoliths of the CODENET species. In H. R. Thierstein, & J. R. Young, (Eds.) *Coccolithophores From Molecular Processes to Global Impact* (pp. 191-216). Berlin, Heidelberg, Germany: Springer-Verlag.

Young, J. R., Andruleit, H., & Probert, I. (2009). Coccolith function and morphogenesis: insights from appendage-bearing coccolithophores of the family Syracosphaeraceae (Haptophyta). *Journal of Phycology*, 45(1), 213–226.

Appendix A.1. Experimental sinking data for all models, conducted in March and September 2013, and the physical calculations derived from them. The characteristic length is the model radius at its widest diameter. Empirical model volumes are based on the weight difference measured in water and in air (see Chapter 2 for details).

Run	Date of run	Characteristic length (m)	Mass (kg)	Time (sec) to travel 10cm)	Velocity (m/s)	Empirical model volume (mL)
Floriform.1	Sept 2-6, 2013	0.0135	2.160E-03	13.7	7.30E-03	5.01E-03
Floriform.2	Sept 2-6, 2014	0.0135	2.160E-03	13.24	7.55E-03	1.00E-02
Floriform.3	Sept 2-6, 2015	0.0135	2.160E-03	13.9	7.19E-03	1.84E-01
Floriform.4	Sept 2-6, 2016	0.0135	2.160E-03	13.75	7.27E-03	2.26E-01
Floriform.5	Sept 2-6, 2017	0.0135	2.160E-03	13.93	7.18E-03	2.24E-01
Floriform.6	Sept 2-6, 2018	0.0135	2.160E-03	13.64	7.33E-03	3.64E-01
Floriform.7	Sept 2-6, 2019	0.0135	2.160E-03	12.36	8.09E-03	4.13E-01
Floriform.8	Sept 2-6, 2020	0.0135	2.160E-03	13.62	7.34E-03	5.53E-01
Floriform.9	Sept 2-6, 2021	0.0135	2.160E-03	13	7.69E-03	5.95E-01
Floriform.10	March, 2013	0.0135	2.160E-03	10.5	9.52E-03	6.84E-01
Floriform.11	March, 2013	0.0135	2.160E-03	12.98	7.70E-03	3.26E-01
Floriform.12	March, 2013	0.0135	2.160E-03	13.71	7.29E-03	3.26E-01
Floriform.13	March, 2013	0.0135	2.160E-03	12.54	7.97E-03	3.26E-01
Small Placoliths.1	Sept 2-6, 2013	0.00575	2.183E-03	11.42	8.76E-03	8.42E-02
Small Placoliths.2	Sept 2-6, 2014	0.00575	2.183E-03	11.43	8.75E-03	4.32E-01
Small Placoliths.3	Sept 2-6, 2015	0.00575	2.183E-03	11.7	8.55E-03	6.30E-01
Small Placoliths.4	Sept 2-6, 2016	0.00575	2.183E-03	10.06	9.94E-03	3.82E-01
Small Placoliths.5	Sept 2-6, 2017	0.00575	2.183E-03	9.73	1.03E-02	3.82E-01
Small Placoliths.6	Sept 2-6, 2018	0.00575	2.183E-03	10.52	9.51E-03	3.82E-01
Small Placoliths.7	Sept 2-6, 2019	0.00575	2.183E-03	10.37	9.64E-03	3.82E-01
Small Placoliths.8	Sept 2-6, 2020	0.00575	2.183E-03	10.53	9.50E-03	3.82E-01
Small Placoliths.9	Sept 2-6, 2021	0.00575	2.183E-03	10.15	9.85E-03	3.82E-01
Small Placoliths.10	Sept 2-6, 2022	0.00575	2.183E-03	10.62	9.42E-03	3.82E-01
Small Placoliths.11	Sept 2-6, 2023	0.00575	2.183E-03	11.21	8.92E-03	3.82E-01
Small Placoliths.12	March, 2013	0.00575	2.183E-03	10.06	9.94E-03	3.82E-01
Small Placoliths.13	March, 2013	0.00575	2.183E-03	10.16	9.84E-03	3.82E-01
Small Placoliths.14	March, 2013	0.00575	2.183E-03	10.17	9.83E-03	3.82E-01
Medium Placoliths.1	Sept 2-6, 2012	0.00575	2.160E-03	9.59	1.04E-02	1.00E-02
Medium Placoliths.2	Sept 2-6, 2013	0.00575	2.160E-03	9.27	1.08E-02	9.03E-02
Medium Placoliths.3	Sept 2-6, 2014	0.00575	2.160E-03	10.18	9.82E-03	3.25E-01
Medium Placoliths.4	Sept 2-6, 2015	0.00575	2.160E-03	9.86	1.01E-02	5.83E-01
Medium Placoliths.5	Sept 2-6, 2016	0.00575	2.160E-03	9.8	1.02E-02	6.40E-01
Medium Placoliths.6	Sept 2-6, 2017	0.00575	2.160E-03	10.36	9.65E-03	7.67E-01
Medium Placoliths.7	Sept 2-6, 2018	0.00575	2.160E-03	9.92	1.01E-02	9.06E-01
Medium Placoliths.8	Sept 2-6, 2019	0.00575	2.160E-03	9.52	1.05E-02	4.74E-01
Medium Placoliths.9	Sept 2-6, 2020	0.00575	2.160E-03	9.78	1.02E-02	4.74E-01
Medium Placoliths.10	Sept 2-6, 2021	0.00575	2.160E-03	9.73	1.03E-02	4.74E-01
Medium Placoliths.11	Sept 2-6, 2022	0.00575	2.160E-03	8.96	1.12E-02	4.74E-01
Medium Placoliths.12	March, 2013	0.00575	2.160E-03	9.6	1.04E-02	4.74E-01
Medium Placoliths.13	March, 2013	0.00575	2.160E-03	9.88	1.01E-02	4.74E-01
Medium Placoliths.14	March, 2013	0.00575	2.160E-03	9.14	1.09E-02	4.74E-01
Large Placoliths.1	Sept 2-6, 2011	0.00575	2.167E-03	13.03	7.67E-03	1.68E-01
Large Placoliths.2	Sept 2-6, 2012	0.00575	2.167E-03	12.65	7.91E-03	3.02E-01
Large Placoliths.3	Sept 2-6, 2013	0.00575	2.167E-03	13.34	7.50E-03	6.93E-01
Large Placoliths.4	Sept 2-6, 2014	0.00575	2.167E-03	12.95	7.72E-03	1.58E+00
Large Placoliths.5	Sept 2-6, 2015	0.00575	2.167E-03	13.59	7.36E-03	6.86E-01
Large Placoliths.6	Sept 2-6, 2016	0.00575	2.167E-03	13.4	7.46E-03	6.86E-01
Large Placoliths.7	Sept 2-6, 2017	0.00575	2.167E-03	13.7	7.30E-03	6.86E-01
Large Placoliths.8	Sept 2-6, 2018	0.00575	2.167E-03	13.28	7.53E-03	6.86E-01
Large Placoliths.9	Sept 2-6, 2019	0.00575	2.167E-03	14	7.14E-03	6.86E-01
Large Placoliths.10	Sept 2-6, 2020	0.00575	2.167E-03	12.3	8.13E-03	6.86E-01
Large Placoliths.11	March, 2013	0.00575	2.167E-03	12.58	7.95E-03	6.86E-01
Large Placoliths.12	March, 2013	0.00575	2.167E-03	12.77	7.83E-03	6.86E-01
Large Placoliths.13	March, 2013	0.00575	2.167E-03	13.34	7.50E-03	6.86E-01
Large Placoliths.14	March, 2013	0.00575	2.167E-03	12.4	8.06E-03	6.86E-01
Umbelliform.1	Sept 2-6, 2008	0.0125	4.207E-03	22.95	4.36E-03	6.29E-01
Umbelliform.2	Sept 2-6, 2009	0.0125	4.207E-03	18.79	5.32E-03	6.80E-01
Umbelliform.3	Sept 2-6, 2010	0.0125	4.207E-03	19.17	5.22E-03	1.52E+00
Umbelliform.4	Sept 2-6, 2011	0.0125	4.207E-03	16.64	6.01E-03	1.65E+00
Umbelliform.5	Sept 2-6, 2012	0.0125	4.207E-03	18.61	5.37E-03	1.70E+00
Umbelliform.6	Sept 2-6, 2013	0.0125	4.207E-03	18.92	5.29E-03	1.73E+00
Umbelliform.7	Sept 2-6, 2014	0.0125	4.207E-03	18.71	5.34E-03	1.89E+00
Umbelliform.8	Sept 2-6, 2015	0.0125	4.207E-03	21.06	4.75E-03	1.95E+00
Umbelliform.9	Sept 2-6, 2016	0.0125	4.207E-03	17.45	5.73E-03	2.05E+00
Umbelliform.10	Sept 2-6, 2017	0.0125	4.207E-03	18.8	5.32E-03	1.53E+00
Umbelliform.11	March, 2013	0.0125	4.207E-03	18.87	5.30E-03	1.53E+00
Umbelliform.12	March, 2013	0.0125	4.207E-03	17.74	5.64E-03	1.53E+00

Appendix A.2. Experimental sinking data for all models, conducted in March and September 2013, and the physical calculations derived from them. Model density calculated using measured mass and empirical volumes. Fluid density calculated using the mass of a known volume of karo syrup. Fluid dynamic viscosity calculated using equation 11.2 in Vogel (2006), and spherical weights of known mass.

Run	Calculated model density (kg/m3)	Fluid density (kg/m^3)	Fluid dynamic viscosity (Pa S or kg/(ms)
Floriform.1	4.307E+05	1.339E+03	4.141E+00
Floriform.2	2.154E+05	1.339E+03	4.141E+00
Floriform.3	1.177E+04	1.339E+03	4.141E+00
Floriform.4	9.572E+03	1.339E+03	4.141E+00
Floriform.5	9.658E+03	1.339E+03	4.141E+00
Floriform.6	5.933E+03	1.339E+03	4.141E+00
Floriform.7	5.227E+03	1.339E+03	4.141E+00
Floriform.8	3.909E+03	1.339E+03	4.141E+00
Floriform.9	3.632E+03	1.339E+03	4.141E+00
Floriform.10	3.158E+03	1.362E+03	3.689E+00
Floriform.11	6.633E+03	1.362E+03	3.689E+00
Floriform.12	6.633E+03	1.362E+03	3.689E+00
Floriform.13	6.633E+03	1.362E+03	3.689E+00
Small Placoliths.1	2.591E+04	1.339E+03	4.141E+00
Small Placoliths.2	5.050E+03	1.339E+03	4.141E+00
Small Placoliths.3	3.466E+03	1.339E+03	4.141E+00
Small Placoliths.4	5.712E+03	1.339E+03	4.141E+00
Small Placoliths.5	5.712E+03	1.339E+03	4.141E+00
Small Placoliths.6	5.712E+03	1.339E+03	4.141E+00
Small Placoliths.7	5.712E+03	1.339E+03	4.141E+00
Small Placoliths.8	5.712E+03	1.339E+03	4.141E+00
Small Placoliths.9	5.712E+03	1.339E+03	4.141E+00
Small Placoliths.10	5.712E+03	1.339E+03	4.141E+00
Small Placoliths.11	5.712E+03	1.339E+03	4.141E+00
Small Placoliths.12	5.712E+03	1.362E+03	3.689E+00
Small Placoliths.13	5.712E+03	1.362E+03	3.689E+00
Small Placoliths.14	5.712E+03	1.362E+03	3.689E+00
Medium Placoliths.1	2.154E+05	1.339E+03	4.141E+00
Medium Placoliths.2	2.393E+04	1.339E+03	4.141E+00
Medium Placoliths.3	6.647E+03	1.339E+03	4.141E+00
Medium Placoliths.4	3.707E+03	1.339E+03	4.141E+00
Medium Placoliths.5	3.376E+03	1.339E+03	4.141E+00
Medium Placoliths.6	2.815E+03	1.339E+03	4.141E+00
Medium Placoliths.7	2.385E+03	1.339E+03	4.141E+00
Medium Placoliths.8	4.553E+03	1.339E+03	4.141E+00
Medium Placoliths.9	4.553E+03	1.339E+03	4.141E+00
Medium Placoliths.10	4.553E+03	1.339E+03	4.141E+00
Medium Placoliths.11	4.553E+03	1.339E+03	4.141E+00
Medium Placoliths.12	4.553E+03	1.362E+03	3.689E+00
Medium Placoliths.13	4.553E+03	1.362E+03	3.689E+00
Medium Placoliths.14	4.553E+03	1.362E+03	3.689E+00
Large Placoliths.1	1.286E+04	1.339E+03	4.141E+00
Large Placoliths.2	7.178E+03	1.339E+03	4.141E+00
Large Placoliths.3	3.127E+03	1.339E+03	4.141E+00
Large Placoliths.4	1.373E+03	1.339E+03	4.141E+00
Large Placoliths.5	3.161E+03	1.339E+03	4.141E+00
Large Placoliths.6	3.161E+03	1.339E+03	4.141E+00
Large Placoliths.7	3.161E+03	1.339E+03	4.141E+00
Large Placoliths.8	3.161E+03	1.339E+03	4.141E+00
Large Placoliths.9	3.161E+03	1.339E+03	4.141E+00
Large Placoliths.10	3.161E+03	1.339E+03	4.141E+00
Large Placoliths.11	3.161E+03	1.362E+03	3.689E+00
Large Placoliths.12	3.161E+03	1.362E+03	3.689E+00
Large Placoliths.13	3.161E+03	1.362E+03	3.689E+00
Large Placoliths.14	3.161E+03	1.362E+03	3.689E+00
Umbelliform.1	6.690E+03	1.339E+03	4.141E+00
Umbelliform.2	6.187E+03	1.339E+03	4.141E+00
Umbelliform.3	2.772E+03	1.339E+03	4.141E+00
Umbelliform.4	2.553E+03	1.339E+03	4.141E+00
Umbelliform.5	2.479E+03	1.339E+03	4.141E+00
Umbelliform.6	2.429E+03	1.339E+03	4.141E+00
Umbelliform.7	2.222E+03	1.339E+03	4.141E+00
Umbelliform.8	2.152E+03	1.339E+03	4.141E+00
Umbelliform.9	2.051E+03	1.339E+03	4.141E+00
Umbelliform.10	2.743E+03	1.339E+03	4.141E+00
Umbelliform.11	2.743E+03	1.362E+03	3.689E+00
Umbelliform.12	2.743E+03	1.362E+03	3.689E+00

Appendix A.3. Experimental sinking data for all models, conducted in March and September 2013, and the physical calculations derived from them. These Stokes radii are based on equation 11.2 in Vogel (2006), and are presented in Mathematica syntax with coefficients multiplied through.

Run	Stokes radius equation (Vogel. 2006 eq. 11.2)	Stokes radius (m)(Vogel 2006, eq. 11.2)
Floriform.1	Solve[(0.021168/(78.0639 *a))==225794.5023*a^2,a]	1.06E-03
Floriform.2	Solve[(0.021168/(78.0639 *a))==112545.2291*a^2,a]	1.34E-03
Floriform.3	Solve[(0.021168/(78.0639 *a))==5484.4192*a^2,a]	3.67E-03
Floriform.4	Solve[(0.021168/(78.0639 *a))==4329.2351*a^2,a]	3.97E-03
Floriform.5	Solve[(0.021168/(78.0639 *a))==4374.3768*a^2,a]	3.96E-03
Floriform.6	Solve[(0.021168/(78.0639 *a))==2415.7485*a^2,a]	4.82E-03
Floriform.7	Solve[(0.021168/(78.0639 *a))==2044.7025*a^2,a]	5.10E-03
Floriform.8	Solve[(0.021168/(78.0639 *a))==1351.2743*a^2,a]	5.85E-03
Floriform.9	Solve[(0.021168/(78.0639 *a))==1205.7021*a^2,a]	4.65E-03
Floriform.10	Solve[(0.021168/(69.5384 *a))==1060.2153*a^2,a]	6.08E-03
Floriform.11	Solve[(0.021168/(69.5384 *a))==3013.7540*a^2,a]	4.66E-03
Floriform.12	Solve[(0.021168/(69.5384 *a))==3013.7540*a^2,a]	4.66E-03
Floriform.13	Solve[(0.021168/(69.5384 *a))==3013.7540*a^2,a]	4.66E-03
Small Placoliths.1	Solve[(0.021392/(78.0639 *a))==12920.9266*a^2,a]	2.77E-03
Small Placoliths.2	Solve[(0.021392/(78.0639 *a))==1951.3844*a^2,a]	5.20E-03
Small Placoliths.3	Solve[(0.021392/(78.0639 *a))==1118.3846*a^2,a]	6.26E-03
Small Placoliths.4	Solve[(0.021392/(78.0639 *a))==2300.8757*a^2,a]	4.92E-03
Small Placoliths.5	Solve[(0.021392/(78.0639 *a))==2300.8757*a^2,a]	4.92E-03
Small Placoliths.6	Solve[(0.021392/(78.0639 *a))==2300.8757*a^2,a]	4.92E-03
Small Placoliths.7	Solve[(0.021392/(78.0639 *a))==2300.8757*a^2,a]	4.92E-03
Small Placoliths.8	Solve[(0.021392/(78.0639 *a))==2300.8757*a^2,a]	4.92E-03
Small Placoliths.9	Solve[(0.021392/(78.0639 *a))==2300.8757*a^2,a]	4.92E-03
Small Placoliths.10	Solve[(0.021392/(78.0639 *a))==2300.8757*a^2,a]	4.92E-03
Small Placoliths.11	Solve[(0.021392/(78.0639 *a))==2300.8757*a^2,a]	4.92E-03
Small Placoliths.12	Solve[(0.021392/(69.5384*a))==2569.4353*a^2,a]	4.93E-03
Small Placoliths.13	Solve[(0.021392/(69.5384*a))==2569.4353*a^2,a]	4.93E-03
Small Placoliths.14	Solve[(0.021392/(69.5384*a))==2569.4353*a^2,a]	4.93E-03
Medium Placoliths.1	Solve[(0.021168/(78.0639 *a))==112545.2291*a^2,a]	1.34E-03
Medium Placoliths.2	Solve[(0.021168/(78.0639 *a))==11879.1878*a^2,a]	2.84E-03
Medium Placoliths.3	Solve[(0.021168/(78.0639 *a))==2791.2818*a^2,a]	4.60E-03
Medium Placoliths.4	Solve[(0.021168/(78.0639 *a))==1245.1466*a^2,a]	6.02E-03
Medium Placoliths.5	Solve[(0.021168/(78.0639 *a))==1071.0005*a^2,a]	6.33E-03
Medium Placoliths.6	Solve[(0.021168/(78.0639 *a))==776.3162*a^2,a]	7.04E-03
Medium Placoliths.7	Solve[(0.021168/(78.0639 *a))==550.0783*a^2,a]	7.90E-03
Medium Placoliths.8	Solve[(0.021168/(78.0639 *a))==1692.2327*a^2,a]	5.43E-03
Medium Placoliths.9	Solve[(0.021168/(78.0639 *a))==1692.2327*a^2,a]	5.43E-03
Medium Placoliths.10	Solve[(0.021168/(78.0639 *a))==1692.2327*a^2,a]	5.43E-03
Medium Placoliths.11	Solve[(0.021168/(78.0639 *a))==1692.2327*a^2,a]	5.43E-03
Medium Placoliths.12	Solve[(0.021168/(69.5384 *a))==1886.1720*a^2,a]	5.44E-03
Medium Placoliths.13	Solve[(0.021168/(69.5384 *a))==1886.1720*a^2,a]	5.44E-03
Medium Placoliths.14	Solve[(0.021168/(69.5384 *a))==1886.1720*a^2,a]	5.44E-03
Large Placoliths.1	Solve[(0.021237/(78.0639 *a))==6058.8085*a^2,a]	3.55E-03
Large Placoliths.2	Solve[(0.021237/(78.0639 *a))==3070.5613*a^2,a]	4.46E-03
Large Placoliths.3	Solve[(0.021237/(78.0639 *a))==940.1634*a^2,a]	6.61E-03
Large Placoliths.4	Solve[(0.021237/(78.0639 *a))==17.76493*a^2,a]	2.48E-02
Large Placoliths.5	Solve[(0.021237/(78.0639 *a))==957.0512*a^2,a]	6.58E-03
Large Placoliths.6	Solve[(0.021237/(78.0639 *a))==957.0512*a^2,a]	6.58E-03
Large Placoliths.7	Solve[(0.021237/(78.0639 *a))==957.0512*a^2,a]	6.58E-03
Large Placoliths.8	Solve[(0.021237/(78.0639 *a))==957.0512*a^2,a]	6.58E-03
Large Placoliths.9	Solve[(0.021237/(78.0639 *a))==957.0512*a^2,a]	6.58E-03
Large Placoliths.10	Solve[(0.021237/(78.0639 *a))==957.0512*a^2,a]	6.58E-03
Large Placoliths.11	Solve[(0.021237/(69.5384 *a))==1060.8565*a^2,a]	6.60E-03
Large Placoliths.12	Solve[(0.021237/(69.5384 *a))==1060.8565*a^2,a]	6.60E-03
Large Placoliths.13	Solve[(0.021237/(69.5384 *a))==1060.8565*a^2,a]	6.60E-03
Large Placoliths.14	Solve[(0.021237/(69.5384 *a))==1060.8565*a^2,a]	6.60E-03
Umbelliform.1	Solve[(0.0412286/(78.0639 *a))==2813.8594*a^2,a]	5.73E-03
Umbelliform.2	Solve[(0.0412286/(78.0639 *a))==2549.2366*a^2,a]	5.92E-03
Umbelliform.3	Solve[(0.0412286/(78.0639 *a))==753.7916*a^2,a]	8.88E-03
Umbelliform.4	Solve[(0.0412286/(78.0639 *a))==638.4407*a^2,a]	9.39E-03
Umbelliform.5	Solve[(0.0412286/(78.0639 *a))==599.5619*a^2,a]	9.59E-03
Umbelliform.6	Solve[(0.0412286/(78.0639 *a))==573.1421*a^2,a]	9.73E-03
Umbelliform.7	Solve[(0.0412286/(78.0639 *a))==464.2276*a^2,a]	1.04E-02
Umbelliform.8	Solve[(0.0412286/(78.0639 *a))==427.6622*a^2,a]	1.07E-02
Umbelliform.9	Solve[(0.0412286/(78.0639 *a))==374.5346*a^2,a]	1.12E-02
Umbelliform.10	Solve[(0.0412286/(78.0639 *a))==738.0912*a^2,a]	8.94E-03
Umbelliform.11	Solve[(0.0412286/(69.5384 *a))==815.0518*a^2,a]	8.99E-03
Umbelliform.12	Solve[(0.0412286/(69.5384 *a))==815.0518*a^2,a]	8.99E-03

Appendix A.4. Experimental sinking data for all models, conducted in March and September 2013, and the physical calculations derived from them. These Stokes radii are based on equation 15.12 in Vogel (194), and are presented in Mathematica syntax with coefficients multiplied through.

Run	Dimensionless Stokes radius (Vogel 2006, eq.11.2)	Stokes radius equation (Vogel. 1994, eq. 15.12)	Stokes radius (m)(Vogel 1994, eq. 15.12)
Floriform.1	7.87E-02	Solve[0.021168-(54962.1663*a^3)==0.5698*a,a]	6.80E-03
Floriform.2	9.93E-02	Solve[0.021168-(54962.1663*a^3)==0.5896*a,a]	6.78E-03
Floriform.3	2.72E-01	Solve[0.021168-(54962.1663*a^3)==0.5616*a,a]	6.81E-03
Floriform.4	2.94E-01	Solve[0.021168-(54962.1663*a^3)==0.5677*a,a]	6.80E-03
Floriform.5	2.93E-01	Solve[0.021168-(54962.1663*a^3)==0.5604*a,a]	6.81E-03
Floriform.6	3.57E-01	Solve[0.021168-(54962.1663*a^3)==0.5723*a,a]	6.80E-03
Floriform.7	3.78E-01	Solve[0.021168-(54962.1663*a^3)==0.6316*a,a]	6.75E-03
Floriform.8	4.34E-01	Solve[0.021168-(54962.1663*a^3)==0.5732*a,a]	6.80E-03
Floriform.9	3.44E-01	Solve[0.021168-(54962.1663*a^3)==0.6005*a,a]	6.78E-03
Floriform.10	4.50E-01	Solve[0.021168-(55903.03784*a^3)==0.6623*a,a]	6.69E-03
Floriform.11	3.45E-01	Solve[0.021168-(55903.03784*a^3)==0.5357*a,a]	6.79E-03
Floriform.12	3.45E-01	Solve[0.021168-(55903.03784*a^3)==0.5072*a,a]	6.82E-03
Floriform.13	3.45E-01	Solve[0.021168-(55903.03784*a^3)==0.5545*a,a]	6.78E-03
Small Placoliths.1	4.81E-01	Solve[0.02139-(54962.1663*a^3)==0.6836*a,a]	6.73E-03
Small Placoliths.2	9.04E-01	Solve[0.02139-(54962.1663*a^3)==0.6830*a,a]	6.73E-03
Small Placoliths.3	1.09E+00	Solve[0.02139-(54962.1663*a^3)==0.6672*a,a]	6.75E-03
Small Placoliths.4	8.56E-01	Solve[0.02139-(54962.1663*a^3)==0.7760*a,a]	6.66E-03
Small Placoliths.5	8.56E-01	Solve[0.02139-(54962.1663*a^3)==0.8023*a,a]	6.64E-03
Small Placoliths.6	8.56E-01	Solve[0.02139-(54962.1663*a^3)==0.7421*a,a]	6.69E-03
Small Placoliths.7	8.56E-01	Solve[0.02139-(54962.1663*a^3)==0.7528*a,a]	6.68E-03
Small Placoliths.8	8.56E-01	Solve[0.02139-(54962.1663*a^3)==0.7413*a,a]	6.69E-03
Small Placoliths.9	8.56E-01	Solve[0.02139-(54962.1663*a^3)==0.7691*a,a]	6.66E-03
Small Placoliths.10	8.56E-01	Solve[0.02139-(54962.1663*a^3)==0.7351*a,a]	6.69E-03
Small Placoliths.11	8.56E-01	Solve[0.02139-(54962.1663*a^3)==0.6964*a,a]	6.72E-03
Small Placoliths.12	8.57E-01	Solve[0.021392-(55903.03784*a^3)==0.6912*a,a]	6.69E-03
Small Placoliths.13	8.57E-01	Solve[0.021392-(55903.03784*a^3)==0.6844*a,a]	6.70E-03
Small Placoliths.14	8.57E-01	Solve[0.021392-(55903.03784*a^3)==0.6838*a,a]	6.70E-03
Medium Placoliths.1	2.33E-01	Solve[0.021168-(54962.1663*a^3)==0.8140*a,a]	6.60E-03
Medium Placoliths.2	4.93E-01	Solve[0.021168-(54962.1663*a^3)==0.8421*a,a]	6.58E-03
Medium Placoliths.3	7.99E-01	Solve[0.021168-(54962.1663*a^3)==0.7668*a,a]	6.64E-03
Medium Placoliths.4	1.05E+00	Solve[0.021168-(54962.1663*a^3)==0.7917*a,a]	6.62E-03
Medium Placoliths.5	1.10E+00	Solve[0.021168-(54962.1663*a^3)==0.7966*a,a]	6.61E-03
Medium Placoliths.6	1.22E+00	Solve[0.021168-(54962.1663*a^3)==0.7535*a,a]	6.66E-03
Medium Placoliths.7	1.37E+00	Solve[0.021168-(54962.1663*a^3)==0.7869*a,a]	6.62E-03
Medium Placoliths.8	9.45E-01	Solve[0.021168-(54962.1663*a^3)==0.8200*a,a]	6.59E-03
Medium Placoliths.9	9.45E-01	Solve[0.021168-(54962.1663*a^3)==0.7982*a,a]	6.61E-03
Medium Placoliths.10	9.45E-01	Solve[0.021168-(54962.1663*a^3)==0.8023*a,a]	6.61E-03
Medium Placoliths.11	9.45E-01	Solve[0.021168-(54962.1663*a^3)==0.8712*a,a]	6.55E-03
Medium Placoliths.12	9.47E-01	Solve[0.021168-(55903.03784*a^3)==0.7244*a,a]	6.64E-03
Medium Placoliths.13	9.47E-01	Solve[0.021168-(55903.03784*a^3)==0.7038*a,a]	6.66E-03
Medium Placoliths.14	9.47E-01	Solve[0.021168-(55903.03784*a^3)==0.7608*a,a]	6.61E-03
Large Placoliths.1	6.18E-01	Solve[0.02124-(54962.1663*a^3)==0.5991*a,a]	6.79E-03
Large Placoliths.2	7.75E-01	Solve[0.02124-(54962.1663*a^3)==0.6171*a,a]	6.77E-03
Large Placoliths.3	1.15E+00	Solve[0.02124-(54962.1663*a^3)==0.5852*a,a]	6.80E-03
Large Placoliths.4	4.32E+00	Solve[0.02124-(54962.1663*a^3)==0.6028*a,a]	6.78E-03
Large Placoliths.5	1.14E+00	Solve[0.02124-(54962.1663*a^3)==0.5744*a,a]	6.81E-03
Large Placoliths.6	1.14E+00	Solve[0.02124-(54962.1663*a^3)==0.5826*a,a]	6.80E-03
Large Placoliths.7	1.14E+00	Solve[0.02124-(54962.1663*a^3)==0.5698*a,a]	6.81E-03
Large Placoliths.8	1.14E+00	Solve[0.02124-(54962.1663*a^3)==0.5878*a,a]	6.80E-03
Large Placoliths.9	1.14E+00	Solve[0.02124-(54962.1663*a^3)==0.5576*a,a]	6.82E-03
Large Placoliths.10	1.14E+00	Solve[0.02124-(54962.1663*a^3)==0.6347*a,a]	6.76E-03
Large Placoliths.11	1.15E+00	Solve[0.02124-(55903.03784*a^3)==0.5528*a,a]	6.79E-03
Large Placoliths.12	1.15E+00	Solve[0.02124-(55903.03784*a^3)==0.5445*a,a]	6.80E-03
Large Placoliths.13	1.15E+00	Solve[0.02124-(55903.03784*a^3)==0.5213*a,a]	6.81E-03
Large Placoliths.14	1.15E+00	Solve[0.02124-(55903.03784*a^3)==0.5608*a,a]	6.78E-03
Umbelliform.1	4.58E-01	Solve[0.04122-(54962.1663*a^3)==0.3401*a,a]	8.86E-03
Umbelliform.2	4.73E-01	Solve[0.04122-(54962.1663*a^3)==0.4155*a,a]	8.81E-03
Umbelliform.3	7.11E-01	Solve[0.04122-(54962.1663*a^3)==0.4072*a,a]	8.81E-03
Umbelliform.4	7.51E-01	Solve[0.04122-(54962.1663*a^3)==0.4691*a,a]	8.77E-03
Umbelliform.5	7.67E-01	Solve[0.04122-(54962.1663*a^3)==0.4195*a,a]	8.81E-03
Umbelliform.6	7.78E-01	Solve[0.04122-(54962.1663*a^3)==0.4126*a,a]	8.81E-03
Umbelliform.7	8.35E-01	Solve[0.04122-(54962.1663*a^3)==0.4172*a,a]	8.81E-03
Umbelliform.8	8.58E-01	Solve[0.04122-(54962.1663*a^3)==0.3707*a,a]	8.81E-03
Umbelliform.9	8.97E-01	Solve[0.04122-(55903.03784*a^3)==0.4474*a,a]	8.74E-03
Umbelliform.10	7.16E-01	Solve[0.04122-(55903.03784*a^3)==0.4152*a,a]	8.76E-03
Umbelliform.11	7.19E-01	Solve[0.04122-(55903.03784*a^3)==0.3685*a,a]	8.79E-03
Umbelliform.12	7.19E-01	Solve[0.04122-(55903.03784*a^3)==0.3920*a,a]	8.78E-03

Appendix B. Part 1. Binary character coding for the 104 species included in this dissertation. Explanation of characters is included as Appendix C. Characters 1 to 44 pertain to coccolith morphology, while characters 45 to 76 pertain to coccosphere morphology.

Coccolith characters																
	Character 1	Character 2	Character 3	Character 4	Character 5	Character 6	Character 7	Character 8	Character 9	Character 10	Character 11	Character 12	Character 13	Character 14	Character 15	Character 16
Emiliania huxleyi-TypeA	0	0	1	0	0	1	0	0	1 NA		1	1 NA		0	0	0
Gephyrocapsa oceanica	0	0	1	0	0	1	0	0	0 NA		0	0 NA		0	0	0
Gephyrocapsa muellerae	0	0	1	0	0	1	0	1	0 NA		0	0 NA		0	0	0
Gephyrocapsa ericsonii-ericsonii	0	0	1	0	0	1	0	1	0 NA		0	1 NA		0	0	0
Gephyrocapsa ornata	0	0	1	0	0	1	0	0	0 NA		0	1 NA		0	0	0
Reticulofenestra parvula	0	0	1	0	0	1	0	0	0 NA		0	0 NA		0	0	0
Reticulofenestra sessilis	0	0	1	0	0	1	0	1	0 NA		0	0 NA		0	0	0
Cruciplacolithus neohelis	0	0	1	0	0	0	0	0	0 NA		1	0	0	0	0	0
Calcidiscus leptoporus-leptoporus	0	1	0	0	0	1	0	0	0 NA		1	0 NA		0	0	0
Oolithotus antillarum	1	0	0	1	1	0	1	0	0	0	0	0	0	0	0	0
Oolithotus fragilis	1	0	0	1	0	0	0	0	0	0	0	0 NA		0	0	0
Hayaster perplexus	1	1	0	0	1	0	0	0	0	1	0	0	0	0	0	0
Umbilicosphaera sibogae	0	1	0	0	0	1	0	0	0 NA		1	0 NA		0	0	0
Umbilicosphaera anulus	0	0	1	0	0	1	0	0	0 NA		0	0 NA		0	0	0
Umbilicosphaera foliosa	0	1	0	0	0	0	0	0	0 NA		1	0 NA		0	0	0
Umbilicosphaera hulburtiana	0	0	1	0	0	0	0	0	0	0	0	0	0	1	0	0
Pleurochrysis carterae-carterae	0	0	1	0	0	0	0	0	0	1	0 NA		0	0	0	0
Pleurochrysis gayraliae	0	1	0	0	1	0	0	0	0	1	0	0	0	0	0	0
Pleurochrysis placolithoides	0	0	0	0	1	0	0	0	0	1	0	0	0	0	0	0
Pleurochrysis roscoffensis	0	0	0	0	1	0	0	0	0	1	0	0	0	1	0	0
Pleurochrysis pseudoroscoffensis	0	0	0	0	1	0	0	0	0	1	0	0	0	0	0	0
Hymenomonas globosa	0	0	1	0	0	1	0	1	0 NA		0	0 NA		0	0	0
Hymenomonas lacuna	0	0	1	0	0	1	0	1	0 NA		0	0 NA		0	0	0
Hymenomonas roseola	0	0	1	0	0	1	0	1	0 NA		0	0 NA		0	0	0
Ochrosphaera neapolitana	0	0	1	0	1	1	0	0	0 NA		0	0 NA		0	0	0
Jomonlithus littoralis	0	0	1	0	0	1	0	0	0 NA		0	0 NA		0	0	0
Helicosphaera carteri	1	0	0	1	0	0	1	0	0 NA		0	0 NA		0	0	0
Helicosphaera hyalina	0	0	0	1	0	0	1	0	0 NA		0	0 NA		1	0	0
Helicosphaera wallichii	0	0	0	1	0	0	1	0	0 NA		0	0 NA		1	0	0
Helicosphaera pavimentum	0	0	0	1	0	0	1	0	0 NA		0	0 NA		1	0	0
Pontosphaera discopora	0	0	0	0	0	0	0	0	0	0	1	0	0	1	0	0
Pontosphaera japonica	0	0	0	0	0	0	0	0	0	0	0	0	0	0	0	0
Pontosphaera multipora	0	0	1	0	0	0	0	0	0	0	1	0	0	0	0	0
Pontosphaera syracusana	0	0	1	0	0	0	0	0	0	0	1	0	0	0	0	0
Scyphosphaera apsteinii	0	0	1	0	0	0	0	0	0	0	0	0	0	0	0	0
Scyphosphaera porosa	0	0	1	0	0	0	0	0	0	0	1	0	0	0	0	0
Calciopappus caudatus	0	0	1	0	0	1	0	0	0 NA		0	0 NA		0	0	0
Calciopappus rigidus	0	0	1	0	0	1	0	0	0 NA		1	0 NA		0	0	0
Michaelsarsia adriaticus	0	0	1	0	0	1	0	0	0 NA		0	0 NA		0	0	0
Michaelsarsia elegans	0	0	1	0	0	1	0	0	0 NA		0	0 NA		0	0	0
Ophiaster hydroideus	0	0	1	0	0	1	0	0	0 NA		0	0 NA		0	0	0
Ophiaster formosus	0	0	1	0	0	1	0	0	0 NA		0	0 NA		0	0	0
Ophiaster reductus	0	0	1	0	0	1	0	0	0 NA		0	0 NA		0	0	0
Syracosphaera anthos	0	0	1	0	0	1	0	0	0 NA		0	0 NA		0	0	0
Syracosphaera lamina	0	0	1	0	0	1	0	1	0 NA		0	0 NA		1	0	0
Syracosphaera tumularis	0	0	1	0	0	1	0	1	0 NA		0	0 NA		1	0	0
Syracosphaera bannockii	0	0	1	0	0	1	0	0	0 NA		0	0 NA		0	0	0
Syracosphaera pulchra	0	0	1	0	0	0	0	0	0	0	0	0 NA		0	0	0
Syracosphaera histrica	0	0	1	0	0	0	0	0	0 NA		0	0	0	0	0	0
Syracosphaera noroitica	0	0	1	0	0	1	0	0	0 NA		0	0 NA		0	0	0
Syracosphaera corolla	0	0	1	0	0	1	0	0	0 NA		1	0 NA		0	0	0
Syracosphaera ossa-Type1	0	0	1	0	0	1	0	0	0 NA		0	0 NA		0	0	0

Appendix B. Part 2. Binary character coding for the 104 species included in this dissertation. Explanation of characters is included as Appendix C. Characters 1 to 44 pertain to coccolith morphology, while characters 45 to 76 pertain to coccosphere morphology.

	Character 17	Character 18	Character 19	Character 20	Character 21	Character 22	Character 23	Character 24	Character 25	Character 26	Character 27	Character 28	Character 29	Character 30	Character 31
Emiliania huxleyi-TypeA	0	0	1	0	0	0	0	0	1	0	0	1	1	0 NA	
Gephyrocapsa oceanica	0	0	1	0	0	0	0	0	1	0	0	1	1	0 NA	
Gephyrocapsa muellerae	0	0	1	0	1	0	0	0	1	0	0	0	1	0 NA	
Gephyrocapsa ericsonii-ericsonii	0	0	1	0	0	0	0	0	1	0	0	0	1	1	0
Gephyrocapsa ornata	0	0	1	0	0	0	0	0	1	0	0	1	1	1	0
Reticulofenestra parvula	0	0	1	0	0	0	0	0	1	0	0	1	1	0 NA	
Reticulofenestra sessilis	0	0	1	0	0	0	0	1	0	0	0	1	0	0 NA	
Cruciplacolithus neohelis	0	0	1	1	0	0	1	0	0	0	0	0 NA		0 NA	
Calcidiscus leptoporus-leptoporus	0	1	0	0	1	0	0	1	0	0	0	0	1	0 NA	0
Oolithotus antillarum	1	1	0	0	1	0	1	0	0	0	0	0	0	0	0
Oolithotus fragilis	0	0	0	0	1	0	0	1	0	0	0	0	1	0	0
Hayaster perplexus	1	1	0	0	1	0	0	1	0	0	0	0	1	1	0
Umbilicosphaera sibogae	0	1	0	0	0	0	1	0	0	0	0	0 NA		0 NA	
Umbilicosphaera anulus	0	0	1	1	0	0	1	0	0	0	0	0 NA		0 NA	
Umbilicosphaera foliosa	0	1	0	0	0	1	1	0	0	0	0	0 NA		1	0
Umbilicosphaera hulburtiana	0	0	1	0	0	1	1	0	0	0	0	0 NA		0 NA	
Pleurochrysis carterae-carterae	0	0	1	1	0	1	1	0	0	0	0	0 NA		0 NA	
Pleurochrysis gayraliae	0	0	1	1	0	0	1	0	0	0	0	0 NA		0 NA	
Pleurochrysis placolithoides	0	0	1	1	0	0	1	0	0	0	0	0 NA		0 NA	
Pleurochrysis roscoffensis	0	0	1	1	0	0	1	0	0	0	0	0 NA		1	0
Pleurochrysis pseudoroscoffensis	0	0	1	1	0	0	1	0	0	0	0	0 NA		1	0
Hymenomonas globosa	0	0	1	1	0	0	1	0	0	0	0	0 NA		0 NA	
Hymenomonas lacuna	0	0	1	1	0	1	1	0	0	0	0	0 NA		0 NA	
Hymenomonas roseola	0	0	1	1	0	0	1	0	0	0	0	0 NA		0 NA	
Ochrosphaera neapolitana	1	0	1	0	0	1	1	0	0	0	0	0 NA		0 NA	
Jomonlithus littoralis	0	0	1	1	0	0	1	0	0	0	0	0 NA		0 NA	
Helicosphaera carteri	0	0	1	1	0	0	0	1	0	0	0	1	0	0 NA	
Helicosphaera hyalina	0	0	1	0	0	0	0	1	0	0	1	0	0	0 NA	
Helicosphaera wallichii	0	0	1	0	0	1	0	1	0	0	0	1	0	0 NA	
Helicosphaera pavimentum	0	0	1	1	0	0	0	1	0	0	0	1	0	0 NA	
Pontosphaera discopora	0	0	1	1	0	0	0	0	0	1	1	0	0	0 NA	
Pontosphaera japonica	0	0	1	0	0	0	0	0	0	0	1	0	0	0 NA	
Pontosphaera multipora	0	0	1	1	0	0	0	0	0	1	0	1	0	0 NA	
Pontosphaera syracusana	0	0	1	1	0	0	0	1	0	0	1	0	0	0 NA	
Scyphosphaera apsteinii	0	0	1	0	0	0	0	1	0	0	1	0	0	0 NA	
Scyphosphaera porosa	0	0	1	1	0	0	0	0	0	1	0	1	1	0	0
Calciopappus caudatus	0	0	1	1	0	0	0	0	1	0	0	1	1	0 NA	
Calciopappus rigidus	0	0	1	1	0	0	0	0	1	0	0	1	1	0 NA	
Michaelsarsia adriaticus	0	0	1	1	0	0	0	0	1	0	0	1	1	0 NA	
Michaelsarsia elegans	0	0	1	1	0	0	0	0	1	0	0	1	1	0 NA	
Ophiaster hydroideus	0	0	1	1	0	0	0	0	1	0	0	1	1	0 NA	
Ophiaster formosus	0	0	1	1	0	0	0	1	1	0	0	0	1	0 NA	
Ophiaster reductus	0	0	1	1	0	0	0	1	0	0	0	0	1	0 NA	
Syracosphaera anthos	0	0	1	1	0	0	0	0	1	0	0	1	1	0 NA	
Syracosphaera lamina	0	0	1	1	0	0	0	0	1	0	0	1	1	1	0
Syracosphaera tumularis	0	0	1	1	0	0	0	0	1	0	0	1	1	0 NA	
Syracosphaera bannockii	0	0	1	1	0	0	0	0	1	0	0	1	1	0 NA	
Syracosphaera pulchra	0	0	1	1	0	0	0	1	0	0	0	1	1	1	0
Syracosphaera histrica	0	0	1	1	0	0	0	0	1	0	0	1	1	0 NA	
Syracosphaera noroitica	0	0	1	1	0	0	0	0	1	0	0	1	1	0 NA	
Syracosphaera corolla	0	0	1	1	0	0	0	0	1	0	0	1	1	0 NA	
Syracosphaera ossa-Type1	0	0	1	0	0	0	0	0	1	0	1	1	1	0 NA	

Appendix B. Part 3. Binary character coding for the 104 species included in this dissertation. Explanation of characters is included as Appendix C. Characters 1 to 44 pertain to coccolith morphology, while characters 45 to 76 pertain to coccosphere morphology.

														Coccosphere characters	
	Character 32	Character 33	Character 34	Character 35	Character 36	Character 37	Character 38	Character 39	Character 40	Character 41	Character 4	Character 43	Character 44	Character 45	Character 46
Emiliania huxleyi-TypeA	NA	NA	NA	0	0	0	0	0	NA	NA	NA	NA	NA	1	0
Gephyrocapsa oceanica	NA	NA	NA	0	0	0	1	0	1	1	0	0	0	1	0
Gephyrocapsa muellerae	NA	NA	NA	0	0	0	0	0	NA	NA	NA	NA	NA	1	1
Gephyrocapsa ericsonii-ericsonii	0	0	0	0	0	0	0	0	NA	NA	NA	NA	NA	1	1
Gephyrocapsa ornata	0	1	0	0	0	0	0	0	NA	NA	NA	NA	NA	1	0
Reticulofenestra parvula	NA	NA	NA	0	0	0	0	0	NA	NA	NA	NA	NA	1	0
Reticulofenestra sessilis	NA	NA	NA	0	0	0	0	0	NA	NA	NA	NA	NA	1	0
Cruciplacolithus neohelis	NA	NA	NA	1	1	1	0	0	NA	NA	NA	NA	NA	1	0
Calcidiscus leptoporus-leptoporus	NA	NA	NA	0	0	0	0	0	NA	NA	NA	NA	NA	1	0
Oolithotus antillarum	0	0	0	0	0	0	0	0	NA	NA	NA	NA	NA	1	0
Oolithotus fragilis	0	0	0	0	0	0	0	0	NA	NA	NA	NA	NA	1	1
Hayaster perplexus	1	0	0	0	0	0	0	0	NA	NA	NA	NA	NA	1	1
Umbilicosphaera sibogae	NA	NA	NA	0	0	0	0	0	NA	NA	NA	NA	NA	1	1
Umbilicosphaera anulus	NA	NA	NA	0	0	0	0	0	NA	NA	NA	NA	NA	1	1
Umbilicosphaera foliosa	0	0	1	0	0	0	0	0	NA	NA	NA	NA	NA	1	0
Umbilicosphaera hulburtiana	NA	NA	NA	0	0	0	0	0	NA	NA	NA	NA	NA	1	1
Pleurochrysis carterae-carterae	NA	NA	NA	0	0	0	0	0	NA	NA	NA	NA	NA	1	1
Pleurochrysis gayraliae	NA	NA	NA	0	0	0	0	0	NA	NA	NA	NA	NA	1	1
Pleurochrysis placolithoides	NA	NA	NA	0	0	0	0	0	NA	NA	NA	NA	NA	1	1
Pleurochrysis roscoffensis	0	0	1	0	0	0	0	0	NA	NA	NA	NA	NA	1	1
Pleurochrysis pseudoroscoffensis	0	0	1	0	0	0	0	0	NA	NA	NA	NA	NA	1	1
Hymenomonas globosa	NA	NA	NA	0	0	0	1	0	0	1	0	1	0	1	1
Hymenomonas lacuna	NA	NA	NA	0	0	0	1	0	0	1	0	1	0	1	1
Hymenomonas roseola	NA	NA	NA	0	0	0	1	0	1	1	0	1	0	1	1
Ochrosphaera neapolitana	NA	NA	NA	0	0	0	1	0	0	0	0	1	0	1	1
Jomonlithus littoralis	NA	NA	NA	0	0	0	0	0	NA	NA	NA	NA	NA	1	1
Helicosphaera carteri	NA	NA	NA	0	0	1	0	0	NA	NA	NA	NA	NA	1	0
Helicosphaera hyalina	NA	NA	NA	0	0	0	0	0	NA	NA	NA	NA	NA	1	0
Helicosphaera wallichii	NA	NA	NA	0	0	1	0	0	NA	NA	NA	NA	NA	1	0
Helicosphaera pavimentum	NA	NA	NA	0	0	1	0	0	NA	NA	NA	NA	NA	1	1
Pontosphaera discopora	NA	NA	NA	0	0	0	0	1	1	1	0	0	0	1	1
Pontosphaera japonica	NA	NA	NA	0	0	0	0	1	1	1	0	0	0	1	1
Pontosphaera multipora	NA	NA	NA	0	0	0	0	1	1	0	0	0	0	1	1
Pontosphaera syracusana	NA	NA	NA	0	0	0	0	1	1	1	0	1	0	1	0
Scyphosphaera apsteinii	NA	NA	NA	0	0	0	0	1	1	0	1	0	0	1	0
Scyphosphaera porosa	0	0	0	0	0	0	0	1	1	1	0	0	0	1	0
Calciopappus caudatus	NA	NA	NA	0	0	0	1	0	1	1	0	0	0	1	0
Calciopappus rigidus	NA	NA	NA	0	0	0	1	0	1	1	0	0	0	1	0
Michaelsarsia adriaticus	NA	NA	NA	0	0	0	1	0	0	1	0	0	0	1	0
Michaelsarsia elegans	NA	NA	NA	0	0	0	1	0	0	1	0	0	0	1	0
Ophiaster hydroideus	NA	NA	NA	0	0	0	1	0	0	1	0	0	0	1	0
Ophiaster formosus	NA	NA	NA	0	0	0	1	0	0	1	0	0	0	1	0
Ophiaster reductus	NA	NA	NA	0	0	0	1	0	0	1	0	0	0	1	0
Syracosphaera anthos	NA	NA	NA	0	0	0	0	1	0	1	0	0	0	1	0
Syracosphaera lamina	0	0	0	0	0	0	0	1	0	1	0	0	0	1	1
Syracosphaera tumularis	NA	NA	NA	0	0	0	0	1	0	1	0	0	0	1	1
Syracosphaera bannockii	NA	NA	NA	0	0	0	0	1	0	1	0	0	0	1	1
Syracosphaera pulchra	1	0	0	0	0	0	1	1	0	1	0	0	0	1	0
Syracosphaera histrica	NA	NA	NA	0	0	0	0	1	0	1	0	0	0	1	0
Syracosphaera noroitica	NA	NA	NA	0	0	0	0	1	0	1	0	0	0	1	1
Syracosphaera corolla	NA	NA	NA	0	0	0	1	0	0	1	0	1	0	1	1
Syracosphaera ossa-Type1	NA	NA	NA	0	0	0	0	0	NA	NA	NA	NA	NA	1	0

Appendix B. Part 4. Binary character coding for the 104 species included in this dissertation. Explanation of characters is included as Appendix C. Characters 1 to 44 pertain to coccolith morphology, while characters 45 to 76 pertain to coccosphere morphology.

	Character 47	Character 48	Character 49	Character 50	Character 51	Character 52	Character 53	Character 54	Character 55	Character 56	Character 57	Character 58	Character 59	Character 60	Character 61
Emiliania huxleyi-TypeA	1	0	0	0	0 NA	0	0	0	1	1	0	0 NA	NA	NA	0
Gephyrocapsa oceanica	NA	0	0	0	0	0	0	0	1	1	1	0	1	0	0
Gephyrocapsa muellerae	0	0	0	0	0 NA	0	0	0	1	1	1	0	1	0	0
Gephyrocapsa ericsonii-ericsonii	0	0	0	0	0 NA	1	0	0	0 NA		1	0	1	0	0
Gephyrocapsa ornata	1	0	0	0	0 NA	0	0	0	1	0	1	0	1	1	0
Reticulofenestra parvula	1	0	0	0	0 NA	0	0	0	1	1	0	0 NA	NA		0
Reticulofenestra sessilis	1	0	0	0	0 NA	0	0	0	1	1	0	0 NA	NA		0
Cruciplacolithus neohelis	1	0	0	0	0 NA	1	0	0	0 NA		0	0 NA	NA		0
Calcidiscus leptoporus-leptoporus	1	0	0	0	0 NA	0	0	0	1	1	0	0 NA	NA		0
Oolithotus antillarum	1	1	0	0	0 NA	1	0	0	0 NA		0	0 NA	NA		0
Oolithotus fragilis	0	0	0	0	0 NA	1	0	0	0	0	0	0 NA	NA		0
Hayaster perplexus	0	0	0	0	0 NA	1	0	0	0 NA		0	0 NA	NA		0
Umbilicosphaera sibogae	0	0	0	0	0 NA	1	0	0	0 NA		0	0 NA	NA		0
Umbilicosphaera anulus	0	0	0	0	0 NA	1	0	0	0 NA		0	0 NA	NA		0
Umbilicosphaera foliosa	1	0	0	0	0 NA	1	0	0	0 NA		0	0 NA	NA		0
Umbilicosphaera hulburtiana	0	0	0	0	0 NA	NA		1	0 NA		0	0 NA	NA		0
Pleurochrysis carterae-carterae	0	0	0	0	0 NA		1	0	0 NA		0	0 NA	NA		0
Pleurochrysis gayraliae	0	0	0	0	0 NA		1	0	0 NA		0	0 NA	NA		0
Pleurochrysis placolithoides	0	0	0	0	0 NA		1	0	0 NA		0	0 NA	NA		0
Pleurochrysis roscoffensis	0	0	0	0	0 NA		1	0	0 NA		0	0 NA	NA		0
Pleurochrysis pseudoroscoffensis	0	0	0	0	0 NA		1	0	0 NA		0	0 NA	NA		0
Hymenomonas globosa	0	0	0	0	0 NA		1	0	0 NA		0	0 NA	NA		0
Hymenomonas lacuna	0	0	0	0	0 NA		1	0	0 NA		0	0 NA	NA		0
Hymenomonas roseola	0	0	0	0	0 NA		1	0	0 NA		0	0 NA	NA		0
Ochrosphaera neapolitana	0	0	0	0	0 NA		1	0	0 NA		0	0 NA	NA		0
Jomonlithus littoralis	0	0	0	0	0 NA		1	0	0 NA		0	0 NA	NA		0
Helicosphaera carteri	1	1	0	1	0 NA		1	0	0 NA		0	0 NA	NA		0
Helicosphaera hyalina	1	1	0	0	0 NA		1	0	0 NA		0	0 NA	NA		0
Helicosphaera wallichii	1	1	0	0	0 NA		1	0	0 NA		0	0 NA	NA		0
Helicosphaera pavimentum	0	1	0	0	1	0	1	0	0 NA		0	0 NA	NA		0
Pontosphaera discopora	0	0	0	0	0 NA		1	0	0 NA		0	0 NA	NA		0
Pontosphaera japonica	0	0	0	0	0 NA		1	0	0 NA		0	0 NA	NA		0
Pontosphaera multipora	0	0	0	0	0 NA		1	0	0 NA		0	0 NA	NA		0
Pontosphaera syracusana	1	0	0	0	0 NA		1	0	0 NA		1	0	1	0	0
Scyphosphaera apsteinii	1	0	0	0	0 NA		1	0	0 NA		1	1	1	1	0
Scyphosphaera porosa	1	0	0	0	0 NA		1	0	0 NA		1	1	1	1	0
Calciopappus caudatus	1	1	1	0	1	1	1	0	0 NA		1	1	1	1	0
Calciopappus rigidus	1	1	0	0	1	0	1	0	0 NA		1	1	1	1	0
Michaelsarsia adriaticus	1	1	0	0	1	0	1	0	0 NA		1	1	1	1	0
Michaelsarsia elegans	1	1	0	0	1	0	1	0	0 NA		1	1	1	1	0
Ophiaster hydroideus	1	0	0	0	0 NA		1	0	0 NA		1	0	0	1	1
Ophiaster formosus	1	0	0	0	0 NA		0	2	0	1	1	0	0	1	1
Ophiaster reductus	1	0	0	0	0 NA		1	0	0 NA		1	0	0	1	1
Syracosphaera anthos	1	0	0	0	0 NA		0	1	0	1	0	0 NA	NA		0
Syracosphaera lamina	0	1	1	0	1	0	0	1	0	0	0	0 NA	NA		0
Syracosphaera tumularis	0	0	0	0	0 NA		0	1	0	0	0	0 NA	NA		0
Syracosphaera bannockii	0	1	0	0	1 NA		0	1	0	1	0	0 NA	NA		0
Syracosphaera pulchra	1	1	0	0	1	0	0	1	0	1	1	1	1	0	0
Syracosphaera histrica	1	1	0	0	1	1	0	1	0	1	1	0	0	0	0
Syracosphaera noroitica	0	1	0	0	0 NA		0	1	0	1	1	0	0	0	0
Syracosphaera corolla	0	1	0	0	1	1	0	1	0	0	0	0 NA	NA		0
Syracosphaera ossa-Type1	1	0	0	0	0 NA		0	1	0	0	1	1	0	0	0

Appendix B. Part 5. Binary character coding for the 104 species included in this dissertation. Explanation of characters is included as Appendix C. Characters 1 to 44 pertain to coccolith morphology, while characters 45 to 76 pertain to coccosphere morphology.

	Character 62	Character 63	Character 64	Character 65	Character 66	Character 67	Character 68	Character 69	Character 70	Character 71	Character 72	Character 73	Character 74	Character 75	Character 76
Emiliania huxleyi-TypeA	1	0	0	0	0	0	0	0	1	0	1	1	0	0	1
Gephyrocapsa oceanica	1	0	0	0	0	0	0	0	1	0	1	0	0	0	1
Gephyrocapsa muellerae	1	0	0	0	0	0	0	0	1	0	1	0	0	0	1
Gephyrocapsa ericsonii-ericsonii	1	0	0	0	0	0	0	0	1	0	1	0	0	0	1
Gephyrocapsa ornata	1	0	0	0	0	0	0	0	1	0	1	0	0	0	1
Reticulofenestra parvula	1	0	0	0	0	0	0	0	1	0	1	0	0	0	1
Reticulofenestra sessilis	1	0	0	0	0	0	0	0	1	1	1	0	0	0	1
Cruciplacolithus neohelis	1	0	0	0	0	0	0	0	1	0	1	0	0	0	1
Calcidiscus leptoporus-leptoporus	1	0	0	0	0	0	0	0	1	1	1	0	0	0	0
Oolithotus antillarum	1	0	0	0	0	1	0	0	1	1	1	0	1	0	0
Oolithotus fragilis	1	0	0	0	NA	1	0	0	1	1	1	0	1	0	0
Hayaster perplexus	1	0	0	0	0	0	0	0	1	1	1	0	0	0	0
Umbilicosphaera sibogae	1	0	0	0	0	0	0	0	1	0	1	0	0	0	1
Umbilicosphaera anulus	1	0	0	0	0	0	0	0	1	1	0	0	0	0	1
Umbilicosphaera foliosa	1	0	0	0	0	0	0	0	1	0	1	0	0	0	1
Umbilicosphaera hulburtiana	1	0	0	0	0	0	0	0	0	NA	1	0	0	0	1
Pleurochrysis carterae-carterae	1	0	0	0	0	0	0	1	0	NA	1	0	0	1	1
Pleurochrysis gayraliae	1	0	0	0	0	0	0	1	0	NA	0	0	0	1	1
Pleurochrysis placolithoides	1	0	0	0	0	0	0	1	1	0	1	0	0	0	1
Pleurochrysis roscoffensis	1	0	0	0	0	0	1	0	1	1	1	0	0	1	1
Pleurochrysis pseudoroscoffensis	1	0	0	0	0	0	0	1	1	0	1	0	0	1	1
Hymenomonas globosa	1	0	0	0	0	0	0	1	0	NA	0	0	0	1	1
Hymenomonas lacuna	1	0	0	0	0	0	0	1	0	NA	0	0	0	1	1
Hymenomonas roseola	1	0	0	0	0	0	0	1	0	NA	0	0	0	1	1
Ochrosphaera neapolitana	1	0	0	0	0	0	0	1	0	NA	1	0	0	1	1
Jomonlithus littoralis	1	0	0	0	0	0	0	1	0	NA	0	0	0	1	1
Helicosphaera carteri	1	0	0	1	NA	1	0	0	1	1	1	0	1	0	1
Helicosphaera hyalina	1	0	0	1	NA	0	1	0	1	1	1	0	1	0	0
Helicosphaera wallichii	1	0	0	1	NA	1	1	0	1	1	1	0	1	1	0
Helicosphaera pavimentum	1	0	0	1	NA	0	1	1	1	1	1	0	1	1	0
Pontosphaera discopora	1	0	0	0		1	0	1	0	NA	0	0	0	1	1
Pontosphaera japonica	1	0	0	0	0	0	0	1	0	NA	0	0	0	1	1
Pontosphaera multipora	0	0	1	0	0	1	0	1	0	NA	0	0	0	1	1
Pontosphaera syracusana	0	0	1	0	0	1	0	1	0	NA	0	0	0	1	1
Scyphosphaera apsteinii	0	1	0	0	0	0	0	1	0	0	1	0	0	1	1
Scyphosphaera porosa	0	1	0	0	0	0	0	1	0	NA	1	0	1	1	1
Calciopappus caudatus	0	1	0	0	1	0	0	1	0	NA	0	0	0	1	1
Calciopappus rigidus	0	0	1	0	1	0	0	1	0	0	0	0	0	1	1
Michaelsarsia adriaticus	0	0	1	0	1	0	0	1	0	NA	0	0	0	1	1
Michaelsarsia elegans	0	0	1	0	1	0	0	1	0	0	0	0	0	1	1
Ophiaster hydroideus	0	0	1	1	1	0	0	1	0	NA	0	0	0	1	1
Ophiaster formosus	0	0	1	0	1	0	0	1	0	NA	0	0	0	1	1
Ophiaster reductus	0	0	1	1	1	0	0	1	0	NA	0	0	0	1	1
Syracosphaera anthos	0	0	1	0	1	0	0	1	0	0	0	0	1	1	1
Syracosphaera lamina	0	1	0	0	0	0	0	1	0	NA	0	0	0	1	1
Syracosphaera tumularis	0	1	0	0	0	0	0	1	0	NA	0	0	0	1	1
Syracosphaera bannockii	0	0	1	0	1	0	0	1	0	0	0	0	0	1	1
Syracosphaera pulchra	0	0	1	0	1	0	1	1	0	NA	0	0	1	1	1
Syracosphaera histrica	0	0	1	1	1	0	0	1	0	NA	0	0	1	1	0
Syracosphaera noroitica	0	0	1	1	1	0	0	1	0	NA	0	0	0	1	1
Syracosphaera corolla	0	1	0	0	0	0	0	1	0	NA	0	0	1	1	1
Syracosphaera ossa-Type1	0	0	1	1	1	1	0	0	1	0	0	0	1	1	1

Appendix B. Part 6. Binary character coding for the 104 species included in this dissertation. Explanation of characters is included as Appendix C. Characters 1 to 44 pertain to coccolith morphology, while characters 45 to 76 pertain to coccosphere morphology.

	Character 1	Character 2	Character 3	Character 4	Character 5	Character 6	Character 7	Character 8	Character 9	Character 10	Character 11	Character 12	Character 13	Character 14	Character 15	Character 16
Syracosphaera epigrosa	0	0	1	0	0	1	0	0	0 NA		0	0 NA		0	0	0
Syracosphaera borealis-Type1	0	0	1	0	0	1	0	0	0 NA		0	0 NA		0	0	0
Syracosphaera exigua	0	0	1	0	0	1	0	0	0 NA		1	0 NA		1	0	0
Syracosphaera rotula	0	0	1	0	0	1	0	0	0 NA		0	0 NA		0	0	0
Syracosphaera ampliora	1	0	1	0	0	1	0	0	0 NA		0	0 NA		0	0	0
Coronosphaera mediterranea	0	0	1	0	0	0	0	0	0	1	1	0	0	0	0	0
Coronosphaera binodata	0	0	1	0	0	0	0	0	0	1	1	0	0	0	0	0
Coronosphaera maxima	0	0	1	0	0	0	0	0	0	1	1	0	0	0	0	0
Calciosolenia murrayi	0	0	1	0	1	1	0	0	0 NA		0	0 NA		0	0	0
Calciosolenia brasiliensis	0	0	1	0	1	1	0	0	0 NA		0	0 NA		0	0	0
Alveosphaera bimurata	0	0	1	0	0	1	0	1	0 NA		0	0 NA		0	0	0
Rhabdosphaera clavigera-clavigera	0	0	1	0	0	0	0	0	0	1	0	0	0	0	0	0
Rhabdosphaera xiphos	0	0	1	0	0	0	0	0	0	0	0	0	0	0	0	0
Palusphaera vandelii	0	1	0	0	0	0	0	0	0	0	0	0	0	0	0	0
Discosphaera tubifera	1	1	0	0	0	0	0	0	0	0	0	0	1	0	0	0
Acanthoica quattrospina	0	0	1	0	0	0	0	0	0	0	0	0	1	0	0	0
Acanthoica janchenii	0	0	1	0	0	0	0	0	0	1	0	0	0	0	0	0
Acanthoica acanthifera	0	0	1	0	0	0	0	0	0	0	0	0	1	0	0	0
Acanthoica biscayensis	0	0	1	0	0	0	0	0	0	0	0	0	1	0	0	0
Anacanthoica acanthos	0	0	1	0	0	0	0	0	0	0	0	0	1	0	0	0
Cyrtosphaera aculeata	0	0	1	0	0	0	0	0	0	1	0	0	1	0	0	0
Algirosphaera robusta	0	0	1	0	0	0	0	0	1	0	0	0	1	0	0	0
Algirosphaera cucullata	0	0	1	0	0	0	0	0	1	0	0	0	1	0	0	0
Algirosphaera meteora	0	0	1	0	0	0	0	0	1	0	0	0	1	0	0	0
Solisphaera emidasia	0	0	1	0	0	0	0	0	0	0	0	0	0	0	0	0
Solisphaera helianthiformis	0	0	1	0	0	0	0	0	0	0	0	0	0	0	0	0
Alisphaera unicornis-spatula	0	0	1	0	0	1	0	0	0 NA		0	0 NA		1	1	0
Alisphaera pinnigera	0	0	1	0	0	1	0	0	0 NA		1	0 NA		1	1	0
Alisphaera capulata	1	0	0	1	0	1	1	0	0 NA		0	0 NA		1	1	1
Alisphaera ordinata	1	0	0	1	0	1	1	0	0 NA		1	0 NA		1	1	1
Alisphaera quadrilatera	1	0	0	1	0	1	1	0	0 NA		0	0 NA		1	1	1
Alisphaera extenta	1	0	0	1	0	1	1	0	0 NA		0	0 NA		0	1	1
Alisphaera gaudii	1	0	0	1	0	1	0	0	0 NA		0	0 NA		1	0	1
Umbellosphaera irregularis	1	0	0	1	0	1	1	0	0 NA		0	0 NA		0	0	0
Umbellosphaera tenuis-Type1	1	0	0	1	0	1	1	0	0 NA		0	0 NA		0	0	0
Papposphaera borealis	0	0	1	0	0	0	0	0	1	0	0	0	0	0	0	0
Papposphaera lepida	1	1	0	0	1	0	0	0	1	0	0	0	0	0	0	0
Pappomonas flabellifera	0	0	1	0	0	0	0	0	1	0	0	0	0	0	0	0
Pappomonas borealis	0	0	1	0	0	0	0	0	1	0	0	0	0	0	0	0
Pappomonas garrisonii	1	0	1	0	0	0	0	1	1	0	0	0	0	0	0	0
Pappomonas weddellensis	0	0	1	0	0	0	0	1	1	0	0	0	0	0	0	0
Picarola margalefii	0	0	1	0	0	1	0	0	0 NA		0	0 NA		0	0	0
Wigwamma arctica	0	1	0	0	0	0	0	0	1	1	0	0	0	1	0	0
Wigwamma triradiata	0	1	0	0	0	0	0	0	1	0	0	0	0	0	0	0
Wigwamma annulifera	0	1	0	0	0	0	0	0	1	0	0	0	0	0	0	0
Wigwamma antarctica	0	0	1	0	0	1	0	0	1 NA		0	0 NA		0	0	0
Wigwamma amatura	0	0	1	0	0	0	0	0	1	0	0	0	0	0	0	0
Kataspinifera baumannii	0	0	1	0	0	1	0	0	1 NA		1	0 NA		0	0	0
Calyptrosphaera sphaeroidea	0	0	1	0	1	1	0	0	0 NA		0	0 NA		0	0	0
Tetralithoides quadrilaminata	1	0	1	0	0	1	0	0	0 NA		1	0 NA		0	1	0
Placorhombus ziveriae	0	0	1	0	1	1	0	0	0 NA		0	0 NA		0	0	0
Tergestiella adriaticus	1	1	0	0	0	0	0	0	0	1	1	0	1	0	0	0

Appendix B. Part 7. Binary character coding for the 104 species included in this dissertation. Explanation of characters is included as Appendix C. Characters 1 to 44 pertain to coccolith morphology, while characters 45 to 76 pertain to coccosphere morphology.

	Character 17	Character 18	Character 19	Character 20	Character 21	Character 22	Character 23	Character 24	Character 25	Character 26	Character 27	Character 28	Character 29	Character 30	Character 31
Syracosphaera epigrosa	0	0	1	0	0	0	0	0	1	0	1	1	1	1	0
Syracosphaera borealis-Type1	0	0	1	0	0	0	0	0	1	0	0	1	1	0 NA	
Syracosphaera exigua	0	0	1	1	0	0	0	0	1	0	0	1	1	0 NA	
Syracosphaera rotula	0	0	1	1	0	0	0	0	1	0	0	1	1	0 NA	
Syracosphaera ampliora	0	0	1	1	0	0	0	0	1	0	0	1	1	0 NA	
Coronosphaera mediterranea	0	0	1	1	0	1	0	1	1	0	0	1	1	0 NA	
Coronosphaera binodata	0	0	1	0	0	0	0	0	1	0	0	1	1	1	0
Coronosphaera maxima	0	0	1	1	0	1	0	1	1	0	0	1	1	0 NA	
Calciosolenia murrayi	1	0	1	1	0	0	0	1	0	0	0	0	1	0 NA	
Calciosolenia brasiliensis	1	0	1	1	0	1	0	0	1	0	0	1	1	0 NA	
Alveosphaera bimurata	0	0	1	1	0	1	1	0	0	0	0	0 NA		0 NA	
Rhabdosphaera clavigera-clavigera	0	0	1	1	0	0	0	1	0	0	0	0	1	1	1
Rhabdosphaera xiphos	0	0	1	1	0	0	0	1	0	0	0	0	0	1	1
Palusphaera vandelii	0	1	0	1	0	0	0	1	0	0	0	0	0	1	1
Discosphaera tubifera	0	1	0	0	0	0	0	1	0	0	0	0	0	1	1
Acanthoica quattrospina	0	0	1	0	0	0	0	1	0	0	0	0	0	0 NA	
Acanthoica janchenii	0	0	1	0	0	0	0	1	0	0	0	0	0	0 NA	
Acanthoica acanthifera	0	0	0	0	0	0	0	1	0	0	0	0	0	0 NA	
Acanthoica biscayensis	0	0	1	1	0	0	0	1	0	0	0	0	0	0 NA	
Anacanthoica acanthos	0	0	1	1	0	0	0	1	0	0	0	0	0	0 NA	
Cyrtosphaera aculeata	0	0	0	0	0	0	0	1	0	0	0	0	0	1	0
Algirosphaera robusta	0	0	1	0	0	1	0	1	0	0	0	0	0	1	0
Algirosphaera cucullata	0	0	1	1	0	1	0	1	0	0	0	0	0	1	0
Algirosphaera meteora	0	0	1	0	0	1	0	1	0	0	0	0	0	1	0
Solisphaera emidasia	0	0	0	0	0	1	0	1	0	0	0	0	0	1	0
Solisphaera helianthiformis	0	0	0	0	0	1	0	1	0	0	0	0	0	1	0
Alisphaera unicornis-spatula	0	0	1	0	0	1	0	1	0	0	0	0	1	0 NA	
Alisphaera pinnigera	0	0	1	0	0	1	0	1	0	0	0	0	1	0 NA	
Alisphaera capulata	0	0	0	0	0	0	0	1	0	0	0	0	1	0 NA	
Alisphaera ordinata	0	0	0	0	0	0	0	1	0	0	0	0	1	0 NA	
Alisphaera quadrilatera	0	0	0	0	0	1	0	1	0	0	0	0	1	0 NA	
Alisphaera extenta	0	0	0	0	0	1	0	1	0	0	0	0	1	0 NA	
Alisphaera gaudii	0	0	1	0	0	1	0	1	0	0	0	0	1	0 NA	
Umbellosphaera irregularis	0	0	1	0	1	0	0	0	1	0	0	0	1	0 NA	
Umbellosphaera tenuis-Type1	0	0	1	0	1	0	0	0	1	0	0	0	1	0 NA	
Papposphaera borealis	0	0	1	1	0	0	0	0	1	0	0	0	0	1	1
Papposphaera lepida	0	0	1	1	0	0	0	0	0	0	0	0 NA		1	1
Pappomonas flabellifera	0	0	1	1	0	0	0	0	0	0	0	1	1	0 NA	
Pappomonas borealis	0	0	1	1	0	0	0	0	0	0	0	1	1	0 NA	
Pappomonas garrisonii	0	0	1	1	0	0	0	0	1	0	0	1	0	0 NA	
Pappomonas weddellensis	0	0	1	1	0	0	1	0	1	0	0	0	0	0 NA	
Picarola margalefii	0	0	1	1	0	0	1	0	0	0	0	0	0	1	1
Wigwamma arctica	0	1	0	1	0	0	1	0	0	0	0	0 NA		0 NA	
Wigwamma triradiata	0	1	0	1	0	0	1	0	0	0	0	0	0	1	0
Wigwamma annulifera	0	1	0	1	0	0	1	0	0	0	0	0	0	0 NA	
Wigwamma antarctica	0	0	1	1	0	0	1	0	1	0	0	1	1	0 NA	
Wigwamma amatura	0	0	1	1	0	0	1	0	0	0	0	0	0	0 NA	
Kataspinifera baumannii	0	0	1	1	0	0	1	0	0	0	0	0 NA		0	0
Calyptrosphaera sphaeroidea	1	0	1	0	0	1	0	1	0	0	0	0	0	0 NA	
Tetralithoides quadrilaminata	0	0	1	1	0	0	0	1	0	0	0	0	0	0 NA	
Placorhombus ziveriae	1	0	1	1	0	0	0	1	0	0	0	0	0	0 NA	
Tergestiella adriaticus	0	1	0	0	1	0	0	1	0	0	0	0	1	0 NA	

Appendix B. Part 8. Binary character coding for the 104 species included in this dissertation. Explanation of characters is included as Appendix C. Characters 1 to 44 pertain to coccolith morphology, while characters 45 to 76 pertain to coccosphere morphology.

	Character 32	Character 33	Character 34	Character 35	Character 36	Character 37	Character 38	Character 39	Character 40	Character 41	Character 42	Character 43	Character 44	Character 45	Character 46
Syracosphaera epigrosa	0	0	0	0	0	0	0	0 NA	NA	NA	NA	NA		1	1
Syracosphaera borealis-Type1	NA	NA	NA	0	0	0	1	0	0	0	0	1	0	1	1
Syracosphaera exigua	NA	NA	NA	0	0	0	0	0 NA	NA	NA	NA	NA		1	0
Syracosphaera rotula	NA	NA	NA	0	0	0	1	0	0	1	0	0	0	1	0
Syracosphaera ampliora	NA	NA	NA	0	0	0	1	1	0	1	0	1	0	1	0
Coronosphaera mediterranea	NA	NA	NA	0	0	0	0	1	1	0	0	1	0	1	1
Coronosphaera binodata	1	0	0	0	0	0	0	1	1	0	0	1	0	1	1
Coronosphaera maxima	NA	NA	NA	0	0	0	0	1	1	0	0	1	0	1	1
Calciosolenia murrayi	NA	NA	NA	0	0	0	0	1	0	1	0	0	0	1	0
Calciosolenia brasiliensis	NA	NA	NA	0	0	0	0	1	0	1	0	0	0	1	0
Alveosphaera bimurata	NA	NA	NA	0	0	0	0	1	0	1	0	0	0	1	1
Rhabdosphaera clavigera-clavigera	0	0	0	0	0	0	0	0 NA	NA	NA	NA	NA		1	0
Rhabdosphaera xiphos	0	0	0	0	0	0	0	0 NA	NA	NA	NA	NA		1	0
Palusphaera vandelii	0	0	0	0	0	0	0	0 NA	NA	NA	NA	NA		1	0
Discosphaera tubifera	0	0	0	0	0	0	0	0 NA	NA	NA	NA	NA		1	0
Acanthoica quattrospina	NA	NA		0	0	0	0	0 NA	NA	NA	NA	NA		1	0
Acanthoica janchenii	NA	NA		0	0	0	0	0 NA	NA	NA	NA	NA		1	0
Acanthoica acanthifera	NA	NA		0	0	0	0	0 NA	NA	NA	NA	NA		1	0
Acanthoica biscayensis	NA	NA		0	0	0	0	0 NA	NA	NA	NA	NA		1	0
Anacanthoica acanthos	NA	NA		0	0	0	0	0 NA	NA	NA	NA	NA		1	1
Cyrtosphaera aculeata	0	0	1	0	0	0	0	0 NA	NA	NA	NA	NA		1	1
Algirosphaera robusta	0	0	0	0	0	0	1	0	1	0	0	0	1	1	0
Algirosphaera cucullata	0	0	0	0	0	0	1	0	0	0	1	0	1	1	1
Algirosphaera meteora	0	0	0	0	0	0	1	0	1	0	1	0	1	1	1
Solisphaera emidasia	0	1	0	0	0	0	0	0 NA	NA	NA	NA	NA		1	0
Solisphaera helianthiformis	0	1	0	0	0	0	0	0 NA	NA	NA	NA	NA		1	1
Alisphaera unicornis-spatula	NA	NA		0	0	0	0	0 NA	NA	NA	NA	NA		1	0
Alisphaera pinnigera	NA	NA		0	0	0	0	0 NA	NA	NA	NA	NA		1	1
Alisphaera capulata	NA	NA		0	0	0	0	0 NA	NA	NA	NA	NA		1	0
Alisphaera ordinata	NA	NA		0	0	0	0	0 NA	NA	NA	NA	NA		1	1
Alisphaera quadrilatera	NA	NA		0	0	0	0	0 NA	NA	NA	NA	NA		1	1
Alisphaera extenta	NA	NA		0	0	0	0	0 NA	NA	NA	NA	NA		1	1
Alisphaera gaudii	NA	NA		0	0	0	0	0 NA	NA	NA	NA	NA		1	1
Umbellosphaera irregularis	NA	NA		0	0	0	1	0	1	1	0	1	0	1	0
Umbellosphaera tenuis-Type1	NA	NA		0	0	0	1	0	0	1	0	1	0	1	0
Papposphaera borealis	0	0	0	0 NA	NA	0	0	1	0	1	0	0	0	1	0
Papposphaera lepida	0	0	0	1	1	1	0	1	0	1	0	0	0	1	0
Pappomonas flabellifera	NA	NA	NA	0 NA	NA		0	1	0	1	0	0	0	1	0
Pappomonas borealis	NA	NA	NA	0 NA	NA		0	1	0	1	0	1	0	1	0
Pappomonas garrisonii	NA	NA	NA	0 NA	NA		0	1	0	1	0	0	0	1	0
Pappomonas weddellensis	NA	NA	NA	1	1	1	0	1	0	1	0	0	0	1	0
Picarola margalefii	0	0	0	1	0	0	0	1	0	1	0	0	0	1	0
Wigwamma arctica	NA	NA	0	0	0	0	0	0 NA	0	NA	NA	NA		0	0
Wigwamma triradiata	0	0	NA	1	0	0	0	0 NA	NA	NA	NA	NA		0	0
Wigwamma annulifera	NA	NA	NA	0	0	0	0	0 NA	NA	NA	NA	NA		0	0
Wigwamma antarctica	NA	NA	NA	0	0	0	0	0 NA	NA	NA	NA	NA		1	0
Wigwamma amatura	NA	NA	NA	0	0	0	0	0 NA	NA	NA	NA	NA		0	0
Kataspinifera baumannii	1	0	0	1	1	1	0	0 NA	NA	NA	NA	NA		1	0
Calyptrosphaera sphaeroidea	NA	NA	NA	0	0	0	0	0 NA	NA	NA	NA	NA		1	1
Tetralithoides quadrilaminata	NA	NA	NA	0	0	0	0	0 NA	NA	NA	NA	NA		1	0
Placorhombus ziveriae	NA	NA	NA	0	0	0	0	0 NA	NA	NA	NA	NA		1	1
Tergestiella adriaticus	NA	NA	NA	0 NA	NA		0	0 NA	NA	NA	NA	NA		1	1

Appendix B. Part 9. Binary character coding for the 104 species included in this dissertation. Explanation of characters is included as Appendix C. Characters 1 to 44 pertain to coccolith morphology, while characters 45 to 76 pertain to coccosphere morphology.

	Character 47	Character 48	Character 49	Character 50	Character 51	Character 52	Character 53	Character 54	Character 55	Character 56	Character 57	Character 58	Character 59	Character 60	Character 61
Syracosphaera epigrosa	0	0	0	0	0 NA		1	0	0 NA		0	0 NA	NA		0
Syracosphaera borealis-Type1	0	0	0	0	0 NA	0	0	1	0	0	0	0 NA	NA		0
Syracosphaera exigua	1	0	0	0	0	0	0	1	0	1	0	0 NA	NA		0
Syracosphaera rotula	1	1	0	0	0 NA	0	0	1	0	1	0	0 NA	NA		0
Syracosphaera ampliora	1	0	0	0	0	0	0	1	0	0	0	0 NA	NA		0
Coronosphaera mediterranea	0	0	0	0	1	0	1	0	0 NA		1	1	1	0	0
Coronosphaera binodata	0	0	0	0	0 NA		1	0	0 NA		1	1	1	0	0
Coronosphaera maxima	0	0	0	0	0 NA		1	0	0 NA		0	1	1	0	0
Calciosolenia murrayi	1	1	1	1	0	0	1	0	0 NA		1	0	0	1	0
Calciosolenia brasiliensis	1	1	1	1	0	0	1	0	0 NA		0	0	0 NA		0
Alveosphaera bimurata	0	1	0	0	1	1	1	0	0 NA		0	0 NA	NA		0
Rhabdosphaera clavigera-clavigera	1	0	0	0	0 NA		0	1	0	1	1	0	1	1	0
Rhabdosphaera xiphos	1	0	0	0	0 NA		1	0	0 NA		1	0	1	1	0
Palusphaera vandelii	1	0	0	0	0 NA		1	0	0 NA		1	0	1	1	0
Discosphaera tubifera	1	0	0	0	0 NA		0	1	0	1	1	0	1	0	0
Acanthoica quattrospina	1	0	0	0	0	0	1	0	0 NA		1	0	0	1	0
Acanthoica janchenii	1	1	0	0	0 NA		1	0	0 NA		1	0	0	1	0
Acanthoica acanthifera	1	1	0	0	0 NA		1	0	0 NA		1	1	0	1	0
Acanthoica biscayensis	1	0	0	0	0 NA		1	0	0 NA		1	0	0	1	0
Anacanthoica acanthos	0	0	0	0	0 NA		1	0	0 NA		0	0	0 NA		0
Cyrtosphaera aculeata	0	0	0	0	0 NA		1	0	0 NA		1	0	0	0	0
Algirosphaera robusta	1	0	0	0	0 NA		1	0	0 NA		1	0	1	0	0
Algirosphaera cucullata	0	0	0	0	0 NA		1	0	0 NA		1	0	1	0	0
Algirosphaera meteora	0	0	0	0	0 NA		1	0	0 NA		1	0	0	0	0
Solisphaera emidasia	1	0	0	0	0 NA		1	0	0 NA		1	1	0	1	0
Solisphaera helianthiformis	0	0	0	0	0 NA		1	0	0 NA		1	1	1	1	0
Alisphaera unicornis-spatula	1	0	0	0	0 NA		1	0	0 NA		0	0 NA	NA		0
Alisphaera pinnigera	0	0	0	0	0 NA		1	0	0 NA		0	0 NA	NA		0
Alisphaera capulata	1	0	0	0	0 NA		1	0	0 NA		1	0	1	1	0
Alisphaera ordinata	0	1	0	0	1	0	1	0	0 NA		1	0	1	0	0
Alisphaera quadrilatera	0	0	0	0	0 NA		1	0	0 NA		0	0	1	1	0
Alisphaera extenta	0	0	0	0	1	0	1	0	0 NA		1	0	1	1	0
Alisphaera gaudii	0	0	0	0	1	0	1	0	0 NA		0	0 NA	NA		0
Umbellosphaera irregularis	1	0	0	0	0 NA		0	1	0	1	1	0	1	0	0
Umbellosphaera tenuis-Type1	1	0	0	0	0 NA		0	1	0	1	1	0	1	0	0
Papposphaera borealis	1	0	0	0	0 NA		1	0	0 NA		1	0	1	1	0
Papposphaera lepida	1	0	0	0	0 NA		0	1	0	1	1	0	1	0	0
Pappomonas flabellifera	1	1	0	0	0 NA		1	0	0 NA		1	1	1	1	0
Pappomonas borealis	1	1	0	0	1	0	1	0	0 NA		1	0	0	1	0
Pappomonas garrisonii	1	0	0	0	0 NA		1	0	0 NA		1	0	1	0	0
Pappomonas weddellensis	1	1	0	0	1	1	1	0	0 NA		1	1	1	1	0
Picarola margalefii	1	1	0	0	1	0	1	0	0	1	1	0	1	1	0
Wigwamma arctica	1	0	0	0	0 NA		1	0	0 NA		1	0	1	1	0
Wigwamma triradiata	1	1	0	0	1	1	1	0	0 NA		1	0	1	1	0
Wigwamma annulifera	1	0	0	0	0 NA		1	0	0 NA		0	1	1	1	0
Wigwamma antarctica	1	1	0	0	1	1	1	0	0 NA		1	1	1	1	0
Wigwamma amatura	1	0	0	0	0 NA		0	0	1 NA		1	0	0	0	0
Kataspinifera baumannii	1	0	0	0	0	0	0	1	0	0	1	0	0	1	0
Calyptrosphaera sphaeroidea	0	0	0	0	0 NA		1	0	0 NA		0	0 NA	NA		0
Tetralithoides quadrilaminata	1	0	0	0	0 NA		1	0	0 NA		0	0 NA	NA		0
Placorhombus ziveriae	0	1	1	1	0	0	1	0	0 NA		0	0 NA	NA		0
Tergestiella adriaticus	0	0	0	0	0 NA		1	0	0 NA		0	0	0 NA		0

Appendix B. Part 10. Binary character coding for the 104 species included in this dissertation. Explanation of characters is included as Appendix C. Characters 1 to 44 pertain to coccolith morphology, while characters 45 to 76 pertain to coccosphere morphology.

	Character 62	Character 63	Character 64	Character 65	Character 66	Character 67	Character 68	Character 69	Character 70	Character 71	Character 72	Character 73	Character 74	Character 75	Character 76
Syracosphaera epigrosa	1	0	0	0	0	0	0	1	1	0	1	0	0	0	1
Syracosphaera borealis-Type1	NA	1	0	0	0	1	1	0	1	1	0	0	0	1	1
Syracosphaera exigua	0	1	0	0	0	0	0	0	1	0	1	0	0	0	1
Syracosphaera rotula	0	1	0	0	0	0	0	1	0	0	0	1	0	1	1
Syracosphaera ampliora	0	1	0	0	0	1	1	1	1	0	0	0	0	1	1
Coronosphaera mediterranea	0	1	0	0	1	0	0	1	0 NA		0	0	0	1	1
Coronosphaera binodata	0	1	0	0	1	0	1	1	0 NA		0	0	0	1	1
Coronosphaera maxima	0	1	0	0	1	0	0	1	0 NA		0	0	0	1	1
Calciosolenia murrayi	0	1	0	1	1	1	0	1	0 NA		0	0	0	0	0
Calciosolenia brasiliensis	1	0	0	1	1	1	0	1	0 NA		0	0	0	0	1
Alveosphaera bimurata	1	0	0	0	0	0	0	1	0	0	0	0	0	1	1
Rhabdosphaera clavigera-clavigera	0	1	0	0	0	0	0	0	1	0	0	0	0	0	0
Rhabdosphaera xiphos	0	1	0	0	0	0	0	0	1	1	0	0	0	0	0
Palusphaera vandelii	1	0	0	0	0	0	0	0	1	0	0	0	0	0	0
Discosphaera tubifera	1	0	0	0	0	0	0	0	1	1	0	0	0	0	1
Acanthoica quattrospina	0	0	1	0	1	0	0	0	1	0	0	0	0	0	1
Acanthoica janchenii	0	1	0	1	0	0	0	0	1	0	0	0	0	0	0
Acanthoica acanthifera	0	1	0	0	0	0	0	0	1	0	0	0	0	0	1
Acanthoica biscayensis	0	0	1	0	1	0	0	0	1	0	0	0	0	0	1
Anacanthoica acanthos	1	0	0	0	0	0	0	0	1	0	0	0	0	0	1
Cyrtosphaera aculeata	0	0	1	1	1	0	0	0	1	0	0	0	0	0	1
Algirosphaera robusta	0	1	0	0	1	0	0	0	1	0	0	0	0	0	1
Algirosphaera cucullata	1	0	0	0	1	1	0	0	1	0	0	1	0	0	0
Algirosphaera meteora	1	0	0	0	0	0	0	0	1	0	0	0	0	0	1
Solisphaera emidasia	0	0	1	0	1	0	0	0	1	0	0	0	0	0	0
Solisphaera helianthiformis	0	1	0	0	0	0	0	0	1	0	0	0	0	0	0
Alisphaera unicornis-spatula	1	0	0	0	0	0	0	0	1	1	1	0	1	0	1
Alisphaera pinnigera	0	1	0	0 NA	0	0	0	0	1	1	0	0	0	0	1
Alisphaera capulata	1	0	0	0	0	0	1	0	1	1	0	0	0	0	1
Alisphaera ordinata	1	0	0	0	0	0	1	0	1	1	1	0	0	0	1
Alisphaera quadrilatera	1	0	0	0	0	0	0	0	1	1	0	0	0	0	1
Alisphaera extenta	1	0	0	1 NA		1	1	0	1	1	0	0	0	0	1
Alisphaera gaudii	1	0	0	1 NA		1	1	0	1	1	0	0	1	0	1
Umbellosphaera irregularis	0	1	0	1	1	1	1	1	1	1	0	0	1	1	0
Umbellosphaera tenuis-Type1	0	1	0	1	1	1	1	1	1	1	0	0	1	1	0
Papposphaera borealis	0	1	0	0	0	0	0	1	0 NA		0	0	0	1	1
Papposphaera lepida	1	0	0	0	0	0	0	1	0 NA		0	0	0	1	1
Pappomonas flabellifera	0	0	1	1	1	0	0	1	0 NA		0	0	0	1	1
Pappomonas borealis	0	0	1	1	1	0	0	1	0	0	0	0	0	1	1
Pappomonas garrisonii	0	1	0	0	1	0	0	1	0 NA		0	0	0	0	1
Pappomonas weddellensis	0	1	0	1	1	1	0	1	0 NA		0	0	0	0	1
Picarola margalefii	0	0	1	1	1	1	0	1	0	0	0	0	1	1	1
Wigwamma arctica	1	0	0	1	1	1	0	1	0	0	0	0	0	1	1
Wigwamma triradiata	0	1	0	0	1	1	0	1	0 NA		0	0	0	1	1
Wigwamma annulifera	0	1	0	0	1	1	0	1	0	0	0	0	0	1	1
Wigwamma antarctica	0	1	0	0	1	0	0	0	1	0	0	0	0	0	1
Wigwamma amatura	0	1	0	0	1	0	0	1	1	0	0	0	0	1	1
Kataspinifera baumannii	0	1	0	0	0	0	0	0	1	0	0	0	0	0	1
Calyptrosphaera sphaeroidea	1	0	0	0	0	0	0	1	0 NA		0	0	0	1	0
Tetralithoides quadrilaminata	1	0	0	0	0	0	0	0	0 NA		1	0	0	1	0
Placorhombus ziveriae	1	0	0	0	0	0	0	1	0 NA		0	0	0	0	0
Tergestiella adriaticus	1	0	0	0	0	0	0	0	0	0	1	0	0	0	0

Coccolith Characters

All coccolith characters refer to features on body coccoliths (BC). The morphology of apical, antapical, and other specialized coccoliths (with the exception of those located on the main body of the cell as in the belt coccoliths of Scyphosphaera apsteinii), is considered under coccosphere traits, since the position on the coccosphere and density of these structures is as important as what they look like. Central area (CA) here refers to the area in the middle of the coccolith enclosed by cycles of crystal units (sensu Young et al. 1997), herein termed the rim (sensu Young et al. 1997). Distal view (DV) is the view of the coccolith showing the face on the outside, facing into the fluid environment. Proximal view (PV) is the view of the coccolith showing the face that lies flush with the cell's surface. A crystal element is a discrete component of a coccolith (sensu Young et al. 1997), such as the proximal shield element. Multiple crystal elements can form larger crystal units, which exhibit crystallographic continuity (sensu Young et al. 1997), such as V and R units. Suture refers to the visible contact of one surface with another in a coccolith (sensu Young et al. 1997).

Character 1: Body Coccolith has distal shield or other over-hanging structure
0= No overhanging structure; top could be smaller or equal in surface area as the bottom
1= Top of coccolith, e.g. distal shield, overhangs the bottom, e.g. proximal shield, of the coccolith.

Character 2: Body Coccolith is [sub]radially symmetric in distal view
0= The upper face of the body coccolith (i.e. distal from cell's surface) is not radially symmetric.
1= The upper face of the body coccolith is radially symmetric (i.e. circular or subcircular, contrast with polygonal profile in character 5).

Character 3: Body Coccolith is elliptical/elongate in distal view
0= The upper face of the body coccolith (i.e. distal from cell's surface) is not elliptical in profile.
1= The upper face of the body coccolith is elliptical, as in *Gephyrocapsa oceanica.*

Character 4: Body Coccolith has an asymmetrical profile in distal view
0= The upper face of the body coccolith (i.e. distal from cell's surface) is symmetric.
1= The upper face of the body coccolith is asymmetric, as in *Helicosphaera hyalina*.

Character 5: Body Coccolith has a polygonal (<15 flat edges) profile in distal view
0= The upper face of the body coccolith (i.e. distal from cell's surface) is not polygonal.
1= The upper face of the body coccolith is polygonal in profile (i.e. has fewer than 15 edges).

Character 6: Body Coccolith's margin is Monocyclic
0= Body coccolith's margin has more than one cycle of crystal elements in the margin or marginal crystal units are not organized in a cycle (i.e. ring).
1=Body coccolith has one, and only one, cycle of crystal units in the margin.

Character 7: Body Coccolith's margin is asymmetrical in distal view
0= Body coccolith's margin is symmetrical, with or without multiple cycles.
1= Body coccolith's margin is asymmetrical, as in *Helicosphaera hyalina.*

Character 8: Body Coccolith with regular marginal concavities or scalloping in distal view
0= Body coccolith margin has a smooth perimeter.
1= Body coccolith has concavities or scalloping, as in *Gephyrocapsa muellerae.*

Character 9: Body Coccolith elements are delicate
0= Body coccolith elements are not delicate.
1=Body coccolith elements are delicate (e.g. thin), as in *Wigwamma arctica*

Character 10: Body Coccolith's margin's inner-most cycle has laevo-dextrogyral sutures
NA= Body coccolith has only one cycle.
0= Sutures in between crystal elements in the inner-most cycle are straight.
1= Sutures in between crystal elements in the inner-most cycle are curving to right (dextrogyre) or curving to the left (laevogyre).

Character 11: Body Coccolith's margin's outer-most cycle has laevo-dextrogyral sutures
0= Sutures in between crystal elements in the outer-most cycle are straight.
1= Sutures in between crystal elements in the outer-most cycle are either curving to right (dextrogyre) or curving to the left (laevogyre).

Character 12: Body Coccolith's margin has slits (aka.pockets) in the outer-most cycle
0= Margin does not have any openings or has perforations in the outer-most cycle.
1= Margin does have slits, defined as a gap forming between two crystal elements, rather than a hole going through a crystal element (i.e. perforation).

Character 13: Body Coccolith's margin has slits (aka.pockets) in the inner-most cycle
NA= Body coccolith only has one cycle.
0= Margin does not have any openings or has perforations in the outer-most cycle.
1= Margin does have slits, defined as a gap forming between two crystal elements, rather than a hole going through a crystal element (i.e. perforation).

Character 14: Body Coccolith's margin with process/protrusion in distal view
0= There are no distinct protruding structures in the margin on the upper face of the coccolith (i.e. distal from cell's surface).
1= There are distinct protruding structures in the central area, as in *Alisphaera ordinata.*

Character 15: Body Coccolith with a single enlarged crystal unit
0= There are no saliently large crystal units.
1= There is one or more saliently large crystal units, which is incorporated into cycles or in the central area, as in *Alisphaera ordinata.*

Character 16: Body Coccolith has an asymmetrical profile in proximal view
0= The lower face of the body coccolith (i.e. proximal to cell's surface) is symmetric.
1= The lower face of the body coccolith is asymmetric, as in *Alisphaera pinnigera*.

Character 17: Body Coccolith has polygonal (<15 flat edges) profile in proximal view
0= The lower face of the body coccolith (i.e. proximal to cell's surface) is not polygonal.

1= The lower face of the body coccolith is polygonal in profile (i.e. has fewer than 15 edges).

Character 18: Body Coccolith has a radially symmetric profile in proximal view
0= The lower face of the body coccolith (i.e. proximal to cell's surface) is not radially symmetric.
1= The lower face of the body coccolith is radially symmetric (i.e. circular or subcircular, contrast with polygonal profile in character 17).

Character 19: Body Coccolith is elliptical/elongate in proximal view
0= The lower face of the body coccolith (i.e. proximal from cell's surface) is not elliptical in profile.
1= The lower face of the body coccolith is elliptical, as in *Gephyrocapsa oceanica.*

Character 20: Body Coccolith's central area is large
0= Body coccolith's central area diameter is less than twice the width of the rim.
1= Body coccolith's central area diameter is more than or equal to twice the width of the rim.

Character 21: Body Coccolith's central area's diameter is small
0= Body Coccolith's central area's diameter is greater than the width of the rim.
1= Body Coccolith's central area's diameter is smaller than or equal to the width of the rim.

C**haracter 22: Body Coccolith's central area is narrow**
0= Length of CA is twice the width of CA or smaller.
1= Length of CA is more than twice the width of CA.

Character 23: Body Coccolith's central area is open
0= central area has mineralized elements in it.
1=central area is unmineralized and open to environment, as in *Umbilicosphaera annulus.*

Character 24: Body Coccolith's central area is mostly to fully infilled
0= CA is partially infilled or fully open.
1= CA is fully mineralized either as a solid plate, e.g. *Scyphosphaera apstenii*, or from converging crystal units, e.g. *Calcidiscus leptoporus.*

Character 25: Body Coccolith's central area is partially infilled with grill morphology.
0= The central area is not partially infilled with grill morphology.
1= The central area is partially infilled with grill morphology, as in *Emiliania huxleyi.*

Character 26: Body Coccolith's central area is partially infilled with net morphology
0= The central area is not partially infilled with a net morphology.
1= The central area is partially mineralized with a net morphology, as in *Scyphospahera porosa.*

Character 27: Body Coccolith's central area has perforations
0= The central area has no perforations.
1= The central area bears perforations, which are any hole that pierces through a crystal unit, as in *Helicosphaera hyalina.*

Character 28: Body coccolith's central area has slits
0= The central area has no slits.
1= The central area bears slits, which are any opening resulting from a gap between two crystal units, as in *Syracospahera lamina*.

Character 29: Body Coccolith's central area's crystals are arranged radially, from the center to the inner edge of the rim
NA= There are no crystal units in the central area.
0= Crystal units in the central area are not arranged radially from the center to the inner edge of the rim.
1= Crystal units in the central area are arranged radially from the center to the inner edge of the rim, as in *Emiliania huxleyi.*

Character 30: Body Coccolith's central area has distinct protruding structure(s)
0= There are no distinct protruding structures in the central area.
1= There are distinct protruding structures in the central area, such as the stem in *Discosphaera tubifera* or the sail in *Gephyrocapsa ornata.*

Character 31: Body coccolith's central area's crystal units form a single stem
NA= There is no distinct protruding structure in the central area.
0= Crystal units in the central area do not form a single stem.
1= Crystal units in the central area form a single hollow stem, as in *Rhabdosphaera clavigera.*

Character 32: Body coccolith's central area's crystal units form a single knob/boss
NA= There is no distinct protruding structure in the central area.
0= Crystal units in the central area do not form a single knob/boss
1= Crystal units in the central area form a single knob or boss, as in *Syracosphaera histrica.*

Character 33: Body coccolith's central area's crystal units form a sail
NA= There is no distinct protruding structure in the central area.
0= Crystal units in the central area do not form a sail.
1= Crystal units in the central area form a sail, as in *Gephyrocapsa ornata.*

Character 34: Body coccolith's central area's crystal units form spine(s)
NA= There is no distinct protruding structure in the central area.
0= Crystal units in the central area do not form spine(s)
1= Crystal units in the central area form one or multiple solid spines, as in *Syracosphaera prolongata*.

Character 35: Body coccolith's central area with cross or spokes
0= There is no cross or spokes across the central area.
1= There is a cross (*sensu* Perch-Nielsen 1985) or spokes across the central area.

Character 36: Body coccolith's central area has disjunct longitudinal bar
NA= No longitudinal bar in the central area

0= Longitudinal bar in central area is conjunct, i.e. formed from crystal units of the rim structure.
1=Longitudinal bar in central area is disjunct, i.e. formed from crystal units that are discrete and separate from the rim, as in *Cruciplacolithus neohelis.*

Character 37: Body coccolith's central area has disjunct traverse bar
NA= No traverse bar in the central area
0= Traverse bar in central area is conjunct, i.e. formed from crystal units of the rim structure as in *Gephyrocapsa oceanica.*
1=Traverse bar in central area is disjunct, i.e. formed from crystal units that are discrete and separate from the rim, as in *Pappomonas weddellensis.*

Character 38: Wall extending from the central area
0= There is no wall extending from the central area
1= There is a wall(s), defined as a vertically built up closed structure made up of continuously joined tall crystal elements, which extends from the [perimeter of the] central area, as in *Gephyrocapsa oceanica.*

Character 39: Wall extending from the margin
0= There is no wall extending from the margin.
1= There is a wall(s), defined as a vertically built up closed structure made up of continuously joined tall crystal elements, which extends from the margin, as in *Coronosphaera mediterranea.*

Character 40: Body coccolith's wall's elements are oblique/imbricated
NA= Body coccolith bears no wall(s)
0= Wall elements are vertically straight, as in *Gephyrocapsa oceanica.*
1= Wall elements are oblique or imbricated, as in *Coronosphaera mediterranea.*

Character 41: Body coccolith has a vertical wall
NA= Body coccolith bears no wall(s)
0= Wall sides are not vertically straight in profile
1= Wall sides are vertically straight in profile throughout the height of the wall.

Character 42: Body coccolith has bowed wall
NA= Body coccolith bears no wall(s)
0=Wall sides are vertically straight in profile
1=Wall side are bend out and are widest at or near mid-height, as in *Scyphosphaera apsteinii*.

Character 43: Body coccolith wall has a flared lip
NA= Body coccolith bears no wall(s)
0=Wall sides are vertically straight in profile
1=Wall sides widen at the top of the wall's height creating a flared lip, as in *Hymenomonas roseola.*

Character 44: Coccolith has Tapering wall
NA= Body coccolith bears no wall(s)
0= Wall sides are vertically straight in profile

1= Wall sides narrow at the top of the wall's height creating a flared lip.

Coccosphere traits

Coccosphere traits pertain to the coccosphere as a whole and to subparts or it, such as the circumflagellar coccoliths. Some address potential functional features, so may not necessarily constitute a particular morphology, but rather some characteristic of it, e.g. fluid access to the cell.

Character 45: Coccosphere covers more than 75% of cell
0= Coccosphere covers less than 75% of the cell, as in *Wigwamma arctica.*
1= Coccosphere covers at least 75% of the cell, as in *Umbilicosphaera foliosa.*

Character 46: Cell defines coccosphere shape
0= No, coccoliths are prominent enough to make up the outline of the planform area, as in *Calciosolenia murrayi*.
1= Yes, the underlying cell defines the coccosphere's shape and it would collapse if the cell were removed, as in *Hymenomonas globosa.*

Character 47: Coccoliths define coccosphere shape
0= No, coccosphere is not predominantly defined by the coccoliths.
1= Yes, coccoliths are prominent enough to make up the outline of the planform area, as in *Umbellosphaera irregularis.*

Character 48: Coccosphere with long axis
0= No, coccosphere is roughly spherical or hemispherical.
1= Yes, coccospheres has one axis longer than the other, thus being either oval, pear/peanut-shaped, or otherwise rod-shaped.

Character 49: Coccosphere is very elongate
0= Long axis is only slightly longer than the short axis, as in *Helicosphaera carteri,* or there is no long axis.
1= Long axis is much longer than the short axis as in the long tube coccospheres in *Placorhombus ziveriae*.

Character 50: Coccosphere tapers at both ends
0= No, coccosphere tapers at one end only or does not taper at all.
1= Yes, coccosphere tapers or pinches in at both the apical and antapical poles, e.g. *Calciosolenia brasiliensis*.

Character 51: Coccosphere tapers at one end
0= No, coccosphere tapers at both ends or does not taper at all
1= Yes, coccosphere tapers at one and only one end, e.g. *Syracospahera pulchra*.

Character 52: Tapering is uniform
NA= Character only applies if coccosphere tapers.

0= No, only tapers at the very end, e.g. *Michaelsarsia adriaticus*, or that curves as it tapers, e.g. *Syracosphaera prolongata*.
1= Yes, tapering is uniform (constant or straight) along the length of the coccosphere, as in *Calciopappus caudatus*.

Character 53: Coccosphere consists of one mineral layer
0= No, coccosphere has multiple coccoliths or mineralized layers on top of one another.
1= Yes, coccosphere has single distinct layer of mineral material around the cell, e.g. *Helicosphaera carteri*.

Character 54: Coccosphere consists of two mineral layers with notable interstices
0= Coccosphere has one layer of coccoliths or undifferentiated piles of coccoliths
1= Coccosphere has two distinct layers of coccoliths with defined interstitial space as is the case for exothecal coccoliths, e.g. *Syracospahera lamina*.

Character 55: Coccosphere consists of undifferentiated piles of coccoliths
0= Coccoliths form at least one distinct mineral layer
1= Multiple coccoliths sit on top of one another in an indistinct fashion, e.g. multilayered coccospheres of *Emiliania huxleyi.*

Character 56: Outermost layer covers at least 50% of innermost layer
NA= Character does not apply to single-layered coccospheres
0= Outer layer covers less than 50% of inner layer, as in *Syracospahaera orbiculus.*
1= Outer layer covers at least 50% of inner layer, as in *Ophiaster formosus.*

Character 57: Mineralized projections in the body of the coccosphere
0= Coccosphere has no projections or has processes that do not significantly extend past the distal plane of the body coccoliths, as in *Alisphaera pinnigera.*
1= Coccosphere hosts independent structure sticking out past the distal plane of the body coccoliths, e.g. the trumpets of *Discosphaera tubifera* and the bridge of *Gephyrocapsa ericsonii*.

Character 58: Single belt of projections on coccospheres
0= No projections on coccosphere or coccosphere bears multiple belts of projections.
1= Coccosphere has a single continuous belt of projections arranged along some of the circumference of some cross-section of the coccosphere, e.g. *Scyphosphaera apsteinii.*

Character 59: Projections are uniformly distributed
NA= Trait only applies if projections are present
0= Projections are irregularly distributed, as in *Acanthoica quattrospina.*
1= Projections are distributed in a uniform pattern, as in *Discosphaera tubifera.*

Character 60: Projections disrupt the "boundary layer"
NA= Trait only applies if projections are present.
0=Projections are short and would likely not disrupt a boundary layer.

1= Projections would be long enough to disrupt the boundary layer that would naturally have formed around the cell, e.g. *Kataspinifera baumannii*; as no formal measurements were conducted, the term in presented in quotations in reference to its approximate nature.

Character 61: Coccosphere has very jointed appendages
NA= Trait only applies if coccosphere bears appendages (*sensu Young et al. 2009*).
0= Appendages are not or only weakly jointed, as in *Calciopappus rigidus.*
0= Appendages are very jointed, as in *Ophiaster formosus.*

Character 62: Coccoliths in coccosphere are monomorphic
0= Body coccoliths are not the same shape.
1= Body coccoliths are the same shape, e.g. *Coccolithus pelagicus*.

Character 63: Coccoliths in coccosphere are dimorphic
0= Body coccoliths are the same shape.
1= Coccosphere bears two discrete coccolith types, as in *Scyphosphaera apsteinii.*

Character 64: Coccoliths in coccosphere are polymorphic
0= Body coccoliths are the same shape.
1= Coccosphere bears more than two discrete coccolith types, as in *Pontosphaera multipora.*

Character 65: Body coccoliths are different from antapical coccoliths
0= Body coccoliths are the same size and shape as antapical coccoliths.
1= Body coccoliths differ in size and/or shape from antapical coccoliths, e.g. *Wigwamma arctica.*

Character 66: Body coccoliths are different from apical coccoliths
0= Body coccoliths are the same size and shape as apical coccoliths.
1= Body coccoliths differ in size and/or shape from apical coccoliths, e.g. *Ophiaster formosus.*

Character 67: Body coccoliths are varimorphic
0= Body coccoliths are the same size and shape
1= Body coccoliths have different sizes and shape depending on the position on the coccosphere, e.g. *Oolithotus antillarum.*

Character 68: Body coccoliths are arranged in a spiral
0= Body coccoliths are not arranged in a spiral.
1= Body coccoliths are arranged in a spiral, as in *Helicosphaera carteri.*

Character 69: Contact between body coccoliths is abutting
0= Contact between body coccoliths is overlapping or interlocking.
1=Body coccoliths abut to one another, as in *Pleurochrysis pseudoroscoffensis.*

Character 70: Contact between body coccoliths is overlapping
0= Contact between body coccoliths does not overlap.
1= Contact between body coccoliths does overlap, as in *Oolithotus fragilis.*

Character 71: Body coccoliths overlap in the same direction
NA= Trait applies only if body coccoliths are overlapping.
0= Body coccoliths overlap in many different directions.
1= Body coccoliths overlap in the same direction, e.g. *Helicosphaera carteri.*

Character 72: Body coccoliths are tightly interlocking
0= Contact between body coccoliths does not interlock tightly.
1= Contact between body coccoliths does interlock tightly, as in *Emiliania huxleyi.*

Character 73: Margin of body coccoliths allows fluid access to the cell
0= There is no fluid access to the cell through the margin of the body coccoliths.
1=There is fluid access to the cell through the margin of the body coccoliths, e.g. *Emiliania huxleyi.*

Character 74: There is fluid access to the cell under one side of the outer-most layer
0= There is no fluid access to the cell through spandrel-shaped gaps forming in between coccoliths on the cell's surface.
1= There is fluid access to the cell through spandrel-shaped gaps forming in between coccoliths on the cell's surface, e.g. *Oolithotus fragilis*.

Character 75: There is fluid access to the cell through the spandrels in between body coccoliths
0= There is no fluid access to the cell through spandrel-shaped gaps forming in between coccoliths on the cell's surface.
1= There is fluid access to the cell through spandrel-shaped gaps forming in between coccoliths on the cell's surface.

Character 76: There is fluid access to the cell through the central area
0= There is no fluid access to the cell through the central area
1= There is fluid access to the cell through the central area, either because it is unmineralized or because it bears many openings that allow a high volume of fluid through, as in *Syracosphaera lamina.*

Appendix D. #1. Geographic occurrence data for the 106 species included in this dissertation. Province occurrences shown in light grey come from *The Atlas of Living Coccolithophores* (Winter & Siesser 1994). Province occurrences shown in medium grey come from both *A Guide To Extant Coccolithophore Taxonomy* (Young et al. 2003) and/or *The Atlas of Living Coccolithophores* (Winter & Siesser 1994). Province occurrences shown in dark grey come from the two aforementioned sources and/or *The Nannotax3 Database* (Young et al., accessed 1-18-2016). Province occurrences of zero are shown in white represent the lack of occurrences of that taxon in that province or an unincorporated occurrence, either because it is only known from coccoliths rather than intact coccospheres or the author was otherwise unable to include it. Numbers reflect the number of records included in the study.

	Biogeographic provinces					
	Arctic	Baltic.Sea	N.European.Continental.Shelf	Subarctic.Atlantic	North.Atlantic.Current	North.Central.Atlantic
Emiliania huxleyi-TypeA	0	0	0	0	4	2
Gephyrocapsa oceanica	0	0	0	2	2	2
Gephyrocapsa muellerae	0	0	0	4	4	2
Gephyrocapsa ericsonii-ericsonii	0	0	0	0	4	4
Gephyrocapsa ornata	0	0	0	2	2	2
Reticulofenestra parvula	0	0	0	2	4	2
Reticulofenestra sessilis	0	0	0	0	0	0
Cruciplacolithus neohelis	0	0	0	2	2	0
Calcidiscus leptoporus-leptoporus	0	0	0	4	2	4
Oolithotus antillarum	0	0	0	0	0	0
Oolithotus fragilis	0	0	0	2	2	0
Hayaster perplexus	0	0	0	2	2	2
Umbilicosphaera sibogae	0	0	0	2	2	4
Umbilicosphaera anulus	0	0	0	0	0	0
Umbilicosphaera foliosa	0	0	0	2	2	2
Umbilicosphaera hulburtiana	0	0	0	2	2	2
Pleurochrysis carterae-carterae	0	0	0	0	0	0
Pleurochrysis gayraliae	0	0	0	0	0	0
Pleurochrysis placolithoides	0	0	5	0	4	0
Pleurochrysis roscoffensis	0	0	0	0	0	0
Pleurochrysis pseudoroscoffensis	0	0	0	0	0	0
Hymenomonas globosa	0	0	0	0	0	0
Hymenomonas lacuna	0	5	0	0	0	0
Hymenomonas roseola	0	0	0	0	0	0
Ochrosphaera neapolitana	0	0	0	0	0	0
Jomonlithus littoralis	0	0	0	0	0	0
Helicosphaera carteri	0	0	0	4	4	2
Helicosphaera hyalina	0	0	0	2	2	2
Helicosphaera wallichii	0	0	0	0	0	0
Helicosphaera pavimentum	0	0	0	2	2	2
Pontosphaera discopora	0	0	0	2	2	2
Pontosphaera japonica	0	0	0	2	2	2
Pontosphaera multipora	0	0	0	0	0	0
Pontosphaera syracusana	0	0	0	2	2	2
Scyphosphaera apsteinii	0	0	0	2	2	4
Scyphosphaera porosa	0	0	0	0	4	0
Calciopappus caudatus	0	0	5	2	0	2
Calciopappus rigidus	0	0	0	0	0	2
Michaelsarsia adriaticus	0	0	0	2	2	0
Michaelsarsia elegans	0	0	0	0	0	2
Ophiaster hydroideus	0	0	0	2	2	4
Ophiaster formosus	0	0	0	0	0	0
Ophiaster reductus	0	0	0	2	2	0
Syracosphaera anthos	0	0	0	2	2	2
Syracosphaera lamina	0	0	0	2	2	2
Syracosphaera tumularis	0	0	0	0	0	0
Syracosphaera bannockii	0	4	0	4	0	4
Syracosphaera pulchra	0	0	0	2	2	2
Syracosphaera histrica	0	0	0	2	2	4
Syracosphaera noroitica	0	0	0	0	0	0
Syracosphaera corolla	0	0	0	2	2	0
Syracosphaera ossa-Type1	0	0	0	2	2	0
Syracosphaera epigrosa	0	0	0	2	2	0

Appendix D. #2**.** Geographic occurrence data for the 106 species included in this dissertation. Province occurrences shown in light grey come from *The Atlas of Living Coccolithophores* (Winter & Siesser 1994). Province occurrences shown in medium grey come from both *A Guide To Extant Coccolithophore Taxonomy* (Young et al. 2003) and/or *The Atlas of Living Coccolithophores* (Winter & Siesser 1994). Province occurrences shown in dark grey come from the two aforementioned sources and/or *The Nannotax3 Database* (Young et al., accessed 1-18-2016). Province occurrences of zero are shown in white represent the lack of occurrences of that taxon in that province or an unincorporated occurrence, either because it is only known from coccoliths rather than intact coccospheres or the author was otherwise unable to include it. Numbers reflect the number of records included in the study.

	Arctic	Baltic.Sea	N.European.Continental.Shelf	Subarctic.Atlantic	North.Atlantic.Current	North.Central.Atlantic
Syracosphaera borealis-Type1	0	5	5	4	2	2
Syracosphaera exigua	0	0	0	2	2	0
Syracosphaera rotula	0	0	0	2	2	0
Syracosphaera ampliora	0	0	0	0	0	0
Coronosphaera mediterranea	0	0	4	4	2	2
Coronosphaera binodata	0	0	0	0	4	0
Coronosphaera maxima	0	0	0	0	0	0
Calciosolenia murrayi	0	0	0	0	2	4
Calciosolenia brasiliensis	0	0	0	0	0	0
Alveosphaera bimurata	0	0	0	2	4	4
Rhabdosphaera clavigera-clavigera	0	0	0	2	2	2
Rhabdosphaera xiphos	0	0	0	2	2	2
Palusphaera vandelii	0	0	0	0	0	0
Discosphaera tubifera	0	0	0	0	2	2
Acanthoica quattrospina	0	0	0	2	2	2
Acanthoica janchenii	0	0	0	0	0	4
Acanthoica acanthifera	0	0	0	2	2	2
Acanthoica biscayensis	0	0	0	0	4	0
Anacanthoica acanthos	0	0	0	2	2	2
Cyrtosphaera aculeata	0	0	0	2	2	2
Algirosphaera robusta	0	0	0	0	0	0
Algirosphaera cucullata	0	0	0	2	2	0
Algirosphaera meteora	0	0	0	2	2	2
Solisphaera emidasia	0	0	0	0	0	0
Solisphaera helianthiformis	0	0	0	0	4	0
Alisphaera unicornis-spatula	0	0	0	0	0	0
Alisphaera pinnigera	0	0	0	0	0	0
Alisphaera capulata	0	0	0	0	0	0
Alisphaera ordinata	0	0	0	0	0	4
Alisphaera quadrilatera	0	0	0	2	2	0
Alisphaera extenta	0	0	4	4	4	0
Alisphaera gaudii	0	0	0	0	0	0
Umbellosphaera irregularis	0	0	0	2	2	2
Umbellosphaera tenuis-TypeI	0	0	0	2	2	2
Papposphaera borealis	4	0	0	0	4	0
Papposphaera lepida	0	0	0	4	4	4
Pappomonas flabellifera	4	0	0	4	0	0
Pappomonas borealis	4	0	0	4	4	0
Pappomonas garrisonii	0	0	0	0	0	0
Pappomonas weddellensis	0	0	0	0	0	0
Picarola margalefii	0	0	0	0	0	0
Wigwamma arctica	4	0	0	0	0	0
Wigwamma triradiata	0	0	0	0	0	0
Wigwamma annulifera	4	0	0	0	0	0
Wigwamma antarctica	0	0	0	0	0	0
Wigwamma amatura	0	0	0	0	0	0
Kataspinifera baumannii	0	0	0	0	0	0
Calyptrosphaera sphaeroidea	0	0	0	0	0	0
Tetralithoides quadrilaminata	0	0	0	2	2	2
Placorhombus ziveriae	0	0	0	0	0	0
Tergestiella adriaticus	0	0	0	0	0	0

Appendix D. #3. Geographic occurrence data for the 106 species included in this dissertation. Province occurrences shown in light grey come from *The Atlas of Living Coccolithophores* (Winter & Siesser 1994). Province occurrences shown in medium grey come from both *A Guide To Extant Coccolithophore Taxonomy* (Young et al. 2003) and/or *The Atlas of Living Coccolithophores* (Winter & Siesser 1994). Province occurrences shown in dark grey come from the two aforementioned sources and/or *The Nannotax3 Database* (Young et al., accessed 1-18-2016). Province occurrences of zero are shown in white represent the lack of occurrences of that taxon in that province or an unincorporated occurrence, either because it is only known from coccoliths rather than intact coccospheres or the author was otherwise unable to include it. Numbers reflect the number of records included in the study.

	Canary.Current	Guinea.Current	Benguela.Current	South.Central.Atlantic	Malvinas.Current	Equatorial.Atlantic
Emiliania huxleyi-TypeA	4	2	2	2	2	2
Gephyrocapsa oceanica	0	0	4	2	2	2
Gephyrocapsa muellerae	0	0	0	0	0	0
Gephyrocapsa ericsonii-ericsonii	4	0	0	0	0	0
Gephyrocapsa ornata	0	0	0	4	0	0
Reticulofenestra parvula	0	0	0	0	0	0
Reticulofenestra sessilis	0	0	4	4	0	4
Cruciplacolithus neohelis	0	0	0	0	0	0
Calcidiscus leptoporus-leptoporus	0	0	0	4	0	2
Oolithotus antillarum	0	0	0	4	6	0
Oolithotus fragilis	0	0	0	0	0	0
Hayaster perplexus	0	0	0	0	0	0
Umbilicosphaera sibogae	4	0	0	4	0	2
Umbilicosphaera anulus	4	0	0	0	0	0
Umbilicosphaera foliosa	0	0	0	0	0	0
Umbilicosphaera hulburtiana	0	0	0	4	2	2
Pleurochrysis carterae-carterae	0	0	0	0	0	0
Pleurochrysis gayraliae	0	0	0	0	0	0
Pleurochrysis placolithoides	0	0	0	0	0	0
Pleurochrysis roscoffensis	0	0	0	0	0	0
Pleurochrysis pseudoroscoffensis	0	0	0	0	0	0
Hymenomonas globosa	0	0	0	0	0	0
Hymenomonas lacuna	0	0	0	0	0	0
Hymenomonas roseola	0	0	0	0	0	0
Ochrosphaera neapolitana	0	0	0	0	0	0
Jomonlithus littoralis	0	0	0	0	0	0
Helicosphaera carteri	4	0	0	2	2	0
Helicosphaera hyalina	4	0	0	4	0	4
Helicosphaera wallichii	0	0	0	0	0	0
Helicosphaera pavimentum	0	0	0	4	0	0
Pontosphaera discopora	0	0	0	2	0	0
Pontosphaera japonica	0	0	0	4	0	0
Pontosphaera multipora	0	0	0	4	0	0
Pontosphaera syracusana	0	0	0	0	0	0
Scyphosphaera apsteinii	0	0	0	0	0	0
Scyphosphaera porosa	4	0	0	4	0	4
Calciopappus caudatus	0	0	0	0	0	0
Calciopappus rigidus	0	0	0	2	0	2
Michaelsarsia adriaticus	0	0	0	0	0	0
Michaelsarsia elegans	4	0	0	4	0	4
Ophiaster hydroideus	0	0	0	4	0	0
Ophiaster formosus	4	0	0	4	0	0
Ophiaster reductus	4	0	0	0	0	0
Syracosphaera anthos	0	0	0	4	0	4
Syracosphaera lamina	0	0	0	2	0	4
Syracosphaera tumularis	4	0	0	0	0	0
Syracosphaera bannockii	4	0	0	4	0	0
Syracosphaera pulchra	0	0	0	4	0	2
Syracosphaera histrica	0	0	4	2	0	2
Syracosphaera noroitica	4	0	0	0	0	0
Syracosphaera corolla	0	0	0	0	0	0
Syracosphaera ossa-Type1	0	0	0	0	0	4
Syracosphaera epigrosa	4	0	0	0	0	0

Appendix D. #4**.** Geographic occurrence data for the 106 species included in this dissertation. Province occurrences shown in light grey come from *The Atlas of Living Coccolithophores* (Winter & Siesser 1994). Province occurrences shown in medium grey come from both *A Guide To Extant Coccolithophore Taxonomy* (Young et al. 2003) and/or *The Atlas of Living Coccolithophores* (Winter & Siesser 1994). Province occurrences shown in dark grey come from the two aforementioned sources and/or *The Nannotax3 Database* (Young et al., accessed 1-18-2016). Province occurrences of zero are shown in white represent the lack of occurrences of that taxon in that province or an unincorporated occurrence, either because it is only known from coccoliths rather than intact coccospheres or the author was otherwise unable to include it. Numbers reflect the number of records included in the study.

	Canary.Current	Guinea.Current	Benguela.Current	South.Central.Atlantic	Malvinas.Current	Equatorial.Atlantic
Syracosphaera borealis-Type1	0	0	0	0	0	0
Syracosphaera exigua	0	0	0	0	0	0
Syracosphaera rotula	0	0	0	0	0	0
Syracosphaera ampliora	0	0	0	0	0	0
Coronosphaera mediterranea	4	0	0	4	0	2
Coronosphaera binodata	4	0	0	0	0	0
Coronosphaera maxima	0	0	0	0	0	0
Calciosolenia murrayi	4	0	0	0	0	0
Calciosolenia brasiliensis	0	0	0	4	0	0
Alveosphaera bimurata	0	0	0	0	0	0
Rhabdosphaera clavigera-clavigera	0	0	2	2	0	0
Rhabdosphaera xiphos	0	0	0	0	0	0
Palusphaera vandelii	0	0	0	0	0	0
Discosphaera tubifera	0	0	0	0	0	2
Acanthoica quattrospina	0	0	0	0	0	0
Acanthoica janchenii	0	0	0	0	0	0
Acanthoica acanthifera	0	0	0	0	0	0
Acanthoica biscayensis	0	0	0	0	0	0
Anacanthoica acanthos	0	0	0	0	0	0
Cyrtosphaera aculeata	0	0	0	0	0	0
Algirosphaera robusta	0	0	0	0	0	0
Algirosphaera cucullata	0	0	0	0	0	0
Algirosphaera meteora	0	0	0	0	0	0
Solisphaera emidasia	0	0	0	0	0	0
Solisphaera helianthiformis	0	0	0	0	0	0
Alisphaera unicornis-spatula	0	0	0	0	0	0
Alisphaera pinnigera	0	0	0	0	0	4
Alisphaera capulata	4	0	0	0	0	0
Alisphaera ordinata	0	0	0	4	0	0
Alisphaera quadrilatera	0	0	0	0	0	0
Alisphaera extenta	0	0	0	0	0	0
Alisphaera gaudii	0	0	0	0	0	0
Umbellosphaera irregularis	0	0	0	4	0	2
Umbellosphaera tenuis-TypeI	4	0	0	2	0	4
Papposphaera borealis	0	0	0	0	0	0
Papposphaera lepida	0	0	0	4	0	0
Pappomonas flabellifera	0	0	0	0	0	0
Pappomonas borealis	0	0	0	0	0	0
Pappomonas garrisonii	0	0	0	0	0	0
Pappomonas weddellensis	0	0	0	0	0	0
Picarola margalefii	0	0	0	0	0	0
Wigwamma arctica	0	0	0	0	0	0
Wigwamma triradiata	0	0	0	0	0	0
Wigwamma annulifera	0	0	0	0	0	0
Wigwamma antarctica	0	0	0	0	0	0
Wigwamma amatura	0	0	0	0	0	0
Kataspinifera baumannii	0	0	0	0	0	0
Calyptrosphaera sphaeroidea	0	0	0	0	0	0
Tetralithoides quadrilaminata	0	0	0	4	0	0
Placorhombus ziveriae	0	0	0	0	0	0
Tergestiella adriaticus	0	0	0	0	0	0

Appendix D. #5. Geographic occurrence data for the 106 species included in this dissertation. Province occurrences shown in light grey come from *The Atlas of Living Coccolithophores* (Winter & Siesser 1994). Province occurrences shown in medium grey come from both *A Guide To Extant Coccolithophore Taxonomy* (Young et al. 2003) and/or *The Atlas of Living Coccolithophores* (Winter & Siesser 1994). Province occurrences shown in dark grey come from the two aforementioned sources and/or *The Nannotax3 Database* (Young et al., accessed 1-18-2016). Province occurrences of zero are shown in white represent the lack of occurrences of that taxon in that province or an unincorporated occurrence, either because it is only known from coccoliths rather than intact coccospheres or the author was otherwise unable to include it. Numbers reflect the number of records included in the study.

	Gulf.Stream	Gulf.of.Mexico	Inter.American.Seas	Black.Sea	Mediterranean.Sea	Caspian.Sea	Red.Sea
Emiliania huxleyi-TypeA	2	0	3	0	4	0	4
Gephyrocapsa oceanica	0	0	4	0	4	0	3
Gephyrocapsa muellerae	0	0	0	0	4	0	0
Gephyrocapsa ericsonii-ericsonii	0	0	0	0	3	0	3
Gephyrocapsa ornata	0	0	0	0	0	0	0
Reticulofenestra parvula	0	0	0	0	4	0	0
Reticulofenestra sessilis	0	4	0	0	0	0	0
Cruciplacolithus neohelis	3	0	0	0	1	0	0
Calcidiscus leptoporus-leptoporus	0	0	3	0	4	0	0
Oolithotus antillarum	0	4	0	0	0	0	0
Oolithotus fragilis	0	0	0	0	4	0	1
Hayaster perplexus	0	0	0	0	0	0	0
Umbilicosphaera sibogae	0	0	3	0	3	0	0
Umbilicosphaera anulus	0	0	0	0	4	0	0
Umbilicosphaera foliosa	0	0	0	0	4	0	0
Umbilicosphaera hulburtiana	0	0	0	0	4	0	0
Pleurochrysis carterae-carterae	0	0	0	0	0	0	0
Pleurochrysis gayraliae	0	0	0	0	0	0	0
Pleurochrysis placolithoides	0	0	0	0	0	0	0
Pleurochrysis roscoffensis	0	0	0	0	0	0	0
Pleurochrysis pseudoroscoffensis	0	0	0	0	0	0	0
Hymenomonas globosa	0	0	0	0	0	0	0
Hymenomonas lacuna	0	0	0	0	0	0	0
Hymenomonas roseola	0	0	0	0	0	0	0
Ochrosphaera neapolitana	0	0	0	0	0	0	0
Jomonlithus littoralis	0	0	0	0	0	0	0
Helicosphaera carteri	0	0	3	0	3	0	0
Helicosphaera hyalina	0	0	0	0	3	0	0
Helicosphaera wallichii	0	4	0	0	0	0	0
Helicosphaera pavimentum	0	0	0	0	4	0	0
Pontosphaera discopora	0	0	0	0	4	0	0
Pontosphaera japonica	0	0	0	0	4	0	0
Pontosphaera multipora	0	4	0	0	0	0	0
Pontosphaera syracusana	0	0	4	0	4	0	0
Scyphosphaera apsteinii	0	4	0	0	4	0	0
Scyphosphaera porosa	0	0	0	0	0	0	0
Calciopappus caudatus	0	0	3	0	4	0	0
Calciopappus rigidus	0	0	3	0	4	0	0
Michaelsarsia adriaticus	0	0	3	0	0	0	0
Michaelsarsia elegans	0	0	3	0	4	0	3
Ophiaster hydroideus	0	0	3	0	4	0	0
Ophiaster formosus	0	0	0	0	4	0	0
Ophiaster reductus	0	0	3	0	3	0	3
Syracosphaera anthos	0	0	0	0	4	0	3
Syracosphaera lamina	0	0	0	0	3	0	0
Syracosphaera tumularis	0	4	0	0	4	0	0
Syracosphaera bannockii	0	0	0	0	0	0	0
Syracosphaera pulchra	0	0	3	0	4	0	3
Syracosphaera histrica	0	0	3	0	3	0	3
Syracosphaera noroitica	0	0	0	0	4	0	0
Syracosphaera corolla	4	0	0	0	3	0	0
Syracosphaera ossa-Type1	0	0	0	0	4	0	0
Syracosphaera epigrosa	0	4	0	0	4	0	0

Appendix D. #6. Geographic occurrence data for the 106 species included in this dissertation. Province occurrences shown in light grey come from *The Atlas of Living Coccolithophores* (Winter & Siesser 1994). Province occurrences shown in medium grey come from both *A Guide To Extant Coccolithophore Taxonomy* (Young et al. 2003) and/or *The Atlas of Living Coccolithophores* (Winter & Siesser 1994). Province occurrences shown in dark grey come from the two aforementioned sources and/or *The Nannotax3 Database* (Young et al., accessed 1-18-2016). Province occurrences of zero are shown in white represent the lack of occurrences of that taxon in that province or an unincorporated occurrence, either because it is only known from coccoliths rather than intact coccospheres or the author was otherwise unable to include it. Numbers reflect the number of records included in the study.

	Gulf.Stream	Gulf.of.Mexico	Inter.American.Seas	Black.Sea	Mediterranean.Sea	Caspian.Sea	Red.Sea
Syracosphaera borealis-Type1	0	0	0	0	0	0	0
Syracosphaera exigua	0	0	0	0	0	0	0
Syracosphaera rotula	0	0	0	0	4	0	3
Syracosphaera ampliora	0	4	0	0	4	0	0
Coronosphaera mediterranea	0	4	0	0	4	0	0
Coronosphaera binodata	0	0	0	0	0	0	0
Coronosphaera maxima	0	4	0	0	0	0	0
Calciosolenia murrayi	0	0	3	0	4	0	0
Calciosolenia brasiliensis	0	0	0	0	4	0	0
Alveosphaera bimurata	0	4	0	0	0	0	0
Rhabdosphaera clavigera-clavigera	0	0	3	0	3	0	3
Rhabdosphaera xiphos	0	0	0	0	3	0	0
Palusphaera vandelii	0	0	0	0	4	0	0
Discosphaera tubifera	0	0	3	0	3	0	3
Acanthoica quattrospina	0	0	3	0	3	0	0
Acanthoica janchenii	0	0	0	0	0	0	0
Acanthoica acanthifera	0	0	0	0	3	0	3
Acanthoica biscayensis	0	0	0	0	0	0	0
Anacanthoica acanthos	0	0	3	0	4	0	0
Cyrtosphaera aculeata	0	0	4	0	3	3	0
Algirosphaera robusta	0	0	0	0	0	0	0
Algirosphaera cucullata	0	0	3	0	4	0	3
Algirosphaera meteora	0	4	0	0	3	0	0
Solisphaera emidasia	0	4	0	0	0	0	0
Solisphaera helianthiformis	0	4	0	0	0	0	0
Alisphaera unicornis-spatula	0	0	0	0	0	0	0
Alisphaera pinnigera	0	0	0	0	4	0	0
Alisphaera capulata	0	0	0	0	4	0	0
Alisphaera ordinata	0	0	0	0	4	0	0
Alisphaera quadrilatera	0	0	0	0	4	0	0
Alisphaera extenta	0	0	0	0	0	0	0
Alisphaera gaudii	0	0	0	0	4	0	0
Umbellosphaera irregularis	0	0	3	0	0	0	3
Umbellosphaera tenuis-TypeI	0	0	3	0	0	0	4
Papposphaera borealis	0	0	0	0	0	0	0
Papposphaera lepida	0	0	0	0	4	0	0
Pappomonas flabellifera	0	0	0	0	0	0	0
Pappomonas borealis	0	0	0	0	0	0	0
Pappomonas garrisonii	0	0	0	0	0	0	0
Pappomonas weddellensis	0	0	0	0	0	0	0
Picarola margalefii	0	0	0	0	4	0	0
Wigwamma arctica	0	0	0	0	0	0	0
Wigwamma triradiata	0	0	0	0	0	0	0
Wigwamma annulifera	0	0	0	0	0	0	0
Wigwamma antarctica	0	0	0	0	0	0	0
Wigwamma amatura	0	0	0	0	0	0	0
Kataspinifera baumannii	0	0	0	0	4	0	0
Calyptrosphaera sphaeroidea	0	0	0	0	0	0	0
Tetralithoides quadrilaminata	0	0	0	0	4	0	0
Placorhombus ziveriae	0	0	0	0	4	0	0
Tergestiella adriaticus	0	0	0	0	4	0	0

Appendix D. #7**.** Geographic occurrence data for the 106 species included in this dissertation. Province occurrences shown in light grey come from *The Atlas of Living Coccolithophores* (Winter & Siesser 1994). Province occurrences shown in medium grey come from both *A Guide To Extant Coccolithophore Taxonomy* (Young et al. 2003) and/or *The Atlas of Living Coccolithophores* (Winter & Siesser 1994). Province occurrences shown in dark grey come from the two aforementioned sources and/or *The Nannotax3 Database* (Young et al., accessed 1-18-2016). Province occurrences of zero are shown in white represent the lack of occurrences of that taxon in that province or an unincorporated occurrence, either because it is only known from coccoliths rather than intact coccospheres or the author was otherwise unable to include it. Numbers reflect the number of records included in the study.

	Persian..Gulf.of.Elat..Aqaba.	Somali.Current	Northeast.Indian.Ocean	Northwest.Indian.Ocean	Agulhas.Current
Emiliania huxleyi-TypeA	1	1	0	1	1
Gephyrocapsa oceanica	0	1	0	4	1
Gephyrocapsa muellerae	0	0	0	0	0
Gephyrocapsa ericsonii-ericsonii	0	1	0	4	1
Gephyrocapsa ornata	0	1	0	1	1
Reticulofenestra parvula	0	0	0	0	0
Reticulofenestra sessilis	0	0	0	0	0
Cruciplacolithus neohelis	0	0	0	0	0
Calcidiscus leptoporus-leptoporus	0	0	0	0	2
Oolithotus antillarum	0	0	0	4	0
Oolithotus fragilis	1	0	0	0	4
Hayaster perplexus	0	0	0	0	0
Umbilicosphaera sibogae	0	1	0	4	1
Umbilicosphaera anulus	0	0	0	0	0
Umbilicosphaera foliosa	0	0	0	0	0
Umbilicosphaera hulburtiana	0	1	0	4	2
Pleurochrysis carterae-carterae	0	0	0	0	0
Pleurochrysis gayraliae	0	0	0	0	0
Pleurochrysis placolithoides	0	0	0	0	0
Pleurochrysis roscoffensis	0	0	0	0	0
Pleurochrysis pseudoroscoffensis	0	0	0	0	0
Hymenomonas globosa	0	0	0	0	0
Hymenomonas lacuna	0	0	0	0	0
Hymenomonas roseola	0	0	0	0	0
Ochrosphaera neapolitana	0	0	0	0	0
Jomonlithus littoralis	0	0	0	0	0
Helicosphaera carteri	0	1	0	1	2
Helicosphaera hyalina	0	0	0	0	2
Helicosphaera wallichii	0	4	0	0	0
Helicosphaera pavimentum	0	1	0	1	3
Pontosphaera discopora	0	0	0	0	0
Pontosphaera japonica	0	0	0	0	0
Pontosphaera multipora	0	0	0	0	0
Pontosphaera syracusana	0	1	0	1	1
Scyphosphaera apsteinii	0	0	0	0	0
Scyphosphaera porosa	0	0	0	0	0
Calciopappus caudatus	0	0	0	0	0
Calciopappus rigidus	0	0	0	4	0
Michaelsarsia adriaticus	0	0	0	4	0
Michaelsarsia elegans	4	0	0	0	0
Ophiaster hydroideus	0	0	0	0	0
Ophiaster formosus	0	0	0	0	0
Ophiaster reductus	0	1	0	4	1
Syracosphaera anthos	0	1	0	1	1
Syracosphaera lamina	0	1	0	1	1
Syracosphaera tumularis	0	0	0	0	0
Syracosphaera bannockii	0	0	0	0	0
Syracosphaera pulchra	0	1	0	4	1
Syracosphaera histrica	0	0	0	0	0
Syracosphaera noroitica	0	0	0	0	0
Syracosphaera corolla	0	1	0	1	2
Syracosphaera ossa-Type1	0	0	0	4	0
Syracosphaera epigrosa	0	0	0	0	0

Appendix D. #8. Geographic occurrence data for the 106 species included in this dissertation. Province occurrences shown in light grey come from *The Atlas of Living Coccolithophores* (Winter & Siesser 1994). Province occurrences shown in medium grey come from both *A Guide To Extant Coccolithophore Taxonomy* (Young et al. 2003) and/or *The Atlas of Living Coccolithophores* (Winter & Siesser 1994). Province occurrences shown in dark grey come from the two aforementioned sources and/or *The Nannotax3 Database* (Young et al., accessed 1-18-2016). Province occurrences of zero are shown in white represent the lack of occurrences of that taxon in that province or an unincorporated occurrence, either because it is only known from coccoliths rather than intact coccospheres or the author was otherwise unable to include it. Numbers reflect the number of records included in the study..

	Persian..Gulf.of.Elat..Aqaba.	Somali.Current	Northeast.Indian.Ocean	Northwest.Indian.Ocean	Agulhas.Current
Syracosphaera borealis-Type1	0	0	0	0	0
Syracosphaera exigua	0	0	0	0	2
Syracosphaera rotula	0	0	0	0	0
Syracosphaera ampliora	0	0	0	0	0
Coronosphaera mediterranea	0	0	0	4	0
Coronosphaera binodata	0	0	0	0	0
Coronosphaera maxima	0	0	0	0	0
Calciosolenia murrayi	0	0	0	4	0
Calciosolenia brasiliensis	0	0	0	4	0
Alveosphaera bimurata	0	0	0	4	0
Rhabdosphaera clavigera-clavigera	0	1	0	1	1
Rhabdosphaera xiphos	0	1	0	1	1
Palusphaera vandelii	0	0	0	0	0
Discosphaera tubifera	0	1	0	4	1
Acanthoica quattrospina	0	1	0	1	1
Acanthoica janchenii	0	0	0	0	0
Acanthoica acanthifera	0	0	0	4	0
Acanthoica biscayensis	0	0	0	0	0
Anacanthoica acanthos	0	1	0	1	1
Cyrtosphaera aculeata	0	0	0	0	0
Algirosphaera robusta	0	0	0	0	0
Algirosphaera cucullata	0	1	0	1	1
Algirosphaera meteora	0	1	0	1	1
Solisphaera emidasia	0	0	0	0	0
Solisphaera helianthiformis	0	0	0	0	0
Alisphaera unicornis-spatula	0	0	0	0	0
Alisphaera pinnigera	0	0	0	0	0
Alisphaera capulata	0	0	0	0	0
Alisphaera ordinata	0	0	0	0	0
Alisphaera quadrilatera	0	0	0	0	0
Alisphaera extenta	0	0	0	0	0
Alisphaera gaudii	0	0	0	0	0
Umbellosphaera irregularis	0	1	0	4	1
Umbellosphaera tenuis-TypeI	0	1	0	1	1
Papposphaera borealis	0	0	0	0	0
Papposphaera lepida	0	0	0	0	0
Pappomonas flabellifera	0	0	0	0	0
Pappomonas borealis	0	0	0	0	0
Pappomonas garrisonii	0	0	0	0	0
Pappomonas weddellensis	0	0	0	0	0
Picarola margalefii	0	0	0	0	0
Wigwamma arctica	0	0	0	0	0
Wigwamma triradiata	0	0	0	0	0
Wigwamma annulifera	0	0	0	0	0
Wigwamma antarctica	0	0	0	0	0
Wigwamma amatura	0	0	0	0	0
Kataspinifera baumannii	0	0	0	0	0
Calyptrosphaera sphaeroidea	0	0	0	0	0
Tetralithoides quadrilaminata	0	0	0	0	0
Placorhombus ziveriae	0	0	0	0	0
Tergestiella adriaticus	0	0	0	0	0

Appendix D. #9. Geographic occurrence data for the 106 species included in this dissertation. Province occurrences shown in light grey come from *The Atlas of Living Coccolithophores* (Winter & Siesser 1994). Province occurrences shown in medium grey come from both *A Guide To Extant Coccolithophore Taxonomy* (Young et al. 2003) and/or *The Atlas of Living Coccolithophores* (Winter & Siesser 1994). Province occurrences shown in dark grey come from the two aforementioned sources and/or *The Nannotax3 Database* (Young et al., accessed 1-18-2016). Province occurrences of zero are shown in white represent the lack of occurrences of that taxon in that province or an unincorporated occurrence, either because it is only known from coccoliths rather than intact coccospheres or the author was otherwise unable to include it. Numbers reflect the number of records included in the study..

	Southern.Indian.Ocean	Leeuwin.Current	Malaysian.Shelf	Indonesian.Through.flow	South.China.Sea
Emiliania huxleyi-TypeA	1	1	1	1	2
Gephyrocapsa oceanica	4	1	1	1	2
Gephyrocapsa muellerae	0	0	0	0	0
Gephyrocapsa ericsonii-ericsonii	1	1	1	1	0
Gephyrocapsa ornata	1	1	1	1	0
Reticulofenestra parvula	0	0	0	0	0
Reticulofenestra sessilis	0	0	0	0	0
Cruciplacolithus neohelis	0	0	0	0	0
Calcidiscus leptoporus-leptoporus	2	0	0	0	0
Oolithotus antillarum	0	0	0	0	0
Oolithotus fragilis	0	0	0	0	0
Hayaster perplexus	0	0	0	0	0
Umbilicosphaera sibogae	1	1	1	1	0
Umbilicosphaera anulus	0	0	0	0	0
Umbilicosphaera foliosa	0	0	0	0	0
Umbilicosphaera hulburtiana	2	1	1	1	0
Pleurochrysis carterae-carterae	0	0	0	0	0
Pleurochrysis gayraliae	0	0	0	0	0
Pleurochrysis placolithoides	0	0	0	0	0
Pleurochrysis roscoffensis	0	0	0	0	0
Pleurochrysis pseudoroscoffensis	0	0	0	0	0
Hymenomonas globosa	0	0	0	0	0
Hymenomonas lacuna	0	0	0	0	0
Hymenomonas roseola	0	0	0	0	0
Ochrosphaera neapolitana	0	0	0	0	0
Jomonlithus littoralis	0	0	0	0	0
Helicosphaera carteri	2	1	1	1	0
Helicosphaera hyalina	2	0	0	0	0
Helicosphaera wallichii	0	0	0	0	0
Helicosphaera pavimentum	3	1	1	1	0
Pontosphaera discopora	0	0	0	0	0
Pontosphaera japonica	0	0	0	0	0
Pontosphaera multipora	0	0	0	0	0
Pontosphaera syracusana	1	1	1	1	0
Scyphosphaera apsteinii	0	0	0	0	0
Scyphosphaera porosa	0	0	0	0	0
Calciopappus caudatus	0	0	0	0	0
Calciopappus rigidus	0	0	0	0	0
Michaelsarsia adriaticus	0	0	0	0	0
Michaelsarsia elegans	0	0	0	0	0
Ophiaster hydroideus	0	0	0	0	0
Ophiaster formosus	0	0	0	0	0
Ophiaster reductus	1	1	1	1	0
Syracosphaera anthos	1	1	1	1	0
Syracosphaera lamina	1	1	1	1	0
Syracosphaera tumularis	0	0	0	0	0
Syracosphaera bannockii	0	0	0	0	0
Syracosphaera pulchra	1	1	1	1	0
Syracosphaera histrica	0	0	0	0	0
Syracosphaera noroitica	0	0	0	0	0
Syracosphaera corolla	2	1	1	1	0
Syracosphaera ossa-Type1	0	0	0	0	0
Syracosphaera epigrosa	0	0	0	0	0

Appendix D. #10. Geographic occurrence data for the 106 species included in this dissertation. Province occurrences shown in light grey come from *The Atlas of Living Coccolithophores* (Winter & Siesser 1994). Province occurrences shown in medium grey come from both *A Guide To Extant Coccolithophore Taxonomy* (Young et al. 2003) and/or *The Atlas of Living Coccolithophores* (Winter & Siesser 1994). Province occurrences shown in dark grey come from the two aforementioned sources and/or *The Nannotax3 Database* (Young et al., accessed 1-18-2016). Province occurrences of zero are shown in white represent the lack of occurrences of that taxon in that province or an unincorporated occurrence, either because it is only known from coccoliths rather than intact coccospheres or the author was otherwise unable to include it. Numbers reflect the number of records included in the study.

	Southern.Indian.Ocean	Leeuwin.Current	Malaysian.Shelf	Indonesian.Through.flow	South.China.Sea
Syracosphaera borealis-Type1	0	0	0	0	0
Syracosphaera exigua	2	0	0	0	0
Syracosphaera rotula	0	0	0	0	0
Syracosphaera ampliora	0	0	0	0	0
Coronosphaera mediterranea	0	0	0	0	0
Coronosphaera binodata	0	0	0	0	0
Coronosphaera maxima	0	0	0	0	0
Calciosolenia murrayi	0	0	0	0	0
Calciosolenia brasiliensis	0	0	0	0	0
Alveosphaera bimurata	0	0	0	0	0
Rhabdosphaera clavigera-clavigera	1	1	1	1	0
Rhabdosphaera xiphos	1	1	1	1	0
Palusphaera vandelii	0	0	0	0	0
Discosphaera tubifera	1	1	1	1	0
Acanthoica quattrospina	1	1	1	1	0
Acanthoica janchenii	0	0	0	0	0
Acanthoica acanthifera	0	0	0	0	0
Acanthoica biscayensis	0	0	0	0	0
Anacanthoica acanthos	1	1	1	1	0
Cyrtosphaera aculeata	0	0	0	0	0
Algirosphaera robusta	0	0	0	0	0
Algirosphaera cucullata	1	1	1	1	0
Algirosphaera meteora	1	1	1	1	0
Solisphaera emidasia	0	0	0	4	0
Solisphaera helianthiformis	0	0	0	0	0
Alisphaera unicornis-spatula	0	0	0	0	0
Alisphaera pinnigera	0	0	0	0	0
Alisphaera capulata	0	0	0	0	0
Alisphaera ordinata	0	0	0	0	0
Alisphaera quadrilatera	0	0	0	0	0
Alisphaera extenta	0	0	0	0	0
Alisphaera gaudii	0	0	0	0	0
Umbellosphaera irregularis	1	1	1	1	0
Umbellosphaera tenuis-TypeI	1	1	1	1	0
Papposphaera borealis	0	0	0	0	0
Papposphaera lepida	0	0	0	0	0
Pappomonas flabellifera	0	0	0	0	0
Pappomonas borealis	0	0	0	0	0
Pappomonas garrisonii	0	0	0	0	0
Pappomonas weddellensis	0	0	0	0	0
Picarola margalefii	0	0	0	0	0
Wigwamma arctica	0	0	0	0	0
Wigwamma triradiata	0	0	0	0	0
Wigwamma annulifera	0	0	0	0	0
Wigwamma antarctica	0	0	0	0	0
Wigwamma amatura	0	0	0	0	0
Kataspinifera baumannii	0	0	0	0	0
Calyptrosphaera sphaeroidea	0	0	0	0	0
Tetralithoides quadrilaminata	0	0	0	0	0
Placorhombus ziveriae	0	0	0	0	0
Tergestiella adriaticus	0	0	0	0	0

Appendix D.#11. Geographic occurrence data for the 106 species included in this dissertation. Province occurrences shown in light grey come from *The Atlas of Living Coccolithophores* (Winter & Siesser 1994). Province occurrences shown in medium grey come from both *A Guide To Extant Coccolithophore Taxonomy* (Young et al. 2003) and/or *The Atlas of Living Coccolithophores* (Winter & Siesser 1994). Province occurrences shown in dark grey come from the two aforementioned sources and/or *The Nannotax3 Database* (Young et al., accessed 1-18-2016). Province occurrences of zero are shown in white represent the lack of occurrences of that taxon in that province or an unincorporated occurrence, either because it is only known from coccoliths rather than intact coccospheres or the author was otherwise unable to include it. Numbers reflect the number of records included in the study..

	Kuroshio.Current	Sea.of.Japan...East.China.Sea	North.Pacific.Current	Subarctic.Pacific	California.Current
Emiliania huxleyi-TypeA	4	2	2	2	2
Gephyrocapsa oceanica	4	2	2	2	2
Gephyrocapsa muellerae	0	0	0	0	0
Gephyrocapsa ericsonii-ericsonii	4	0	2	0	2
Gephyrocapsa ornata	4	0	2	0	2
Reticulofenestra parvula	0	0	0	0	0
Reticulofenestra sessilis	2	2	2	2	2
Cruciplacolithus neohelis	0	0	0	0	0
Calcidiscus leptoporus-leptoporus	0	0	0	0	0
Oolithotus antillarum	4	0	0	0	0
Oolithotus fragilis	0	0	2	0	2
Hayaster perplexus	1	0	2	0	2
Umbilicosphaera sibogae	0	0	2	0	2
Umbilicosphaera anulus	0	0	0	0	0
Umbilicosphaera foliosa	0	0	2	0	2
Umbilicosphaera hulburtiana	0	0	2	0	2
Pleurochrysis carterae-carterae	0	0	0	0	0
Pleurochrysis gayraliae	0	0	0	0	0
Pleurochrysis placolithoides	0	0	0	0	0
Pleurochrysis roscoffensis	0	0	0	0	0
Pleurochrysis pseudoroscoffensis	0	0	0	0	0
Hymenomonas globosa	0	0	0	0	0
Hymenomonas lacuna	0	0	0	0	0
Hymenomonas roseola	0	0	0	0	0
Ochrosphaera neapolitana	0	0	0	0	0
Jomonlithus littoralis	0	0	0	0	0
Helicosphaera carteri	0	0	2	0	2
Helicosphaera hyalina	0	0	2	0	2
Helicosphaera wallichii	4	0	0	0	0
Helicosphaera pavimentum	0	0	2	2	2
Pontosphaera discopora	0	0	0	0	2
Pontosphaera japonica	0	0	2	2	2
Pontosphaera multipora	0	0	0	0	0
Pontosphaera syracusana	0	0	2	0	2
Scyphosphaera apsteinii	0	0	2	0	2
Scyphosphaera porosa	0	0	0	0	0
Calciopappus caudatus	0	0	2	2	2
Calciopappus rigidus	0	0	0	0	0
Michaelsarsia adriaticus	4	0	2	2	2
Michaelsarsia elegans	0	0	0	0	0
Ophiaster hydroideus	0	0	2	2	2
Ophiaster formosus	0	0	0	0	0
Ophiaster reductus	0	0	0	0	0
Syracosphaera anthos	0	0	2	2	2
Syracosphaera lamina	0	4	2	2	2
Syracosphaera tumularis	4	0	0	0	0
Syracosphaera bannockii	0	0	0	0	0
Syracosphaera pulchra	0	0	2	2	2
Syracosphaera histrica	0	0	2	2	2
Syracosphaera noroitica	0	0	0	0	0
Syracosphaera corolla	0	0	2	2	2
Syracosphaera ossa-Type1	0	0	2	2	2
Syracosphaera epigrosa	0	0	2	2	2

Appendix D.#12. Geographic occurrence data for the 106 species included in this dissertation. Province occurrences shown in light grey come from *The Atlas of Living Coccolithophores* (Winter & Siesser 1994). Province occurrences shown in medium grey come from both *A Guide To Extant Coccolithophore Taxonomy* (Young et al. 2003) and/or *The Atlas of Living Coccolithophores* (Winter & Siesser 1994). Province occurrences shown in dark grey come from the two aforementioned sources and/or *The Nannotax3 Database* (Young et al., accessed 1-18-2016). Province occurrences of zero are shown in white represent the lack of occurrences of that taxon in that province or an unincorporated occurrence, either because it is only known from coccoliths rather than intact coccospheres or the author was otherwise unable to include it. Numbers reflect the number of records included in the study.

	Kuroshio.Current	Sea.of.Japan...East.China.Sea	North.Pacific.Current	Subarctic.Pacific	California.Current
Syracosphaera borealis-Type1	0	0	2	2	2
Syracosphaera exigua	0	0	2	2	2
Syracosphaera rotula	0	0	2	2	2
Syracosphaera ampliora	0	0	0	0	0
Coronosphaera mediterranea	0	0	2	0	2
Coronosphaera binodata	0	0	4	0	0
Coronosphaera maxima	0	0	0	0	0
Calciosolenia murrayi	0	0	2	0	2
Calciosolenia brasiliensis	4	0	0	0	0
Alveosphaera bimurata	0	0	2	2	2
Rhabdosphaera clavigera-clavigera	0	0	2	2	2
Rhabdosphaera xiphos	0	0	2	2	0
Palusphaera vandelii	4	0	0	0	0
Discosphaera tubifera	0	0	2	0	2
Acanthoica quattrospina	0	4	2	2	2
Acanthoica janchenii	0	0	0	0	0
Acanthoica acanthifera	0	0	2	2	2
Acanthoica biscayensis	0	0	0	0	0
Anacanthoica acanthos	0	0	0	0	0
Cyrtosphaera aculeata	0	0	2	2	2
Algirosphaera robusta	0	0	0	0	0
Algirosphaera cucullata	0	0	2	2	2
Algirosphaera meteora	0	0	0	0	0
Solisphaera emidasia	0	0	0	0	0
Solisphaera helianthiformis	0	0	0	0	0
Alisphaera unicornis-spatula	0	0	0	0	0
Alisphaera pinnigera	0	0	0	0	0
Alisphaera capulata	0	0	0	0	0
Alisphaera ordinata	0	0	0	0	0
Alisphaera quadrilatera	2	2	2	2	2
Alisphaera extenta	0	0	0	0	0
Alisphaera gaudii	0	0	0	0	0
Umbellosphaera irregularis	4	0	2	2	2
Umbellosphaera tenuis-TypeI	0	0	2	2	2
Papposphaera borealis	0	0	0	0	0
Papposphaera lepida	0	0	0	0	0
Pappomonas flabellifera	0	0	0	0	4
Pappomonas borealis	0	0	0	0	0
Pappomonas garrisonii	0	0	0	0	0
Pappomonas weddellensis	0	0	0	0	0
Picarola margalefii	0	0	0	0	0
Wigwamma arctica	0	0	0	0	0
Wigwamma triradiata	0	0	0	0	0
Wigwamma annulifera	0	0	0	0	0
Wigwamma antarctica	0	0	0	0	0
Wigwamma amatura	0	0	0	0	0
Kataspinifera baumannii	0	0	0	0	0
Calyptrosphaera sphaeroidea	4	0	0	0	0
Tetralithoides quadrilaminata	0	0	2	0	2
Placorhombus ziveriae	0	0	0	0	0
Tergestiella adriaticus	0	4	0	0	0

Appendix D. #13. Geographic occurrence data for the 106 species included in this dissertation. Province occurrences shown in light grey come from *The Atlas of Living Coccolithophores* (Winter & Siesser 1994). Province occurrences shown in medium grey come from both *A Guide To Extant Coccolithophore Taxonomy* (Young et al. 2003) and/or *The Atlas of Living Coccolithophores* (Winter & Siesser 1994). Province occurrences shown in dark grey come from the two aforementioned sources and/or *The Nannotax3 Database* (Young et al., accessed 1-18-2016). Province occurrences of zero are shown in white represent the lack of occurrences of that taxon in that province or an unincorporated occurrence, either because it is only known from coccoliths rather than intact coccospheres or the author was otherwise unable to include it. Numbers reflect the number of records included in the study.

	Eastern.Tropical.Pacific	Humboldt.Current	North.Central.Pacific	Equatorial.Pacific	South.Central.Pacific
Emiliania huxleyi-TypeA	2	2	2	4	2
Gephyrocapsa oceanica	2	2	4	4	2
Gephyrocapsa muellerae	0	0	0	0	0
Gephyrocapsa ericsonii-ericsonii	2	0	2	4	2
Gephyrocapsa ornata	2	0	2	2	2
Reticulofenestra parvula	0	0	2	2	2
Reticulofenestra sessilis	2	0	4	2	2
Cruciplacolithus neohelis	0	0	0	4	0
Calcidiscus leptoporus-leptoporus	0	0	4	2	2
Oolithotus antillarum	0	0	4	0	0
Oolithotus fragilis	2	0	2	2	0
Hayaster perplexus	2	0	2	2	2
Umbilicosphaera sibogae	2	0	2	4	2
Umbilicosphaera anulus	0	0	0	0	0
Umbilicosphaera foliosa	2	0	2	2	2
Umbilicosphaera hulburtiana	2	4	2	4	2
Pleurochrysis carterae-carterae	0	0	0	0	0
Pleurochrysis gayraliae	0	0	0	0	0
Pleurochrysis placolithoides	0	0	0	0	0
Pleurochrysis roscoffensis	0	0	0	0	0
Pleurochrysis pseudoroscoffensis	0	0	0	0	0
Hymenomonas globosa	0	0	0	0	0
Hymenomonas lacuna	0	0	0	0	0
Hymenomonas roseola	0	0	0	0	0
Ochrosphaera neapolitana	0	0	0	0	0
Jomonlithus littoralis	0	0	0	0	0
Helicosphaera carteri	2	0	2	4	2
Helicosphaera hyalina	2	0	2	2	2
Helicosphaera wallichii	0	0	4	0	0
Helicosphaera pavimentum	0	0	2	2	2
Pontosphaera discopora	2	0	4	2	2
Pontosphaera japonica	2	0	4	2	2
Pontosphaera multipora	0	0	0	0	0
Pontosphaera syracusana	2	0	2	2	2
Scyphosphaera apsteinii	2	0	4	2	2
Scyphosphaera porosa	0	0	0	0	0
Calciopappus caudatus	2	0	2	2	2
Calciopappus rigidus	0	0	0	4	0
Michaelsarsia adriaticus	0	0	2	2	0
Michaelsarsia elegans	0	0	0	0	0
Ophiaster hydroideus	2	0	2	2	0
Ophiaster formosus	0	0	0	0	4
Ophiaster reductus	2	0	2	2	2
Syracosphaera anthos	2	0	2	2	0
Syracosphaera lamina	2	0	2	2	2
Syracosphaera tumularis	0	0	0	0	0
Syracosphaera bannockii	0	0	0	0	0
Syracosphaera pulchra	2	0	2	2	2
Syracosphaera histrica	2	0	2	2	2
Syracosphaera noroitica	0	0	0	0	0
Syracosphaera corolla	2	0	2	2	0
Syracosphaera ossa-Type1	2	0	2	2	2
Syracosphaera epigrosa	0	0	0	0	0

Appendix D. #14. Geographic occurrence data for the 106 species included in this dissertation. Province occurrences shown in light grey come from *The Atlas of Living Coccolithophores* (Winter & Siesser 1994). Province occurrences shown in medium grey come from both *A Guide To Extant Coccolithophore Taxonomy* (Young et al. 2003) and/or *The Atlas of Living Coccolithophores* (Winter & Siesser 1994). Province occurrences shown in dark grey come from the two aforementioned sources and/or *The Nannotax3 Database* (Young et al., accessed 1-18-2016). Province occurrences of zero are shown in white represent the lack of occurrences of that taxon in that province or an unincorporated occurrence, either because it is only known from coccoliths rather than intact coccospheres or the author was otherwise unable to include it. Numbers reflect the number of records included in the study.

	Eastern.Tropical.Pacific	Humboldt.Current	North.Central.Pacific	Equatorial.Pacific	South.Central.Pacific
Syracosphaera borealis-Type1	2	0	2	2	0
Syracosphaera exigua	2	0	2	2	2
Syracosphaera rotula	2	0	2	2	2
Syracosphaera ampliora	0	0	0	0	0
Coronosphaera mediterranea	0	0	2	4	2
Coronosphaera binodata	0	0	0	0	0
Coronosphaera maxima	0	0	0	0	0
Calciosolenia murrayi	2	0	2	2	2
Calciosolenia brasiliensis	0	0	0	4	0
Alveosphaera bimurata	0	0	2	2	0
Rhabdosphaera clavigera-clavigera	2	0	2	2	2
Rhabdosphaera xiphos	0	0	2	0	0
Palusphaera vandelii	0	0	0	0	0
Discosphaera tubifera	2	0	2	2	2
Acanthoica quattrospina	2	0	2	2	0
Acanthoica janchenii	0	0	4	0	0
Acanthoica acanthifera	0	0	2	2	0
Acanthoica biscayensis	0	0	0	0	0
Anacanthoica acanthos	0	0	0	0	0
Cyrtosphaera aculeata	2	0	2	2	0
Algirosphaera robusta	0	0	0	0	0
Algirosphaera cucullata	2	0	2	2	0
Algirosphaera meteora	0	0	0	0	0
Solisphaera emidasia	0	0	0	0	0
Solisphaera helianthiformis	0	0	0	0	0
Alisphaera unicornis-spatula	0	0	0	0	0
Alisphaera pinnigera	0	0	0	0	0
Alisphaera capulata	0	0	0	0	0
Alisphaera ordinata	0	0	0	0	0
Alisphaera quadrilatera	2	0	2	2	0
Alisphaera extenta	0	0	0	0	0
Alisphaera gaudii	0	0	0	0	0
Umbellosphaera irregularis	2	0	4	4	2
Umbellosphaera tenuis-TypeI	2	0	2	4	2
Papposphaera borealis	0	0	0	0	0
Papposphaera lepida	0	0	0	0	0
Pappomonas flabellifera	4	0	0	0	0
Pappomonas borealis	0	0	0	0	0
Pappomonas garrisonii	0	0	0	0	0
Pappomonas weddellensis	0	0	0	0	0
Picarola margalefii	0	0	0	0	0
Wigwamma arctica	0	0	0	0	0
Wigwamma triradiata	0	0	0	0	0
Wigwamma annulifera	0	0	0	0	0
Wigwamma antarctica	0	0	0	0	0
Wigwamma amatura	0	0	0	0	0
Kataspinifera baumannii	0	0	0	0	0
Calyptrosphaera sphaeroidea	0	0	0	0	0
Tetralithoides quadrilaminata	2	0	2	2	2
Placorhombus ziveriae	0	0	0	0	0
Tergestiella adriaticus	0	0	0	0	0

Appendix D. #15. Geographic occurrence data for the 106 species included in this dissertation. Province occurrences shown in light grey come from *The Atlas of Living Coccolithophores* (Winter & Siesser 1994). Province occurrences shown in medium grey come from both *A Guide To Extant Coccolithophore Taxonomy* (Young et al. 2003) and/or *The Atlas of Living Coccolithophores* (Winter & Siesser 1994). Province occurrences shown in dark grey come from the two aforementioned sources and/or *The Nannotax3 Database* (Young et al., accessed 1-18-2016). Province occurrences of zero are shown in white represent the lack of occurrences of that taxon in that province or an unincorporated occurrence, either because it is only known from coccoliths rather than intact coccospheres or the author was otherwise unable to include it. Numbers reflect the number of records included in the study.

	Southwest.Pacific	New.Zealand	Southern.subtropical.front	Subantarctic	Antarctic.Polar.Front	Antarctic	Ross.Sea
Emiliania huxleyi-TypeA	2	0	0	0	0	0	0
Gephyrocapsa oceanica	4	0	0	0	0	0	0
Gephyrocapsa muellerae	0	0	0	0	0	0	0
Gephyrocapsa ericsonii-ericsonii	0	0	0	0	0	0	0
Gephyrocapsa ornata	0	0	0	0	0	0	0
Reticulofenestra parvula	0	0	0	0	0	0	0
Reticulofenestra sessilis	0	0	0	0	0	0	0
Cruciplacolithus neohelis	0	0	0	0	0	0	0
Calcidiscus leptoporus-leptoporus	0	0	0	0	0	0	0
Oolithotus antillarum	0	0	6	6	0	0	0
Oolithotus fragilis	0	0	0	0	0	0	0
Hayaster perplexus	0	0	0	0	0	0	0
Umbilicosphaera sibogae	0	0	0	0	0	0	0
Umbilicosphaera anulus	0	0	0	0	0	0	0
Umbilicosphaera foliosa	0	0	0	0	0	0	0
Umbilicosphaera hulburtiana	0	0	0	0	0	0	0
Pleurochrysis carterae-carterae	0	0	0	0	0	0	0
Pleurochrysis gayraliae	0	0	0	0	0	0	0
Pleurochrysis placolithoides	0	0	0	0	0	0	0
Pleurochrysis roscoffensis	0	0	0	0	0	0	0
Pleurochrysis pseudoroscoffensis	0	0	0	0	0	0	0
Hymenomonas globosa	0	0	0	0	0	0	0
Hymenomonas lacuna	0	0	0	0	0	0	0
Hymenomonas roseola	0	0	0	0	0	0	0
Ochrosphaera neapolitana	0	0	0	0	0	0	0
Jomonlithus littoralis	0	0	0	0	0	0	0
Helicosphaera carteri	0	0	0	0	0	0	0
Helicosphaera hyalina	0	0	0	0	0	0	0
Helicosphaera wallichii	0	0	0	0	0	0	0
Helicosphaera pavimentum	0	0	0	0	0	0	0
Pontosphaera discopora	4	0	0	0	0	0	0
Pontosphaera japonica	0	0	0	0	0	0	0
Pontosphaera multipora	0	0	0	0	0	0	0
Pontosphaera syracusana	0	0	0	0	0	0	0
Scyphosphaera apsteinii	0	0	0	0	0	0	0
Scyphosphaera porosa	0	0	0	0	0	0	0
Calciopappus caudatus	0	0	0	0	0	0	0
Calciopappus rigidus	0	0	0	0	0	0	0
Michaelsarsia adriaticus	0	0	0	0	0	0	0
Michaelsarsia elegans	0	0	0	0	0	0	0
Ophiaster hydroideus	0	0	0	0	0	0	0
Ophiaster formosus	0	0	0	0	0	0	0
Ophiaster reductus	0	0	0	0	0	0	0
Syracosphaera anthos	0	0	0	0	0	0	0
Syracosphaera lamina	0	0	0	0	0	0	0
Syracosphaera tumularis	0	0	0	0	0	0	0
Syracosphaera bannockii	0	0	4	0	0	0	0
Syracosphaera pulchra	0	0	4	0	0	0	0
Syracosphaera histrica	0	4	0	0	0	0	0
Syracosphaera noroitica	0	0	0	0	0	0	0
Syracosphaera corolla	0	4	0	0	0	0	0
Syracosphaera ossa-Type1	0	0	0	0	0	0	0
Syracosphaera epigrosa	0	0	4	0	0	0	0

Appendix D.#16. Geographic occurrence data for the 106 species included in this dissertation. Province occurrences shown in light grey come from *The Atlas of Living Coccolithophores* (Winter & Siesser 1994). Province occurrences shown in medium grey come from both *A Guide To Extant Coccolithophore Taxonomy* (Young et al. 2003) and/or *The Atlas of Living Coccolithophores* (Winter & Siesser 1994). Province occurrences shown in dark grey come from the two aforementioned sources and/or *The Nannotax3 Database* (Young et al., accessed 1-18-2016). Province occurrences of zero are shown in white represent the lack of occurrences of that taxon in that province or an unincorporated occurrence, either because it is only known from coccoliths rather than intact coccospheres or the author was otherwise unable to include it. Numbers reflect the number of records included in the study.

	Southwest.Pacific	New.Zealand	Southern.subtropical.front	Subantarctic	Antarctic.Polar.Front	Antarctic	Ross.Sea
Syracosphaera borealis-Type1	0	0	0	0	0	0	0
Syracosphaera exigua	0	0	0	0	0	0	0
Syracosphaera rotula	0	0	0	0	0	0	0
Syracosphaera ampliora	0	0	0	0	0	0	0
Coronosphaera mediterranea	0	0	0	0	0	0	0
Coronosphaera binodata	0	0	0	0	0	0	0
Coronosphaera maxima	0	0	0	0	0	0	0
Calciosolenia murrayi	0	0	0	0	0	0	0
Calciosolenia brasiliensis	0	0	0	0	0	0	0
Alveosphaera bimurata	0	0	0	0	0	0	0
Rhabdosphaera clavigera-clavigera	0	0	0	0	0	0	0
Rhabdosphaera xiphos	0	0	0	0	0	0	0
Palusphaera vandelii	0	0	4	0	0	0	0
Discosphaera tubifera	0	0	0	0	0	0	0
Acanthoica quattrospina	0	0	0	0	0	0	0
Acanthoica janchenii	0	0	0	0	0	0	0
Acanthoica acanthifera	0	0	0	0	0	0	0
Acanthoica biscayensis	0	0	0	0	0	0	0
Anacanthoica acanthos	0	0	0	0	0	0	0
Cyrtosphaera aculeata	0	0	0	0	0	0	0
Algirosphaera robusta	0	0	0	0	0	0	0
Algirosphaera cucullata	0	0	0	0	0	0	0
Algirosphaera meteora	0	0	0	0	0	0	0
Solisphaera emidasia	0	0	0	0	0	0	0
Solisphaera helianthiformis	0	0	4	0	0	0	0
Alisphaera unicornis-spatula	0	0	0	0	0	0	0
Alisphaera pinnigera	0	0	4	0	0	0	0
Alisphaera capulata	0	0	0	0	0	0	0
Alisphaera ordinata	0	0	0	0	0	0	0
Alisphaera quadrilatera	0	0	0	0	0	0	0
Alisphaera extenta	0	0	0	0	0	0	0
Alisphaera gaudii	0	0	4	0	0	0	0
Umbellosphaera irregularis	0	0	0	0	0	0	0
Umbellosphaera tenuis-TypeI	0	0	0	0	0	0	0
Papposphaera borealis	0	0	0	0	0	0	0
Papposphaera lepida	0	0	0	0	0	0	0
Pappomonas flabellifera	0	0	0	0	0	0	0
Pappomonas borealis	0	0	0	0	0	0	0
Pappomonas garrisonii	0	0	0	0	0	4	0
Pappomonas weddellensis	0	0	0	0	4	4	0
Picarola margalefii	0	0	0	0	0	0	0
Wigwamma arctica	0	0	0	0	4	4	0
Wigwamma triradiata	0	0	0	0	4	4	0
Wigwamma annulifera	0	0	0	0	4	0	0
Wigwamma antarctica	0	0	0	0	4	0	0
Wigwamma amatura	0	0	0	0	0	4	0
Kataspinifera baumannii	0	0	4	0	0	0	0
Calyptrosphaera sphaeroidea	0	0	0	0	0	0	0
Tetralithoides quadrilaminata	0	0	0	0	0	0	0
Placorhombus ziveriae	0	0	0	0	0	0	0
Tergestiella adriaticus	0	0	0	0	0	0	0

Appendix D.#17. Geographic occurrence data for the 106 species included in this dissertation. Province occurrences shown in light grey come from *The Atlas of Living Coccolithophores* (Winter & Siesser 1994). Province occurrences shown in medium grey come from both *A Guide To Extant Coccolithophore Taxonomy* (Young et al. 2003) and/or *The Atlas of Living Coccolithophores* (Winter & Siesser 1994). Province occurrences shown in dark grey come from the two aforementioned sources and/or *The Nannotax3 Database* (Young et al., accessed 1-18-2016). Province occurrences of zero are shown in white represent the lack of occurrences of that taxon in that province or an unincorporated occurrence, either because it is only known from coccoliths rather than intact coccospheres or the author was otherwise unable to include it. Numbers reflect the number of records included in the study. Biome and latitude occurrences represent a summary of the provincial information and are based on the assignment of that province to a given biome or latitude category (see Appendix E).

									Latitudes
	Weddell.Sea	E.Boundary	Gyre	W.Boundary	Transitional	Semi.enclosed.Sea	Enclosed.Sea	Shallow	PAC_Pola
Emiliania huxleyi-TypeA	3	1	1	1	1	1	0	1	0
Gephyrocapsa oceanica	3	1	1	1	1	1	0	1	0
Gephyrocapsa muellerae	0	0	1	0	1	1	0	0	0
Gephyrocapsa ericsonii-ericsonii	0	1	1	1	1	1	0	0	0
Gephyrocapsa ornata	0	0	1	1	0	0	0	0	0
Reticulofenestra parvula	0	0	0	0	1	1	0	0	0
Reticulofenestra sessilis	0	1	1	0	0	0	0	0	0
Cruciplacolithus neohelis	0	0	0	1	0	0	0	0	0
Calcidiscus leptoporus-leptoporus	0	0	1	0	0	1	0	1	0
Oolithotus antillarum	0	0	1	1	1	0	0	0	0
Oolithotus fragilis	0	0	0	1	0	1	0	0	0
Hayaster perplexus	0	0	0	0	0	0	0	0	0
Umbilicosphaera sibogae	0	1	1	0	0	1	0	1	0
Umbilicosphaera anulus	0	1	0	0	0	1	0	0	0
Umbilicosphaera foliosa	0	0	0	0	0	1	0	0	0
Umbilicosphaera hulburtiana	0	1	1	0	0	1	0	0	0
Pleurochrysis carterae-carterae	0	0	0	0	0	0	0	0	0
Pleurochrysis gayraliae	0	0	0	0	0	0	0	0	0
Pleurochrysis placolithoides	0	0	0	0	1	0	0	0	0
Pleurochrysis roscoffensis	0	0	0	0	0	0	0	0	0
Pleurochrysis pseudoroscoffensis	0	0	0	0	0	0	0	0	0
Hymenomonas globosa	0	0	0	0	0	0	0	0	0
Hymenomonas lacuna	0	0	0	0	0	1	0	1	0
Hymenomonas roseola	0	0	0	0	0	0	0	0	0
Ochrosphaera neapolitana	0	0	0	0	0	0	0	0	0
Jomonlithus littoralis	0	0	0	0	0	0	0	0	0
Helicosphaera carteri	0	1	1	0	1	1	0	1	0
Helicosphaera hyalina	0	1	1	0	0	1	0	0	0
Helicosphaera wallichii	0	0	1	1	0	0	0	0	0
Helicosphaera pavimentum	0	0	1	1	0	1	0	0	0
Pontosphaera discopora	0	0	1	0	1	1	0	0	0
Pontosphaera japonica	0	0	1	0	0	1	0	0	0
Pontosphaera multipora	0	0	1	0	0	0	0	0	0
Pontosphaera syracusana	0	0	0	0	0	1	0	1	0
Scyphosphaera apsteinii	0	0	1	0	0	1	0	0	0
Scyphosphaera porosa	0	1	1	0	1	0	0	0	0
Calciopappus caudatus	0	0	0	0	0	1	0	1	0
Calciopappus rigidus	0	0	1	0	0	1	0	1	0
Michaelsarsia adriaticus	0	0	1	1	0	1	0	1	0
Michaelsarsia elegans	0	1	1	0	0	1	0	1	0
Ophiaster hydroideus	0	0	1	0	0	1	0	1	0
Ophiaster formosus	0	1	1	0	0	1	0	0	0
Ophiaster reductus	0	1	1	0	0	1	0	1	0
Syracosphaera anthos	0	0	1	0	0	1	0	0	0
Syracosphaera lamina	0	0	0	0	0	1	0	1	0
Syracosphaera tumularis	0	1	1	1	0	1	0	0	0
Syracosphaera bannockii	0	1	1	0	1	1	0	1	0
Syracosphaera pulchra	0	0	1	0	1	1	0	1	0
Syracosphaera histrica	0	1	1	0	0	1	0	1	0
Syracosphaera noroitica	0	1	0	0	0	1	0	0	0
Syracosphaera corolla	0	0	0	1	0	1	0	1	0
Syracosphaera ossa-Type1	0	0	1	0	0	1	0	0	0
Syracosphaera epigrosa	0	1	1	0	1	1	0	0	0

Appendix D.#18. Geographic occurrence data for the 106 species included in this dissertation. Biome and latitude occurrences represent a summary of the provincial information and are based on the assignment of that province to a given biome or latitude category (see Appendix E).

	Weddell.Sea	E.Boundary	Gyre	W.Boundary	Transitional	Semi.enclosed.Sea	Enclosed.Sea	Shallow	PAC_Pola
Syracosphaera borealis-Type1	0	0	1	0	0	1	0	1	0
Syracosphaera exigua	0	0	0	0	0	0	0	0	0
Syracosphaera rotula	0	0	0	0	0	1	0	0	0
Syracosphaera ampliora	0	0	1	0	0	1	0	0	0
Coronosphaera mediterranea	0	1	1	0	0	1	0	0	0
Coronosphaera binodata	0	1	0	0	1	0	0	0	0
Coronosphaera maxima	0	0	1	0	0	0	0	0	0
Calciosolenia murrayi	0	1	1	0	0	1	0	1	0
Calciosolenia brasiliensis	0	0	1	1	0	1	0	0	0
Alveosphaera bimurata	0	0	1	0	1	0	0	0	0
Rhabdosphaera clavigera-clavigera	0	0	0	0	0	1	0	1	0
Rhabdosphaera xiphos	0	0	0	0	0	1	0	0	0
Palusphaera vandelii	0	0	0	1	1	1	0	0	0
Discosphaera tubifera	0	0	1	0	0	1	0	1	0
Acanthoica quattrospina	0	0	0	0	0	1	0	1	0
Acanthoica janchenii	0	0	1	0	0	0	0	0	0
Acanthoica acanthifera	0	0	1	0	0	1	0	0	0
Acanthoica biscayensis	0	0	0	0	1	0	0	0	0
Anacanthoica acanthos	0	0	0	0	0	1	0	1	0
Cyrtosphaera aculeata	0	0	0	0	0	1	1	1	0
Algirosphaera robusta	0	0	0	0	0	0	0	0	0
Algirosphaera cucullata	0	0	0	0	0	1	0	1	0
Algirosphaera meteora	0	0	1	0	0	1	0	0	0
Solisphaera emidasia	0	0	1	0	0	1	0	0	0
Solisphaera helianthiformis	0	0	1	0	1	0	0	0	0
Alisphaera unicornis-spatula	0	0	0	0	0	0	0	0	0
Alisphaera pinnigera	0	0	0	0	1	1	0	0	0
Alisphaera capulata	0	1	0	0	0	1	0	0	0
Alisphaera ordinata	0	0	1	0	0	1	0	0	0
Alisphaera quadrilatera	0	0	0	0	0	1	0	0	0
Alisphaera extenta	0	0	1	0	1	0	0	0	0
Alisphaera gaudii	0	0	0	0	1	1	0	0	0
Umbellosphaera irregularis	0	0	1	1	0	1	0	1	0
Umbellosphaera tenuis-TypeI	0	1	0	0	0	1	0	1	0
Papposphaera borealis	0	0	0	0	1	0	0	0	0
Papposphaera lepida	0	0	1	0	1	1	0	0	0
Pappomonas flabellifera	0	1	1	0	0	0	0	0	0
Pappomonas borealis	0	0	1	0	1	0	0	0	0
Pappomonas garrisonii	0	0	0	0	0	0	0	0	0
Pappomonas weddellensis	0	0	0	0	0	0	0	0	0
Picarola margalefii	0	0	0	0	0	1	0	0	0
Wigwamma arctica	0	0	0	0	0	0	0	0	0
Wigwamma triradiata	0	0	0	0	0	0	0	0	0
Wigwamma annulifera	0	0	0	0	0	0	0	0	0
Wigwamma antarctica	0	0	0	0	0	0	0	0	0
Wigwamma amatura	0	0	0	0	0	0	0	0	0
Kataspinifera baumannii	0	0	0	0	1	1	0	0	0
Calyptrosphaera sphaeroidea	0	0	0	1	0	0	0	0	0
Tetralithoides quadrilaminata	0	0	1	0	0	1	0	0	0
Placorhombus ziveriae	0	0	0	0	0	1	0	0	0
Tergestiella adriaticus	0	0	0	0	0	1	0	1	0

Appendix D.#19. Geographic occurrence data for the 106 species included in this dissertation. Biome and latitude occurrences represent a summary of the provincial information and are based on the assignment of that province to a given biome or latitude category (see Appendix E).

	s by ocean						
	PAC_Temperate	PAC_Subtropical	PAC_Tropical	ATL_Polar	ATL_Temperate	ATL_Subtropical	ATL_Tropical
Emiliania huxleyi-TypeA	0	1	1	0	1	1	0
Gephyrocapsa oceanica	0	1	1	0	1	0	0
Gephyrocapsa muellerae	0	0	0	1	1	0	0
Gephyrocapsa ericsonii-ericsonii	0	1	1	0	1	1	0
Gephyrocapsa ornata	0	1	0	0	0	1	0
Reticulofenestra parvula	0	0	0	0	1	0	0
Reticulofenestra sessilis	0	1	0	0	1	1	1
Cruciplacolithus neohelis	0	0	1	0	0	0	1
Calcidiscus leptoporus-leptoporus	0	1	0	1	0	1	0
Oolithotus antillarum	0	1	0	0	1	1	0
Oolithotus fragilis	0	0	0	0	0	0	0
Hayaster perplexus	0	0	0	0	0	0	0
Umbilicosphaera sibogae	0	0	1	0	0	1	0
Umbilicosphaera anulus	0	0	0	0	0	1	0
Umbilicosphaera foliosa	0	0	0	0	0	0	0
Umbilicosphaera hulburtiana	1	0	1	0	0	1	0
Pleurochrysis carterae-carterae	0	0	0	0	0	0	0
Pleurochrysis gayraliae	0	0	0	0	0	0	0
Pleurochrysis placolithoides	0	0	0	0	1	0	0
Pleurochrysis roscoffensis	0	0	0	0	0	0	0
Pleurochrysis pseudoroscoffensis	0	0	0	0	0	0	0
Hymenomonas globosa	0	0	0	0	0	0	0
Hymenomonas lacuna	0	0	0	0	0	0	0
Hymenomonas roseola	0	0	0	0	0	0	0
Ochrosphaera neapolitana	0	0	0	0	0	0	0
Jomonlithus littoralis	0	0	0	0	0	0	0
Helicosphaera carteri	0	0	1	1	1	1	0
Helicosphaera hyalina	0	0	0	0	0	1	1
Helicosphaera wallichii	0	1	0	0	0	0	0
Helicosphaera pavimentum	0	0	0	0	0	1	0
Pontosphaera discopora	0	1	0	0	0	0	0
Pontosphaera japonica	0	1	0	0	0	1	0
Pontosphaera multipora	0	0	0	0	0	1	0
Pontosphaera syracusana	0	0	0	0	0	0	0
Scyphosphaera apsteinii	0	1	0	0	0	1	0
Scyphosphaera porosa	0	0	0	0	1	1	1
Calciopappus caudatus	0	0	0	0	0	0	0
Calciopappus rigidus	0	0	1	0	0	0	0
Michaelsarsia adriaticus	0	1	0	0	0	0	0
Michaelsarsia elegans	0	0	0	0	0	1	1
Ophiaster hydroideus	0	0	0	0	0	1	0
Ophiaster formosus	0	1	0	0	0	1	0
Ophiaster reductus	0	0	0	0	0	1	0
Syracosphaera anthos	0	0	0	0	0	1	1
Syracosphaera lamina	1	0	0	0	0	0	1
Syracosphaera tumularis	0	1	0	0	0	1	0
Syracosphaera bannockii	0	0	0	1	0	1	0
Syracosphaera pulchra	0	0	0	0	0	1	0
Syracosphaera histrica	0	0	0	0	1	1	0
Syracosphaera noroitica	0	0	0	0	0	1	0
Syracosphaera corolla	0	0	0	0	0	0	1
Syracosphaera ossa-Type1	0	0	0	0	0	0	1
Syracosphaera epigrosa	0	0	0	0	0	1	0

Appendix D.#20. Geographic occurrence data for the 106 species included in this dissertation. Biome and latitude occurrences represent a summary of the provincial information and are based on the assignment of that province to a given biome or latitude category (see Appendix E).

	PAC_Temperate	PAC_Subtropical	PAC_Tropical	ATL_Polar	ATL_Temperate	ATL_Subtropical	ATL_Tropical
Syracosphaera borealis-Type1	0	0	0	1	0	0	0
Syracosphaera exigua	0	0	0	0	0	0	0
Syracosphaera rotula	0	0	0	0	0	0	0
Syracosphaera ampliora	0	0	0	0	0	0	0
Coronosphaera mediterranea	0	0	1	1	0	1	0
Coronosphaera binodata	1	0	0	0	1	1	0
Coronosphaera maxima	0	0	0	0	0	0	0
Calciosolenia murrayi	0	0	0	0	0	1	0
Calciosolenia brasiliensis	0	1	1	0	0	1	0
Alveosphaera bimurata	0	0	0	0	1	1	0
Rhabdosphaera clavigera-clavigera	0	0	0	0	0	0	0
Rhabdosphaera xiphos	0	0	0	0	0	0	0
Palusphaera vandelii	0	1	0	0	0	0	0
Discosphaera tubifera	0	0	0	0	0	0	0
Acanthoica quattrospina	1	0	0	0	0	0	0
Acanthoica janchenii	0	1	0	0	0	1	0
Acanthoica acanthifera	0	0	0	0	0	0	0
Acanthoica biscayensis	0	0	0	0	1	0	0
Anacanthoica acanthos	0	0	0	0	0	0	0
Cyrtosphaera aculeata	0	0	0	0	0	0	0
Algirosphaera robusta	0	0	0	0	0	0	0
Algirosphaera cucullata	0	0	0	0	0	0	0
Algirosphaera meteora	0	0	0	0	0	0	0
Solisphaera emidasia	0	0	0	0	0	0	0
Solisphaera helianthiformis	0	0	0	0	1	0	0
Alisphaera unicornis-spatula	0	0	0	0	0	0	0
Alisphaera pinnigera	0	0	0	0	0	0	1
Alisphaera capulata	0	0	0	0	0	1	0
Alisphaera ordinata	0	0	0	0	0	1	0
Alisphaera quadrilatera	0	0	0	0	0	0	0
Alisphaera extenta	0	0	0	1	1	0	0
Alisphaera gaudii	0	0	0	0	0	0	0
Umbellosphaera irregularis	0	1	1	0	0	1	0
Umbellosphaera tenuis-TypeI	0	0	1	0	0	1	1
Papposphaera borealis	0	0	0	0	1	0	0
Papposphaera lepida	0	0	0	1	1	1	0
Pappomonas flabellifera	1	0	1	1	0	0	0
Pappomonas borealis	0	0	0	1	1	0	0
Pappomonas garrisonii	0	0	0	0	0	0	0
Pappomonas weddellensis	0	0	0	0	0	0	0
Picarola margalefii	0	0	0	0	0	0	0
Wigwamma arctica	0	0	0	0	0	0	0
Wigwamma triradiata	0	0	0	0	0	0	0
Wigwamma annulifera	0	0	0	0	0	0	0
Wigwamma antarctica	0	0	0	0	0	0	0
Wigwamma amatura	0	0	0	0	0	0	0
Kataspinifera baumannii	0	0	0	0	0	0	0
Calyptrosphaera sphaeroidea	0	1	0	0	0	0	0
Tetralithoides quadrilaminata	0	0	0	0	0	1	0
Placorhombus ziveriae	0	0	0	0	0	0	0
Tergestiella adriaticus	1	0	0	0	0	0	0

Appendix D.#21. Geographic occurrence data for the 106 species included in this dissertation. Biome and latitude occurrences represent a summary of the provincial information and are based on the assignment of that province to a given biome or latitude category (see Appendix E).

	AMS_Tropical	IND_Subtropical	IND_Tropical	MED.RED_Temperate	MED.RED_Subtropical	ARC_Temperate
Emiliania huxleyi-TypeA	1	0	0	0	1	0
Gephyrocapsa oceanica	1	1	0	0	1	0
Gephyrocapsa muellerae	0	0	0	0	1	0
Gephyrocapsa ericsonii-ericsonii	0	1	0	0	1	0
Gephyrocapsa ornata	0	0	0	0	0	0
Reticulofenestra parvula	0	0	0	0	1	0
Reticulofenestra sessilis	1	0	0	0	0	0
Cruciplacolithus neohelis	0	0	0	0	0	0
Calcidiscus leptoporus-leptoporus	1	0	0	0	1	0
Oolithotus antillarum	1	1	0	0	0	0
Oolithotus fragilis	0	1	0	0	1	0
Hayaster perplexus	0	0	0	0	0	0
Umbilicosphaera sibogae	1	1	0	0	1	0
Umbilicosphaera anulus	0	0	0	0	1	0
Umbilicosphaera foliosa	0	0	0	0	1	0
Umbilicosphaera hulburtiana	0	1	0	0	1	0
Pleurochrysis carterae-carterae	0	0	0	0	0	0
Pleurochrysis gayraliae	0	0	0	0	0	0
Pleurochrysis placolithoides	0	0	0	0	0	1
Pleurochrysis roscoffensis	0	0	0	0	0	0
Pleurochrysis pseudoroscoffensis	0	0	0	0	0	0
Hymenomonas globosa	0	0	0	0	0	0
Hymenomonas lacuna	0	0	0	0	0	1
Hymenomonas roseola	0	0	0	0	0	0
Ochrosphaera neapolitana	0	0	0	0	0	0
Jomonlithus littoralis	0	0	0	0	0	0
Helicosphaera carteri	1	0	0	0	1	0
Helicosphaera hyalina	0	0	0	0	1	0
Helicosphaera wallichii	1	1	0	0	0	0
Helicosphaera pavimentum	0	1	0	0	1	0
Pontosphaera discopora	0	0	0	0	1	0
Pontosphaera japonica	0	0	0	0	1	0
Pontosphaera multipora	1	0	0	0	0	0
Pontosphaera syracusana	1	0	0	0	1	0
Scyphosphaera apsteinii	1	0	0	0	1	0
Scyphosphaera porosa	0	0	0	0	0	0
Calciopappus caudatus	1	0	0	0	1	1
Calciopappus rigidus	1	1	0	0	1	0
Michaelsarsia adriaticus	1	1	0	0	0	0
Michaelsarsia elegans	1	0	0	0	1	0
Ophiaster hydroideus	1	0	0	0	1	0
Ophiaster formosus	0	0	0	0	1	0
Ophiaster reductus	1	1	0	0	1	0
Syracosphaera anthos	0	0	0	0	1	0
Syracosphaera lamina	0	0	0	0	1	0
Syracosphaera tumularis	1	0	0	0	1	0
Syracosphaera bannockii	0	0	0	0	0	1
Syracosphaera pulchra	1	1	0	0	1	0
Syracosphaera histrica	1	0	0	0	1	0
Syracosphaera noroitica	0	0	0	0	1	0
Syracosphaera corolla	0	0	0	0	1	0
Syracosphaera ossa-Type1	0	1	0	0	1	0
Syracosphaera epigrosa	1	0	0	0	1	0

Appendix D.#22. Geographic occurrence data for the 106 species included in this dissertation. Biome and latitude occurrences represent a summary of the provincial information and are based on the assignment of that province to a given biome or latitude category (see Appendix E).

	AMS_Tropical	IND_Subtropical	IND_Tropical	MED.RED_Temperate	MED.RED_Subtropical	ARC_Temperate
Syracosphaera borealis-Type1	0	0	0	0	0	1
Syracosphaera exigua	0	0	0	0	0	0
Syracosphaera rotula	0	0	0	0	1	0
Syracosphaera ampliora	1	0	0	0	1	0
Coronosphaera mediterranea	1	1	0	0	1	1
Coronosphaera binodata	0	0	0	0	0	0
Coronosphaera maxima	1	0	0	0	0	0
Calciosolenia murrayi	1	1	0	0	1	0
Calciosolenia brasiliensis	0	1	0	0	1	0
Alveosphaera bimurata	1	1	0	0	0	0
Rhabdosphaera clavigera-clavigera	1	0	0	0	1	0
Rhabdosphaera xiphos	0	0	0	0	1	0
Palusphaera vandelii	0	0	0	0	1	0
Discosphaera tubifera	1	1	0	0	1	0
Acanthoica quattrospina	1	0	0	0	1	0
Acanthoica janchenii	0	0	0	0	0	0
Acanthoica acanthifera	0	1	0	0	1	0
Acanthoica biscayensis	0	0	0	0	0	0
Anacanthoica acanthos	1	0	0	0	1	0
Cyrtosphaera aculeata	1	0	0	1	1	0
Algirosphaera robusta	0	0	0	0	0	0
Algirosphaera cucullata	1	0	0	0	1	0
Algirosphaera meteora	1	0	0	0	1	0
Solisphaera emidasia	1	0	1	0	0	0
Solisphaera helianthiformis	1	0	0	0	0	0
Alisphaera unicornis-spatula	0	0	0	0	0	0
Alisphaera pinnigera	0	0	0	0	1	0
Alisphaera capulata	0	0	0	0	1	0
Alisphaera ordinata	0	0	0	0	1	0
Alisphaera quadrilatera	0	0	0	0	1	0
Alisphaera extenta	0	0	0	0	0	1
Alisphaera gaudii	0	0	0	0	1	0
Umbellosphaera irregularis	1	1	0	0	1	0
Umbellosphaera tenuis-TypeI	1	0	0	0	1	0
Papposphaera borealis	0	0	0	0	0	0
Papposphaera lepida	0	0	0	0	1	0
Pappomonas flabellifera	0	0	0	0	0	0
Pappomonas borealis	0	0	0	0	0	0
Pappomonas garrisonii	0	0	0	0	0	0
Pappomonas weddellensis	0	0	0	0	0	0
Picarola margalefii	0	0	0	0	1	0
Wigwamma arctica	0	0	0	0	0	0
Wigwamma triradiata	0	0	0	0	0	0
Wigwamma annulifera	0	0	0	0	0	0
Wigwamma antarctica	0	0	0	0	0	0
Wigwamma amatura	0	0	0	0	0	0
Kataspinifera baumannii	0	0	0	0	1	0
Calyptrosphaera sphaeroidea	0	0	0	0	0	0
Tetralithoides quadrilaminata	0	0	0	0	1	0
Placorhombus ziveriae	0	0	0	0	1	0
Tergestiella adriaticus	0	0	0	0	1	0

Appendix D. #23. Geographic occurrence data for the 106 species included in this dissertation. Biome and latitude occurrences represent a summary of the provincial information and are based on the assignment of that province to a given biome or latitude category (see Appendix E).

				Latitudes (global summary of oceans)			
	ARC_Polar	ANT_Temperate	ANT_Polar	No.Polar.realms	No.Temp.realms	No.Subtrop.realms	No.Trop.realms
Emiliania huxleyi-TypeA	0	0	1	1	1	3	2
Gephyrocapsa oceanica	0	0	1	1	1	3	2
Gephyrocapsa muellerae	1	0	0	2	1	1	0
Gephyrocapsa ericsonii-ericsonii	0	0	0	0	1	4	1
Gephyrocapsa ornata	0	0	0	0	0	2	0
Reticulofenestra parvula	0	0	0	0	1	1	0
Reticulofenestra sessilis	0	0	0	0	1	2	2
Cruciplacolithus neohelis	0	0	0	0	0	0	2
Calcidiscus leptoporus-leptoporus	1	0	0	2	0	3	1
Oolithotus antillarum	0	1	0	0	2	3	1
Oolithotus fragilis	0	0	0	0	0	2	0
Hayaster perplexus	0	0	0	0	0	0	0
Umbilicosphaera sibogae	0	0	0	0	0	3	2
Umbilicosphaera anulus	0	0	0	0	0	2	0
Umbilicosphaera foliosa	0	0	0	0	0	1	0
Umbilicosphaera hulburtiana	0	0	0	0	1	3	1
Pleurochrysis carterae-carterae	0	0	0	0	0	0	0
Pleurochrysis gayraliae	0	0	0	0	0	0	0
Pleurochrysis placolithoides	0	0	0	0	2	0	0
Pleurochrysis roscoffensis	0	0	0	0	0	0	0
Pleurochrysis pseudoroscoffensis	0	0	0	0	0	0	0
Hymenomonas globosa	0	0	0	0	0	0	0
Hymenomonas lacuna	0	0	0	0	1	0	0
Hymenomonas roseola	0	0	0	0	0	0	0
Ochrosphaera neapolitana	0	0	0	0	0	0	0
Jomonlithus littoralis	0	0	0	0	0	0	0
Helicosphaera carteri	1	0	0	2	1	2	2
Helicosphaera hyalina	0	0	0	0	0	2	1
Helicosphaera wallichii	0	0	0	0	0	2	1
Helicosphaera pavimentum	0	0	0	0	0	3	0
Pontosphaera discopora	0	0	0	0	0	2	0
Pontosphaera japonica	0	0	0	0	0	3	0
Pontosphaera multipora	0	0	0	0	0	1	1
Pontosphaera syracusana	0	0	0	0	0	1	1
Scyphosphaera apsteinii	0	0	0	0	0	3	1
Scyphosphaera porosa	0	0	0	0	1	1	1
Calciopappus caudatus	0	0	0	0	1	1	1
Calciopappus rigidus	0	0	0	0	0	2	2
Michaelsarsia adriaticus	0	0	0	0	0	2	1
Michaelsarsia elegans	0	0	0	0	0	2	2
Ophiaster hydroideus	0	0	0	0	0	2	1
Ophiaster formosus	0	0	0	0	0	3	0
Ophiaster reductus	0	0	0	0	0	3	1
Syracosphaera anthos	0	0	0	0	0	2	1
Syracosphaera lamina	0	0	0	0	1	1	1
Syracosphaera tumularis	0	0	0	0	0	3	1
Syracosphaera bannockii	1	1	0	2	2	1	0
Syracosphaera pulchra	0	1	0	0	1	3	1
Syracosphaera histrica	0	1	0	0	2	2	1
Syracosphaera noroitica	0	0	0	0	0	2	0
Syracosphaera corolla	0	1	0	0	1	1	1
Syracosphaera ossa-Type1	0	0	0	0	0	2	1
Syracosphaera epigrosa	0	1	0	0	1	2	1

Appendix D.#24. Geographic occurrence data for the 106 species included in this dissertation. Biome and latitude occurrences represent a summary of the provincial information and are based on the assignment of that province to a given biome or latitude category (see Appendix E).

	ARC_Polar	ANT_Temperate	ANT_Polar	No.Polar.realms	No.Temp.realms	No.Subtrop.realms	No.Trop.realms
Syracosphaera borealis-Type1	1	0	0	2	1	0	0
Syracosphaera exigua	0	0	0	0	0	0	0
Syracosphaera rotula	0	0	0	0	0	1	0
Syracosphaera ampliora	0	0	0	0	0	1	1
Coronosphaera mediterranea	1	0	0	2	1	3	2
Coronosphaera binodata	0	0	0	0	2	1	0
Coronosphaera maxima	0	0	0	0	0	0	1
Calciosolenia murrayi	0	0	0	0	0	3	1
Calciosolenia brasiliensis	0	0	0	0	0	4	1
Alveosphaera bimurata	0	0	0	0	1	2	1
Rhabdosphaera clavigera-clavigera	0	0	0	0	0	1	1
Rhabdosphaera xiphos	0	0	0	0	0	1	0
Palusphaera vandelii	0	1	0	0	1	2	0
Discosphaera tubifera	0	0	0	0	0	2	1
Acanthoica quattrospina	0	0	0	0	1	1	1
Acanthoica janchenii	0	0	0	0	0	2	0
Acanthoica acanthifera	0	0	0	0	0	2	0
Acanthoica biscayensis	0	0	0	0	1	0	0
Anacanthoica acanthos	0	0	0	0	0	1	1
Cyrtosphaera aculeata	0	0	0	0	1	1	1
Algirosphaera robusta	0	0	0	0	0	0	0
Algirosphaera cucullata	0	0	0	0	0	1	1
Algirosphaera meteora	0	0	0	0	0	1	1
Solisphaera emidasia	0	0	0	0	0	0	2
Solisphaera helianthiformis	0	1	0	0	2	0	1
Alisphaera unicornis-spatula	0	0	0	0	0	0	0
Alisphaera pinnigera	0	1	0	0	1	1	1
Alisphaera capulata	0	0	0	0	0	2	0
Alisphaera ordinata	0	0	0	0	0	2	0
Alisphaera quadrilatera	0	0	0	0	0	1	0
Alisphaera extenta	1	0	0	2	2	0	0
Alisphaera gaudii	0	1	0	0	1	1	0
Umbellosphaera irregularis	0	0	0	0	0	4	2
Umbellosphaera tenuis-TypeI	0	0	0	0	0	2	3
Papposphaera borealis	1	0	0	1	1	0	0
Papposphaera lepida	1	0	0	2	1	2	0
Pappomonas flabellifera	1	0	0	2	1	0	1
Pappomonas borealis	1	0	0	2	1	0	0
Pappomonas garrisonii	0	0	1	1	0	0	0
Pappomonas weddellensis	0	0	1	1	0	0	0
Picarola margalefii	0	0	0	0	0	1	0
Wigwamma arctica	1	0	1	2	0	0	0
Wigwamma triradiata	0	0	1	1	0	0	0
Wigwamma annulifera	1	0	1	2	0	0	0
Wigwamma antarctica	0	0	1	1	0	0	0
Wigwamma amatura	0	0	1	1	0	0	0
Kataspinifera baumannii	0	1	0	0	1	1	0
Calyptrosphaera sphaeroidea	0	0	0	0	0	1	0
Tetralithoides quadrilaminata	0	0	0	0	0	2	0
Placorhombus ziveriae	0	0	0	0	0	1	0
Tergestiella adriaticus	0	0	0	0	1	1	0

Appendix E. Map of pelagic biogeographic provinces generated using Google Earth Pro (kmz and kml files included as supplementary files and will be available on Dryad following publication). Colored markers denote "ocean basin" assignment: dark blue is Arctic, green is Atlantic, Pacific is purple, Indian is orange, Mediterranean to Arabian Sea, Teal is the Southern Subtropical Transition Zone, light-blue is Antarctic. Full key to province markers in Appendix F.

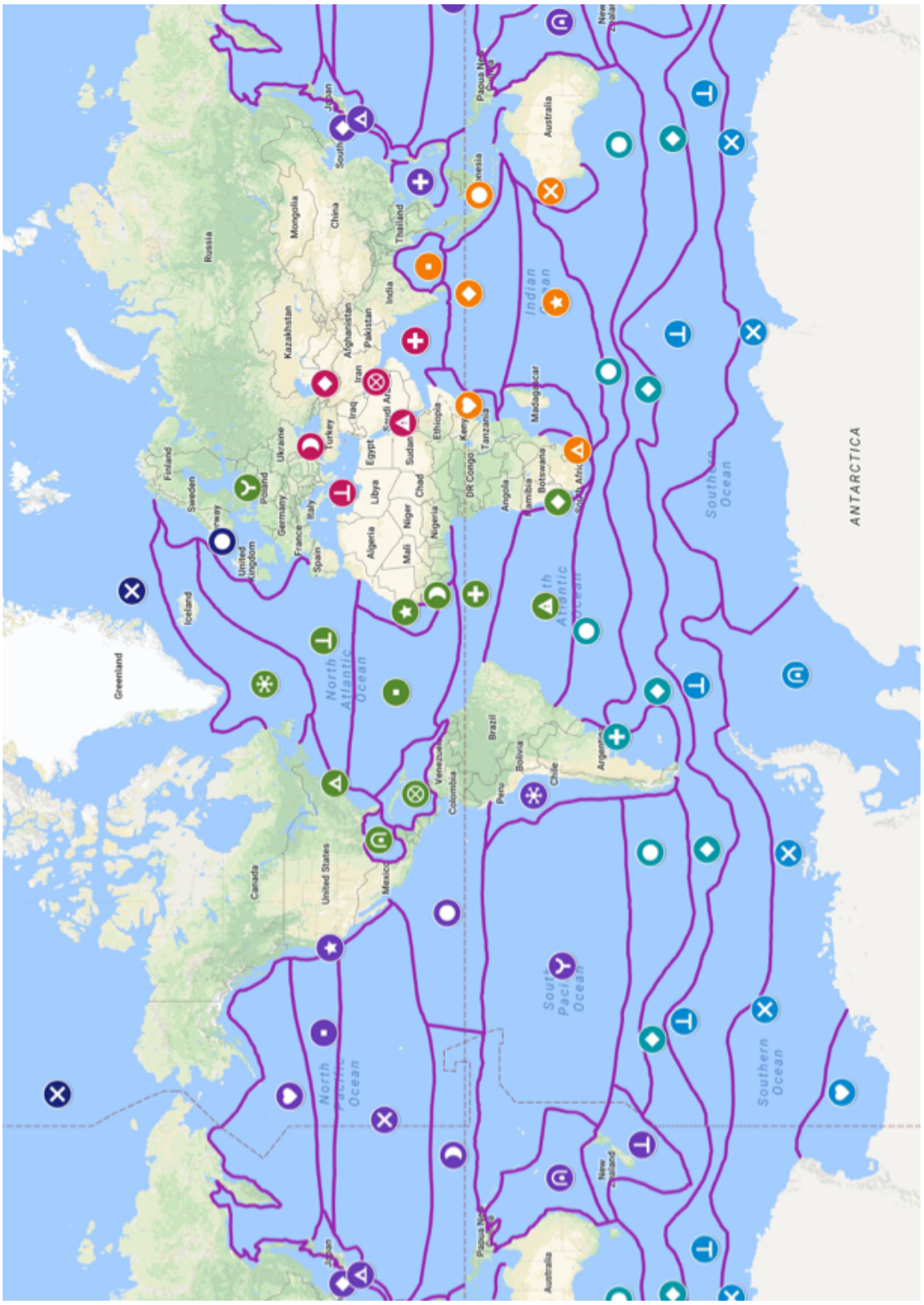

Appendix F. Table of pelagic biogeographic provinces (see Chapter 3 for details on how boundaries were delimited). Markers correspond to markers found in the map included as Appendix E. "Ocean Basin" refers to the oceanic sector where the province is located, which may not be an ocean basin, hence the quotations. Latitude is assigned according to Winter et al. (1994). Biomes are assigned based on Spalding et al (2012).

Province	Map marker	"Ocean Basin"	Latitude	Biome(s)
Arctic Ocean		Arctic	Polar	Polar
Northern European Shelf		Arctic	Temperate	Polar, Shallow, Semi-Enclosed Sea
Subarctic Atlantic		Atlantic Ocean	Temperate	
North Atlantic Current		Atlantic Ocean	Temperate	Transitional
Gulf Stream Current		Atlantic Ocean	Subtropical	Western Boundary Current
North Central Atlantic		Atlantic Ocean	Subtropical	Gyre
Interamerican Seas		Atlantic Ocean	Tropical	Semi-Enclosed
Canary Current System		Atlantic Ocean	Subtropical	Eastern Boundary current
Equatorial Atlantic		Atlantic Ocean	Tropical	Equatorial
Benguela Current		Atlantic Ocean	Temperate	Eastern Boundary current
South Central Atlantic		Atlantic Ocean	Subtropical	Gyre
Guinea Current		Atlantic Ocean	Tropical	Eastern Boundary current
Baltic Sea		Atlantic Ocean	Temperate	Enclosed Sea
Gulf of Mexico		Atlantic Ocean	Tropical	Gyre
Humboldt Current		Pacific Ocean	Temperate	Eastern Boundary Current
North Central Pacific		Pacific Ocean	Subtropical	Gyre
South Central Pacific		Pacific Ocean	Subtropical	Gyre
Kuroshio-Oyashio Current		Pacific Ocean	Subtropical	Shallow, Western Boundary Current
North Pacific Current		Pacific Ocean	Temperate	Transitional, Gyre
Southwest Pacific		Pacific Ocean	Subtropical	Shallow
New Zealand Shelf		Pacific Ocean	Temperate	Shallow
Equatorial Pacific		Pacific Ocean	Tropical	Equatorial
California Current		Pacific Ocean	Temperate	Eastern Boundary Current
South China Sea		Pacific Ocean	Tropical	Western Boundary Current
Eastern Tropical Pacific		Pacific Ocean	Tropical	Eastern Boundary Current
Subarctic Pacific		Pacific Ocean	Polar	Eastern Boundary Current

Appendix F. Table of pelagic biogeographic provinces (see Chapter 3 for details on how boundaries were delimited), continued.

Province	Map marker	"Ocean Basin"	Latitude	Biome(s)
Sea of Japan & East China Sea		Pacific Ocean	Temperate	Transitional
North East Indian Ocean		Indian Ocean	Subtropical	Gyre
North Equatorial Indian Ocean		Indian Ocean	Tropical	Gyre
Somali Current		Indian Ocean	Subtropical	Western Boundary Current
Agulhas Current		Indian Ocean	Subtropical	Western Boundary Current
South Indian Ocean		Indian Ocean	Subtropical	Gyre
Indonesian Flow-Through		Indian Ocean	Tropical	Shallow, Semi-Enclosed
Leeuwin Current		Indian Ocean	Subtropical	Eastern Boundary current, Shallow
Arabian and associated Seas		Mediterranean - Arabian Sea	Subtropical	Gyre
Gulf of Elat (Persian Gulf)		Mediterranean-Arabian Sea	Subtropical	Semi-Enclosed Sea
Red Sea		Mediterranean-Arabian Sea	Subtropical	Semi-Enclosed Sea
Black Sea		Mediterranean-Arabian Sea	Temperate	Enclosed Sea
Mediterranean Seas		Mediterranean-Arabian Sea	Subtropical	Semi-Enclosed Sea
Caspian Sea		Mediterranean-Arabian Sea	Temperate	Enclosed Sea
Malvinas Current		Southern Subtropical Transition Zone	Temperate	Transitional, Western Boundary Current
Southern Subtropical Front		Southern Subtropical Transition Zone	Temperate	Transitional
Subantarctic		Southern Subtropical Transition Zone	Temperate	Transitional
Antarctic		Antarctic	Polar	Gyre, Polar
Weddell Sea		Antarctic	Polar	Polar
Antarctic Polar Front		Antarctic	Polar	Polar
Ross Sea		Antarctic	Polar	Gyre, Polar